TEXTILE RESEARCH JOURNAL

VOLUME XXVI August 1956 NUMBER 8

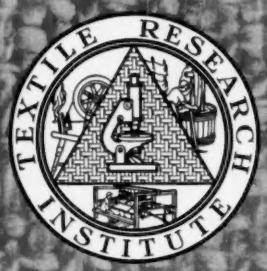

PUBLICATION OF

TEXTILE RESEARCH INSTITUTE

Publications Department: P. O. Box 625, Princeton, N. J.

Will

RHOPLEX

Acrylic Emulsions

Trigger the Next Big Idea

in Textiles?

NOW COMMERCIALLY AVAILABLE

A new and comprehensive series of Rohm & Haas acrylic emulsion polymers and copolymers is now available in commercial quantities.

Already, these low-cost emulsion polymers have made a name for themselves in . . . fabric finishes . . . pigment binders . . . non-woven fabric binders . . . fabric backings . . . warp sizes.

The films of these resins vary from extremely soft and flexible to hard and stiff. Like all acrylic resins, the films also display unusual clarity and resistance to light and aging. The polymers applied to fibers range from completely hydrophilic to strongly hydrophobic.

With Rohm & Haas acrylic emulsions, the next big development in textiles may be yours. Write today to Department R for complete information.

ACRYLIC MONOMERS ALSO AVAILABLE

Methyl acrylate	Methyl methacrylate
Ethyl acrylate	Ethyl methacrylate
Butyl acrylate	Butyl methacrylate
Glacial acrylic acid	Glacial methacrylic acid

2-Ethylhexyl acrylate

RHOPLEX *is a trade-mark, Reg. U.S. Pat. Off. and in principal foreign countries.*

Chemicals for Industry

ROHM & HAAS COMPANY

WASHINGTON SQUARE, PHILADELPHIA 5, PA.

Representatives in principal foreign countries

TEXTILE RESEARCH JOURNAL

VOL. XXVI, NO. 8 AUGUST 1956

IN THIS ISSUE

THE DETERMINATION OF NEPPINESS IN CARDED WEBS. N. H. Chamberlain and G. Jordan 579

EFFECT OF ALKALINE HYDROLYSIS ON THE PROPERTIES OF CYANOETHYLATED COTTON. Laurence W. Mazzeno, Jr., Robert M. Reinhardt, J. David Reid, and John B. Dickson 597

DEFINITION AND MEASUREMENTS OF CRIMP OF TEXTILE FIBERS. Ernst Alexander, Menachem Lewin, Helmut V. Muhsam, and Miriam Shiloh . 606

Letters to the Editor

THE DISTRIBUTION OF ORTHO- AND PARA-CORTICAL CELLS IN WOOL AND MOHAIR. R. D. B. Fraser and T. P. Macrae 618

A FABRIC DESIGNED FOR RAPID PREPARATION OF UNIFORM RAVELED TEST SPECIMENS. Samuel Shapiro 620

Industrial Section

LUBRICATION OF THE TEXTILE SPINDLE BEARING. J. P. Vidosic and R. D. Cheverton 622

A COPPER PROCESS FOR PROLONGED MICROBIOLOGICAL PROTECTION OF CELLULOSIC FABRICS BY CHEMICAL MODIFICATION. Edward Abrams and Robert R. Bottoms 630

PHYSICAL PROPERTIES OF CHEMICALLY MODIFIED COTTONS. *PART I:* PROPERTIES OF THE UNTREATED COTTONS. Allan W. McDonald, Geraldine C. Humphreys, Ora M. Kromhout, and James N. Grant . 641

PART II: EFFECTS OF PARTIAL ACETYLATION. Allan W. McDonald, Geraldine C. Humphreys, Rollin S. Orr, and James N. Grant 646

BOOK REVIEWS 652

Editor: Julian S. Jacobs *Production Editor:* Ellen Vogel

Associate Editors

H. J. Ball, Earl E. Berkley, Henry Eyring, W. J. Hamburger, Milton Harris, K. L. Hertel, Harold P. Lundgren, H. Mark, E. R. Schwarz

TEXTILE RESEARCH JOURNAL, published monthly at Prince and Lemon Streets, Lancaster, Pa., is devoted to the interest of research in textile and allied industries. It is published by Textile Research Institute.

Entered as second-class matter, April 27, 1945, at the post office at Lancaster, Pa., under the Act of August 24, 1912. Accepted for mailing at special rate of postage provided for in paragraph (d-2), Section 34.40, P. L. & R. of 1948, authorized May 9, 1950.

Manuscripts and communications should be sent to the Publications Department, P.O. Box 625, Princeton, N. J.

Subscription rates: $20.00 per year; additional for postage, 50 cents to Canada, $1.00 to all other countries. Single copies, $2.00 each.

Contents copyrighted © 1956 by Textile Research Institute. Advertising rates supplied on request.

The Perkin Centennial

The Waldorf-Astoria
New York City
Week of September 10, 1956

A large attendance is assured at the centennial celebration of Sir William Henry Perkin's discovery of the first synthetic dye. The variety of features of the week-long program holds something of interest to every one. Speakers from abroad as well as from the U. S. A. will discuss developments in the application of color; there will be luncheons and banquets with speakers of prominence, and elaborate exhibits of colored materials of all types including fibers and fabrics. Exhibits of functional finishes applied to fabrics will be a feature. Twenty-nine industry associations, scientific and research organizations are participating in the program. T. R. I. is sponsoring a symposium: "Theories of Dyeing" with Howard J. White, Jr., Associate Director of Research, presiding. This symposium will be held Saturday morning, September 15.

Complete information sheet with form for general registration and registration for special events may be obtained from Roy R. Hamilton, c/o Interchemical Corporation, 150 Waganow Road, Hawthorne, New Jersey. Deadline for hotel reservations is said to be August 20. These are handled solely by the Housing Bureau, New York Convention and Visitors Bureau, 90 East 42nd Street, New York 17, N. Y.

TEXTILE RESEARCH JOURNAL

VOL. XXVI, NO. 8 AUGUST 1956

The Determination of Neppiness in Carded Webs

N. H. Chamberlain and G. Jordan

Department of Textile Industries, Leeds University, Leeds, England

Abstract

The general problems encountered in determining the number and average size of a population of opaque particles randomly distributed on a transparent or translucent ground are discussed, with particular reference to the use of optical scanning methods for such determinations. An apparatus suitable for scanning specimens of carded webs, with a view to determining their nep content, is described, and it is shown that, when used with "ideal" samples consisting of small black paper disks randomly distributed between glass plates, it is capable of counting and sizing the particle array within very close limits. The particular difficulties encountered with carded web samples are then discussed with reference to actual experimental results, and a method of computing the "neppiness index" is described. It is suggested that this index may be a more reliable and consistent measure of the neppiness of a sample of carded web than the "nep count" which has hitherto been used for this purpose.

Introduction

The importance, from a commercial standpoint, of the nep content or neppiness of worsted slivers, tops, and rovings, needs no emphasis. These small bunches, or knots, of unopened fibers and entangled fiber fragments, are formed mainly during the carding process, and are remarkably persistent in later operations. Though their number may be modified by backwashing, combing, gilling, etc., it is impossible to eliminate them completely once they have been formed, and their deleterious effects in later spinning operations, particularly when fine counts are in question, is well known. Very little is known, however, as to the nature of the physical mechanism of nep formation, or indeed as to which part of the carding operation is mainly responsible. This lack of knowledge is largely attributable to the experimental difficulties encountered in attempts to determine the nep content of carded webs with speed and accuracy. The most commonly used method, that of examining a known area of the web by transmitted light, and counting the neps present individually, is not only very tedious, but also is found to be highly subjective, the results obtained by different operators for the same set of specimens often showing considerable divergence. A more objective and automatic method would therefore seem to be of value not only from the point of view of quality control in industry, but also as a research tool in the investigation of the causes of neppiness, which, once understood, may then be minimized or abolished.

Many modifications to the simple visual counting method have been suggested with a view to increasing its accuracy. Some experimenters have used transmitted light, and some reflected light; some have used low-power magnifiers, while others have relied on the unaided eye; some have picked out the neps from the web with tweezers, and some have

counted them *in situ*. The results have remained disappointing. Stenersen [14], for example, found it necessary to count each sample of 10 g. of sliver four times in order to obtain more reproducible results. Even so, computation from Stenersen's data shows in fact a coefficient of variation between counts of 38.5%. The difficulty appears to be twofold. First, different observers, or even the same observer on different occasions, disagree as to the size or prominence of the fiber aggregate which is to qualify as a nep; and second, it is very difficult to ensure that every nep within a given area is counted, if the area is at all large, say 10 × 10 in., as it should be to ensure adequate sampling. Several workers [1, 7, 14] have attempted to overcome the latter difficulty by ruling off the area to be examined into smaller squares, rectangles, or circles, and counting the neps within these smaller areas one at a time; but this device eliminates one problem only to introduce another, i.e., whether a nep falling on the boundary of a defined areas should be included or excluded from the count. This is a well-recognized difficulty in the counting of red blood corpuscles on squared counting slides, and one way of overcoming it is to include in the count all boundary particles falling on the left-hand side and bottom of each rectangular area, and to omit all those falling on the right-hand side and top. Even so, "doubtful" cases occur, and the accuracy of the count suffers. But even if this mechanical problem is dealt with, there remains the difficulty of deciding what constitutes a nep and what does not. The only answer here would seem to be that of removing the criterion from the sphere of human judgment and opinion, and setting up some optical or electro-optical device for the purpose which, being constant and reproducible, will not vary its standard from machine to machine or from day to day. Thus, the indications would seem to point to an optical scanning device, associated preferably with an electrical recorder, both for detecting the neps in a web, deciding what shall be counted, and what shall not, and making the actual count. The remainder of the present contribution is an account of an attempt to create such an instrument, and of some of the results obtained with it.

Experimental

I. *Particle Counting by Scanning Methods*

Considerable attention has been directed in recent years to the problem of counting and sizing populations of small particles, such as red blood cells, coal and stone dust particles, spray droplets, etc. In general, optical scanning systems with photoelectric detection of the particle have been employed [9], and much information has been gained regarding the most suitable type of scanning system for use in any particular case. The mathematics of particle counting has also been examined in some detail. As all this information is relevant to the present case, a summary of some of the leading results follows.

(*a*) *Mechanical considerations.* The methods used up to the present may be divided roughly into two types, i.e., those involving the use of reciprocating or rectilinear scanners, and those employing continuous spiral or cylindrical scanners.

In the former case, either the specimen or the scanning head is moved to and fro, with a lateral displacement between each scan stroke. Apparatus of this type has been used by Cooke-Yarborough and Hawksley [2, 6]. The major objection to this type of system seems to be the tendency to vibration of the apparatus, caused by the intermittent motion and the inertia of the moving parts. It has been found necessary to scan relatively slowly, and to accelerate and decelerate the scanner gradually at the ends of each scan stroke. As it is generally desirable to have a reasonably constant scanning speed, only the center portion of each stroke can, in consequence, be utilized, and this further reduces the effective speed of scanning, in terms of the area scanned in unit time.

Taken over-all, rectilinear scanning has proved rather troublesome and inefficient compared with continuous scanning systems. Of these, that used by Courshee [3] and adapted directly from the type of scanner used in facsimile picture transmitters, is a good example. The specimen to be scanned is wrapped around a cylindrical drum which is rotated at constant speed, while the scanning head moves parallel to the axis of the drum, and also at constant speed. The scanning track takes the form of a helix, but when the specimen is removed from the cylinder, successive scan tracks approximate to straight lines very nearly parallel to the edges. The scanning speed is constant, and can be quite high, so that large areas can be rapidly covered. It is, of course, applicable only to specimens of reasonably large area, which are flexible enough to conform to the scanning cylinder. Normally, scanning is by reflected light, and the use of transmitted light would involve putting either the light source and

optical system, or the detecting photocell, within the cylinder. While this is by no means impossible, it was felt in the present case that this complication, and the additional difficulty of wrapping a very fragile web specimen around the cylinder and securing it without damage or distortion, made the use of this type of scanner inadvisable.

There remains a further type of spiral scanning, namely that used on gramophone disks, in which the scanning track forms a continuous spiral from the edge to a point as near the center as possible. This method, applied to optical scanning, involves sandwiching the specimen between two transparent rigid disks, revolving at constant speed, preferably in a horizontal plane, and traversing the scanning head at constant speed along a fixed radius of the disks. It has all the advantages of cylindrical scanning save one, and in addition can be used equally easily with transmitted or reflected light. The disadvantage of the method is that the scanning speed is not constant, but decreases as the scanning head approaches the center of the disks. This continuous change in the linear scanning speed will affect the nature of the signal output from the scanning head. It is possible, however, by suitable design of the apparatus, at least when photoelectric scanning is employed, to overcome this difficulty by making the action of the counting part depend largely on the amplitude of the voltage pulse produced by the scanner when a particle intercepts the light beam, rather than on pulse duration. The amplitudes are almost independent of scanning speed, whereas pulse duration is, of course, inversely proportional to it.

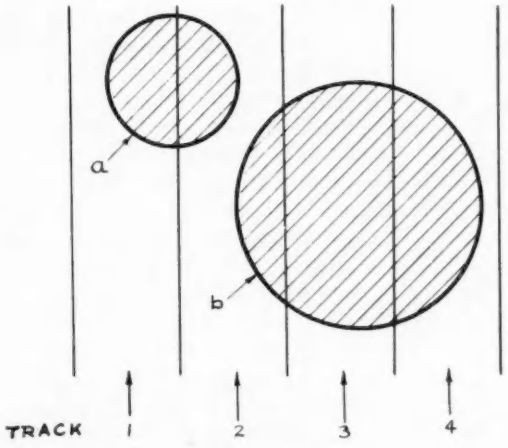

Fig. 1.

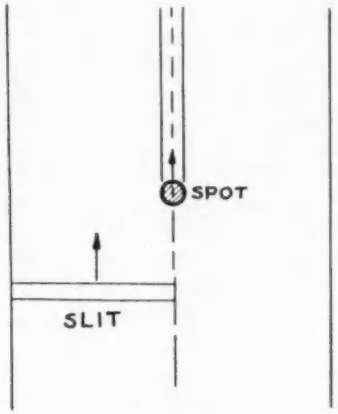

Fig. 2.

As the flat spiral scanner was in all other respects apparently ideal for the purpose of scanning web samples, which could be mounted very easily and without distortion between plate-glass disks, it was adopted in the present work, as will later be described.

(*b*) *Mathematical considerations.* The main problem involved in counting particles randomly distributed over an area by photoelectric track-scanning is essentially the same as that already mentioned in connection with the visual counting of particles in an area circumscribed by a rectangle, namely that of counting the particles falling on the boundary of a counting area. In the visual case, in order to prevent boundary particles from being counted twice, all particles touching the bottom and left-hand boundaries of the rectangle are counted, while those touching the top and right-hand side are neglected. When the experimental field is scanned by a light spot moving over it in a series of parallel tracks, similar conditions are encountered. The particle, if it falls on the boundary between two scanning tracks, is counted in both tracks, and registered twice instead of once, as in Figure 1, *a*. If the diameter of the particle exceeds twice the width of the scan track, it will be counted three times as in Figure 1, *b*.

One method of dealing with this problem, closely imitating the visual method, was suggested by Meyer [11] who used a scanning system consisting of small light spot and an illuminated slit, as shown in Figure 2. The slit scanned the specimen in successive tracks, while the spot scanned one of the two edges of each track. Both slit and spot were

furnished with separate detecting photocells, and a separate counting system. The count obtained from the spot system was subtracted from that of the slit system to obtain the true particle count. The constructional difficulties inherent in such an arrangement are considerable, since the spot must have dimensions small compared with the slit length, and the latter itself must not be large if good sensitivity and resolution are to be maintained.

Another ingenious method for eliminating edge double counts was suggested by Lagerkrantz and Wolff [10, 15]. For reasonably large samples, in which the particles to be counted are distributed randomly, the number of particles touching each track boundary will be approximately equal. If the sample is scanned twice, using two scanning slits of different widths, but keeping the total length of scanned track the same in both cases, then the number of particles overlapping each boundary of the wider track must be equal to the number overlapping each boundary of the narrower one, since the lengths of the two tracks are equal. The difference between the total counts obtained in the two cases therefore represents the number of particles present in the additional area swept over by the wider track.

Roberts and Young [12, 13] have suggested the use of a guard-spot scanning system. The particles, randomly distributed over a plane area, are scanned by two light spots whose centers are on a line perpendicular to the direction of scan. Each spot has its own photocell, receiving light transmitted from the spot through the specimen. One photocell is arranged to give a positive pulse, the other a negative pulse, when the corresponding light spot is obscured by a particle, and the two are connected to the counter *via* an anticoincidence circuit which passes a signal to the counter only on receipt of a single positive pulse. As the two spots scan the specimen and a particle is approached, the light from one of the spots is ultimately interrupted and a positive pulse is passed by the corresponding photocell to the anticoincidence circuit and thence to the counter. When this spot returns to the same particle on the next scan line (i.e., one line lower), the companion spot occupies its former position, on the original scan line. If the distance between the spots is smaller than the diameter of the particle (which would normally give rise to a multiple count), both spots are simultaneously obscured and the anticoincidence circuit receives a paired pulse, one positive and one negative, neither of which affects the counter. This state of affairs persists for successive lines, no further counts being registered, until the leading spot clears the particle, and only the guard spot is obscured on the last scan line. Since this spot generates only a negative pulse, the anticoincidence circuit does not operate the counter. Thus, though both spots may have been obscured several times by the same particle, only one count is registered. This method may also be used for sizing the particles, by obtaining a series of counts with successively greater distances between the scan spots. It is theoretically very attractive, but the practical difficulties involved in setting up the twin optical systems within a very short distance of each other, and yet in such a way that they do not interfere with each other, are considerable.

Courshee [3] and Hoare [8] have counted and sized spray droplet stains on paper, using an intercept length method. Briefly, this method involves the scanning of a random population of small circular stains by a spot of light and a photocell, and the recording of the frequency distribution of pulse lengths in the resultant output. A spot of light, of sufficiently small dimensions, draws during rectilinear scanning a series of parallel and equally spaced lines across the specimen. A circular stain of a given diameter gives under these circumstances a characteristic number and size distribution of chords (pulse lengths). A population of circles of different sizes gives a family of chords characteristic of that population. At present the mathematical analysis of the chord length distribution is available only for circular particles; considerable computation is necessary in order to extract the particle size distribution and particle number from the scanning data, so that the method, though of considerable theoretical interest, is difficult to apply in practice, and the apparatus required is considerable, since many counters must be used, one counting each group of the frequency distribution of pulse lengths.

Hawksley [5] has shown that the count and size distribution of a random population of particles may also be obtained by a slit scanning method in which the sample is scanned by a series of narrow slits, whose length (perpendicular to the scanning direction) is varied on repeated scans from a length less than the diameter of the smallest particle present to a length greater than the diameter of the largest particle. If counts are recorded only on each occasion that the slit is totally obscured, Hawksley shows that the size distribution is given by the reciprocal

of the number of particles per unit area multiplied by the second derivative of the observed frequency distribution of counts. A major difficulty of this method is the mechanical one of making accurate changes in the dimensions of very small slit apertures.

All the foregoing methods suffer from various disadvantages when considered from the standpoint of nep counting. With one exception, all require complex optical systems and/or electronic apparatus. This exception, the method suggested by Wolff [15] and Lagerkrantz [10], requires only a change in slit length. The use of this system in the present instance was not considered advisable, however, since it requires that the particles to be counted shall be clearly delineated and that the background shall be either transparent or uniformly translucent. With carded webs, the background varies considerably in transparency, thus generating a background signal which must be eliminated in some way to prevent it from interfering with the counting of pulses due to neps.

A reconsideration of the mathematics of track-scanning has shown, however, that if a simple constant-width track-scanning system is combined with a pulse amplitude discriminator, which enables the pulses generated by the particles to be sorted into groups according to their amplitude distribution, a very simple equation can be derived from which both the number and the average diameter of the particles present may be evaluated. The practical form and utility of this expression seems to have been overlooked by Hawksley [6] and Courshee [3] since the former placed emphasis on variable track width systems rather than on pulse amplitude discriminators, and the latter was concerned with pulse durations and the frequency distribution of pulse widths. Hawksley [5] has, however, clearly foreshadowed the theoretical possibility of a counting and sizing system based on amplitude discrimination, but for some reason failed to follow it up in practice.

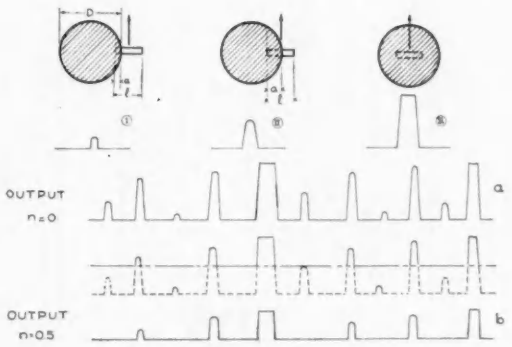

Fig. 3.

(*c*) *Particle counting by means of an amplitude discriminator.* The following analysis is based upon the following two assumptions.

(i) The particles in the array to be counted are considered separate and discrete, without overlapping.

(ii) They are considered to be uniformly opaque; it is not necessary that they should be totally opaque, as the equations are equally valid for semi-opaque particles provided the light-stopping power of all of them is the same.

If an array of randomly distributed particles conforming to the above assumptions is scanned by a narrow rectangular spot of light, moving at right angles to its long axis to form the scan track, and the light from the spot is received on a photocell, a voltage pulse (positive or negative at will) is produced each time a particle intercepts part or all of the spot. If the illuminated rectangle constituting the scan spot is of equal intensity at all points within its area, the amplitude of the voltage pulse will be proportional to the length of the spot obscured, i.e., to the distance a in Figure 3, I and II. Maximum pulse amplitude will correspond to complete interception of the spot, i.e., to $a = l$ in Figure 3, III. It should be noted that if this essential proportionality between pulse amplitude and length of spot intercept is to be preserved, photocells and amplifiers with linear characteristics are essential.

During the scanning process, the rectangular spot describes over the specimen a series of parallel scan tracks of width l. In the general case, these tracks will be separated by an unscanned track of width d, as shown in Figures 4 and 5. When $d = 0$, the scan tracks join at their edges and the whole area of the field is scanned, but this is really a special case, though a very important one as will later appear. Let a particle of radius r overlap the scan track by a distance a, and let a be expressed as a fraction n of the width of the track, i.e., $n = a/l$. Now, if the detecting photocell and its associated amplifier have linear characteristics, and if the width of the scanning spot is small compared with its length, then n is also the ratio of amplitudes of the pulses produced by this partial interception of the slit, and by a complete interception of the slit respectively. Thus, $n =$

1 when the slit is completely obstructed, i.e., when $a = l$, and $n = 0$ if the slit is not obstructed at all, i.e., when $a = 0$.

For a random series of partial interceptions of the slit by the scanned particles, the photocell output will consist of a series of mixed pulses varying in amplitude from zero to a maximum corresponding to complete obstruction of the scanning spot. The total number of pulses in the series will be several times greater than the number of particles present, and may be represented as shown in Fig. 3, *a*. Let this photocell output be fed to a clipper circuit (to be described later) which allows only those parts of the pulse train which lie above a certain predetermined and adjustable level to pass forward to later stages and ultimately to be recorded by the counter. Then the "clipping level" so established corresponds exactly to the value of n as defined above. All particles having their centers within the distance xy (Figure 4) will give pulses larger than n, and after passing through the clipper all such pulses will score a count; but particles having their centers outside the distance xy will be clipped out completely when the clipping level is set at n, and so will fail to score a count. Now

$$xy = l + 2(r - nl)$$

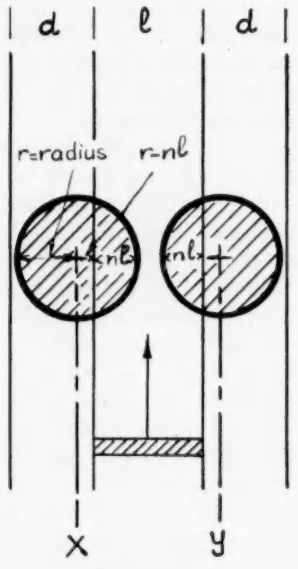

Fig. 4.

If

$$D = \text{particle diameter } (= 2r)$$

Then

$$xy = l + D - 2nl$$

The effective area scanned when a slit of length l travels over a distance L is $xy \cdot L$, and the count recorded C is equal to the number of particles having their centers within the area $xy \cdot L$ and is

$$C = xy \cdot L \cdot K = LK(l + D - 2nl) \qquad (1)$$

where K is the number of particle centers per unit area. This equation assumes that all particles have the same diameter D, that L is very large, and that $D > l$.

The number of particle centers, N, present in a rectangle of width $(d + l)$ and length L is $LK(d + l)$ (d is the width of the unscanned track between scan tracks), and if the rectangle represents the total area of p pairs of parallel tracks, which together scan the whole specimen area (Figure 5), then

$$N = pLK(d + l) \qquad (2)$$

and the total count recorded by the counter will be

$$C = pLK(l + D - 2nl)$$

Finally, if F is the number of counts recorded per particle present in the scanned area,

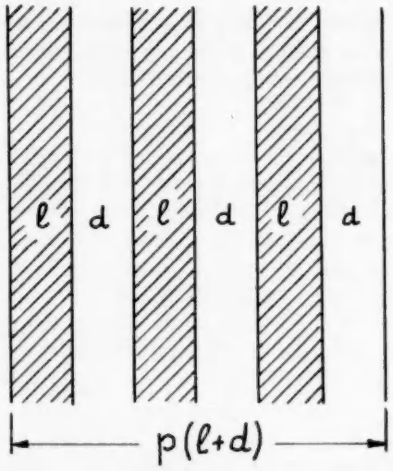

Fig. 5.

$$F = \frac{C}{N} = \frac{pLK(l + D - 2nl)}{pLK(d + l)}$$

or

$$F = \frac{l + D - 2nl}{d + l} \tag{3}$$

A special case of this equation is when $d = 0$, i.e., when successive scan tracks just join at their edges so that the whole area of the field is covered by the scan. Then

$$\frac{C}{N} = 1 + \frac{D}{l} - 2n$$

$$C = N\left[1 + \frac{D}{l} - 2n\right] \tag{4}$$

In this case, if C, the count experimentally recorded, is plotted against n, the number of particles actually present, a straight line is obtained, as shown at ABC in Figure 6. Putting $C = 0$ in Equation 4, the intercept on the n axis is given by $n = \frac{1}{2}\,[1 + (D/l)]$, and putting $n = 0$, the intercept on the C axis is $C = N\,[1 + (D/l)]$. The value of C when $n = 1$ is $C = N\,[(D/l) - 1]$. Since the part AB of the theoretical relation cannot be realized in practice, since n cannot have values > 1, a perpendicular dropped from point B intercepts the C axis at a point distant from C by a distance equal to $2N$. Hence, if a specimen is scanned repeatedly using different values of n, with a slit of constant known length l and $d = 0$, and the experimental count so obtained is plotted against the corresponding n value, then in theory both N, the total number of particles present, and D, their diameter, can be obtained from the resulting figure. This method appears to possess so many advantages over any previously suggested that it was adopted in the present case, and an electronic circuit was designed to enable the plot of C against n to be made conveniently and quickly.

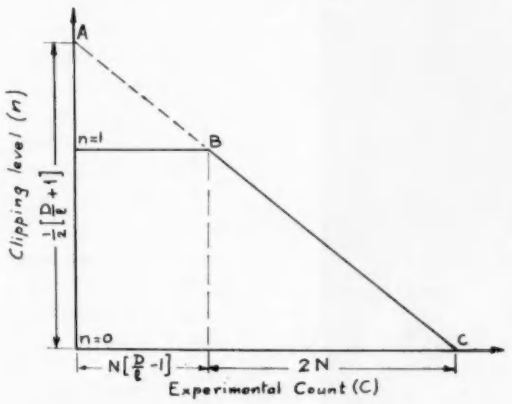

Fig. 6.

The derivation of Equation 4 above assumes that all the particles present are of equal diameter. It is, however, easy to show that for particle arrays having particles of varying diameter, the equation remains valid provided that D is then the number-weighted average particle diameter $\bar{D}$. This result follows from the fact that the particles present may be considered as divided into a number of size groups, the diameter of all particles in any group being the same. Each group of particles will behave in counting as if all the other groups were absent, and the counts obtained from each group are additive to give the total count registered. Thus, Equation 4 for the case of particle arrays of varying particle diameter is

$$C = N\left[1 + \frac{\bar{D}}{l} - 2n\right]$$

and the sole restriction imposed (apart from the two basic assumptions already mentioned) is that the diameter of the smallest particle present must not be less than l, the width of the scan track.

As regards arrays of noncircular particles, D becomes the projected particle diameter, the projection being taken parallel to the direction of scan; and for noncircular particle arrays of varying particle size, $\bar{D}$ is the mean weighted projected diameter of the particles in the scan direction.

II. *Experimental Apparatus for Web Scanning*

(*a*) *Details of construction.* The scanning apparatus designed for the purpose of implementing the foregoing theory is illustrated in Figure 7. The sample to be scanned is contained between two plate-glass disks, 1, 14 in. in diameter, which are clamped together by the milled head 2, and mounted on a vertical spindle. The drive from the geared-down motor 3 *via* the front shaft 4 passes through two pairs of bevel gears 5, giving the specimen disks a constant speed of 0.5 rev./sec. very approximately. The lamphouse 6, condenser 7, and photocell housing 8 are all rigidly attached to a ⊏-shaped bracket, which in turn is fastened to a carriage 9, free to move on slide rails 10, and driven by a leadscrew 11. The latter is rotated by a chain and sprocket drive 12 from the end of the front shaft. The leadscrew drive consists of a spring-loaded split nut,

which enabled the carriage to be disengaged from the leadscrew and returned to its starting position at will. Normally, the ratio of the sprocket and chain drive is such that the scanning carriage moves inward by 1/20 in./rev. of the specimen disks, so that the specimen is scanned at 20 lines to the inch, the length of the scanning spot at right angles to the direction of scan, in the specimen plane being 1/20 in. ($d = 0$).

The driving motor is controlled by a switch 13 and a carriage-operated microswitch 14, connected in series. When the carriage reaches the inner end of the scanning run, it operates the latter and stops the motor, so that overrunning is impossible. Similarly, the light source is switched by a mercury-break relay 15 operated from a cam 16 on the carriage. The lamp is switched on only after the scanning head has traveled in far enough for the optical axis to be inside the periphery of the disks, so that no false counts can be registered as the disk edges intercept the light beam. When the scanning head is returned to its extreme outward position, the lamp is automatically extinguished.

The optical system is shown in Figure 8. The light source, a 10-volt, 7.5-amp. projector lamp, is contained in a ventilated lamp house, into the side of which is inserted a sliding tube containing a finely ground diffusing screen and a metal diaphragm pierced in its center by an accurately cut rectangular aperture. An image of this aperture is focussed in the plane of the specimen by a microscope substage

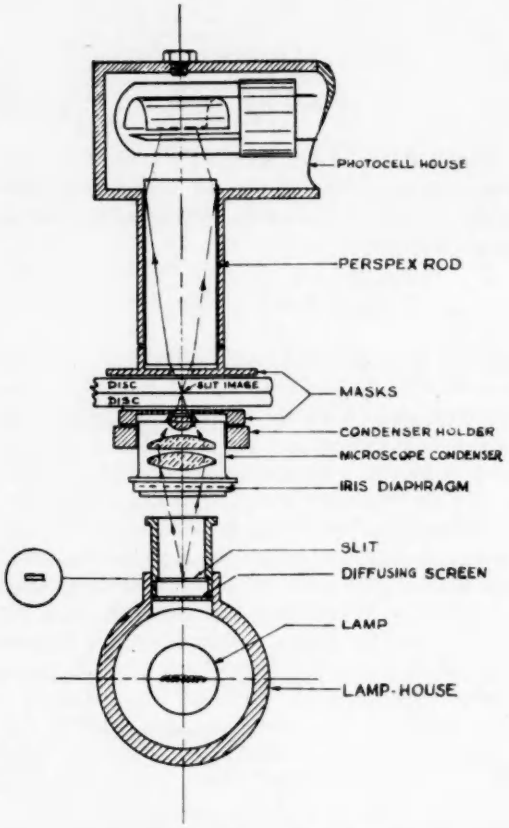

Fig. 8. Diagram of optical system.

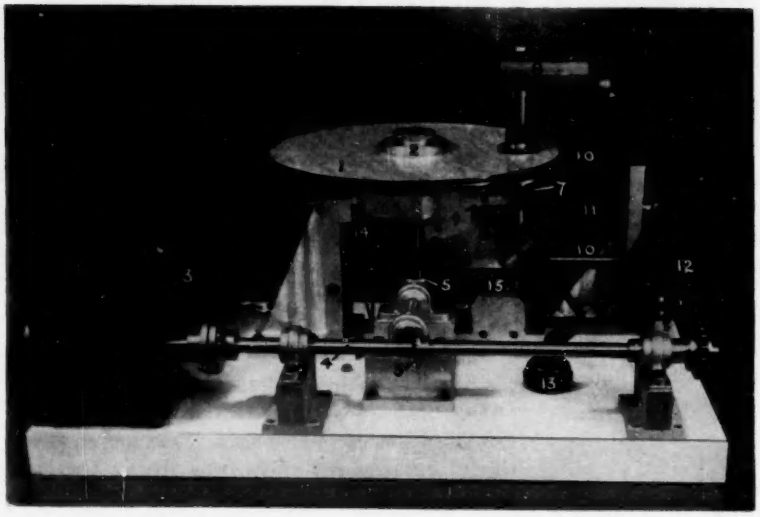

Fig. 7. Photograph of electronic scanning apparatus for counting neps.

condenser; the lamphouse, slit, and condenser are all relatively adjustable so that this slit image can be made to have the exact dimensions required. After passing through the specimen, the light is received on the end of a short length of Perspex rod, acting as a light guide, and delivering the transmitted light direct to the cathode of the photocell, a cesium–silver oxide vacuum-type emission cell mounted in a light-tight housing as shown. Masks of blackened metal are arranged to exclude stray daylight from the system, though total exclusion is not essential, as the photocell amplifier is resistance-capacity coupled and thus does not transmit any steady component of the photocell output due to stray daylight, but only the pulse components due to interception of the scanning beam by a particle. The lamp is normally supplied from a large 6-volt accumulator, thus being underrun by 4 volts, which prolongs its life and minimizes the internal blackening to which high-power projector lamps are prone.

In setting up the optical system to give the correct size of scanning spot, the following procedure was adopted:

(i) The photocell housing was removed, and a low-power microscope, fixed in position relative to the scanning disks, was substituted for it. The microscope carried a cross hair in the eyepiece.

(ii) A few fibers were placed between the scanning discs to define the specimen plane, and the microscope focussed on them. It was thereafter not altered as to focus.

(iii) The substage condenser was adjusted as to height to bring the slit image into focus in the microscope, i.e., in the specimen plane.

(iv) One end of the slit image was brought on to the cross hair of the microscope by rotating the scanning disks with the leadscrew nut engaged; and then the disks were given one complete revolution from this position. If the image is the right length, this should displace it by exactly its own length, thus bringing the other end into coincidence with the cross hair.

(v) If the image length was incorrect, the lamphouse was moved slightly in the appropriate direction, and the whole of the foregoing procedure repeated, until the correct adjustment was found, after which all adjustments were locked, the microscope removed, and the photocell and its housing replaced.

(*b*) *The electronic clipper and counter circuits.* The diagram of the electronic circuit used with the foregoing scanner, together with details of its operation may be obtained by writing to the authors.

(*c*) *Performance of the apparatus with "ideal" samples.* The performance of the completed apparatus, as regards agreement with the mathematical theory given previously, was checked by employing it to count and size a series of "ideal" particle populations, consisting of a number of small round disks punched from black paper and distributed at random between the plate glass scanning disks. In this way the assumptions made in the theoretical argument are very closely fulfilled, and results in reasonable agreement with theory may be expected.

The procedure adopted was as follows: The sample disks having been arranged between the scanning plates, the clipping level dial was set at $n = 1$ and a dummy run carried out, the gain of the amplifier being adjusted during this run so that the counter just failed to register any counts. In practice it was safer to set the gain so that at $n = 1$ a very few (< 5) counts were registered during the complete scan. This ensured the correct setting of the clipping level. The sample was then scanned repeatedly, using successively smaller values of n, and the resulting relation between counts registered and n value was plotted. Figure 9 shows a typical plot, the circles representing the experimental points, while the thick line shows the expected relation between counts and n value for this sample (30 disks of diameter 0.104 in.). There is some undercounting at n values just below $n = 1$, resulting in a rounding-off of the sharp corner of the theoretical curve. Hawksley [6], Cook-Yarborough [2] and

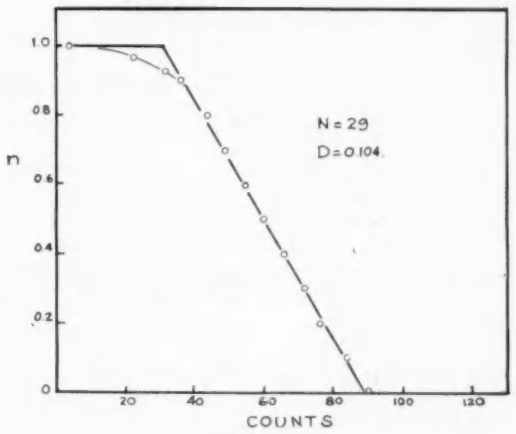

Fig. 9.

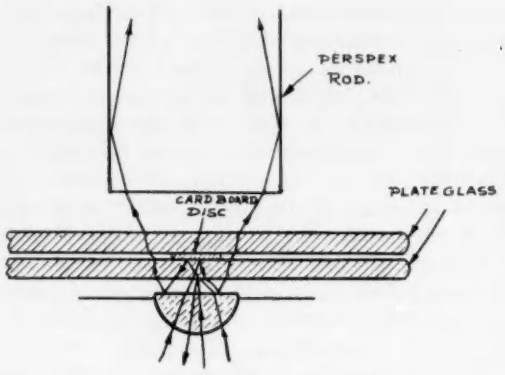

Fig. 10.

others have noted similar undercounting under comparable circumstances and have not been able to offer a fully satisfactory explanation. It is believed that it is mainly due, in the present case at least, to diffuse reflection of light from the back of the intercepting particle (see Figure 10). When the particle intercepts the light beam in the sample plane, a certain amount of light is reflected from the back surface, and reflected upward again from the upper and lower surfaces of the lower scanning disk and from the top lens of the condenser. Some of this light is thus passed around the edge of the particle and ultimately finds its way to the photocell cathode. Seen from above, the particle is surrounded by a slight but definite halo, which varies in intensity to some extent according as the particle intercepts the light spot symmetrically or slightly off center. This halo has the effect of making the height of the maximum amplitude pulses, corresponding to complete cut-off, somewhat irregular, and so spreads the maximum amplitude group out somewhat, resulting in the dispersion noticeable on the experimental plot. The effect is of no significance, however, as the particle number is obtained direct from the gradient of the sloping part of the experimental curve, and this can be accurately determined in spite of the rounding of the corner. Table I shows the results obtained in four such check experiments on different particle populations.

From the results it is apparent that the apparatus set up gives results closely in accordance with theory, and enables mixed populations of circular opaque particles to be counted and sized with an error not exceeding $\pm 3\%$. Errors of this order would be quite without significance in nep counting, and therefore the apparatus was considered to have fulfilled design requirements satisfactorily, showing behavior sufficiently close to theoretical for all practical requirements.

III. *Additional Factors Influencing the Counting of Neps in Actual Web Samples*

When scanning actual webs as opposed to the "ideal" samples so far considered, two problems immediately arise, connected with the intrinsic properties of this type of material. These are

(*a*) The presence of a variable background to the actual "particles" or neps.

(*b*) The variation in the opacity or optical density of the neps themselves.

They will be considered in turn.

(*a*) *The problem of background fluctuation.* The background of the "ideal" samples consisted simply

TABLE I. Counting and Sizing Experiments on "Ideal" Samples *

Details of actual array			Experimental results obtained			
					% error of	
No. and size of particles	N	$\bar{D}$ (in.)	N	$\bar{D}$	N	$\bar{D}$
90 of diam. 0.1 in.	90	0.1	87.5	0.10	−2.78	0
30 of diam. 0.1 in.	30	0.1	29.5	0.100[2]	−1.6	+0.2
30 of diam. 0.1 in. 30 of diam. 0.1275 in.	60	0.113[7]	61.2	0.110[8]	+2.0	−2.5
10 of diam. 0.084 in. 10 of diam. 0.10 in. 10 of diam. 0.1275 in.	30	0.104	29.1	0.104[8]	−3.0	−0.8

* Each experimental value is the mean of five determinations.

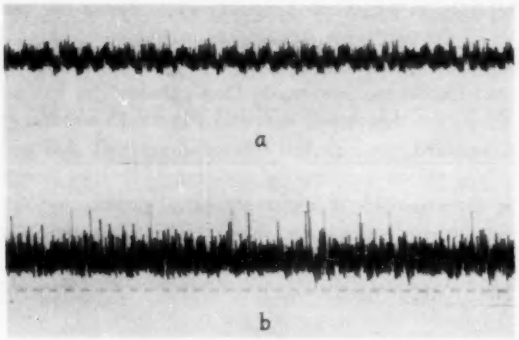

Fig. 11.

of transparent glass, and the photocell output obtained when scanning such a background, if particles are absent, is zero as far as any A.C. component is concerned. In an actual web, the particles to be counted are distributed on a background of randomly arranged fibers, and this background has great irregularity in a short-term sense (i.e., over areas comparable with the dimensions of the scanning beam), though the mean fiber weight per unit area may be reasonably constant when measured over larger areas. As a result, the photocell output when scanning the background of such a web is not zero, but fluctuates with the short-term irregularity. Figure 11 shows two actual records of photocell output from wool web specimens, obtained by means of a cathode ray oscillograph from the photocell amplifier, the clipper being bypassed. A moving-film camera was used to obtain the records. The pulses due to the presence of neps can be clearly seen standing above the general background irregularity, particularly in the lower record, which was taken from a very neppy sample. The presence of this background prevents the use of any value of n (clipping level) less than that corresponding to complete removal of the background. If n is reduced below a certain value, which varies from sample to sample, the extreme peaks of the background variation are not clipped out, and the background begins to give a count of its own which very rapidly increases as n is further decreased. Naturally, small pulses due to edge interceptions by neps themselves are merged in the background and lost; in fact the only part of the counts $-$ n value curve which can be obtained is that corresponding to values of n greater than peak background level.

(*b*) *The problem of variable nep density.* A second effect which greatly influences results when scanning actual web samples, is that due to the varying optical density of the neps, both from one individual to another, and also at different points in the same nep. In the "ideal" samples, the cross section of the particles was as shown in Figure 12, *a* of uniform thickness and with vertical edges giving a practically instantaneous transformation from transparency to complete opacity, the latter being uniformly maintained over the whole area of the particle. The cross section of a nep in a carded web, however, is much more like Figure 12, *b* or *c*. It is approximately biconvex in section, with the result that the opacity increases from the edge to the center and then decreases again to the edge as the scanning spot traverses it. This would be the case even in a "good" (i.e., well-formed and approximately circular) nep. Many neps, in wool webs at least, are more complex than this, only approximately circular, and of irregular thickness, as shown in Figure 12, *c*.

The effect of the variation in optical density of the particles on the shape of n value-counts curve

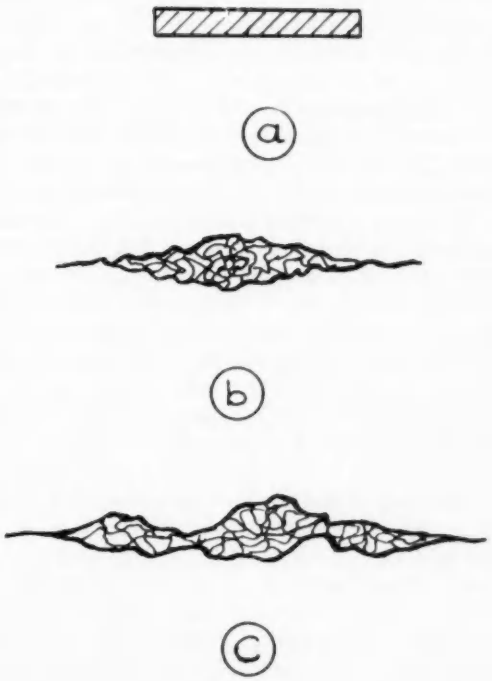

Fig. 12.

may be examined as follows: The particles present may be divided inot a series of groups, all individuals within a group having the same optical density, which differs from group to group. Each group will follow Equation 4 after correction for nep optical density: the corrected equation is

$$C = N\left[1 + \frac{D}{l} - 2n\right]\left[1 - \frac{\rho_g}{\rho_n}\right]$$

where ρn is the optical density of the nep, and ρg that of the uniform background. When the particle is completely opaque

$$\frac{\rho_g}{\rho_n} = 0 \qquad \text{and} \qquad \left[1 - \frac{\rho_g}{\rho_n}\right] = 1$$

When

$$\rho_n = \rho_g, \qquad \left[1 - \frac{\rho_g}{\rho_n}\right] = 0.$$

When several such groups are scanned as one population, the maximum clipping level (i.e., the level at which the pulse of greatest amplitude is just clipped out) is proportional to the particle density, because the height of the pulse caused by a particle which completely obstructs the scanning beam is proportional to the amount of light cut off, i.e., to the optical density of the particle. Figure 13 *A, B,* and *C* shows the *n* value-counts curves for three groups of particles superimposed, each group having the same number of particles of the same mean diameter, but with different optical densities for each group, the latter increasing from *A* to *C*. When such an array of particles is scanned as one population, the *n* value-counts curve of the total array will be as shown by the full line in Figure 14. In actual webs, the nep density will vary continuously rather than in finite groups, and the resulting *n*-value-counts relation becomes a smooth curve concave upward, as shown by dotted line in Figure 14. Such a curve cannot be conveniently analyzed by the mathematical theory already developed, especially when a background is present.

The effect of the biconvex section of the neps on the *n*-value-counts curve, in an ideal case in which the neps are of constant optical density at their centers, is shown in Figure 15, *a*. The theoretical relation for neps or particles of rectangular cross section and constant optical density is shown by the heavy line. With biconvex neps, pulses of maximum amplitude will be obtained only from interceptions in which the scanning spot crosses the center of the nep symmetrically, as in Figure 15, *b*. All other complete interceptions will give pulses of less than maximum amplitude, thus causing the flat top *AB* of the theoretical curve in Figure 15, *a* to slope downward. All partial interceptions will also give pulses whose amplitudes are less than they would be for a particle of constant optical density, so that the curve assumes the shape *ABC* (thin line) of Figure 15, *a*.

IV. *Experimental Counts on Web Samples*

(*a*) *The background effect.* The general nature of the effect of the background was investigated by superimposing a uniform nep-free rayon web on an

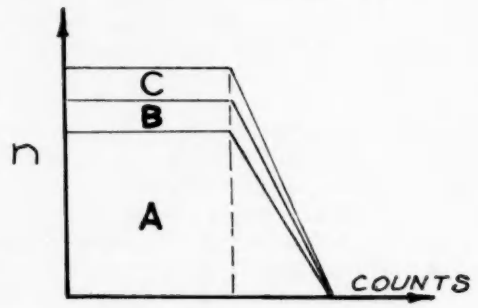

Fig. 13.

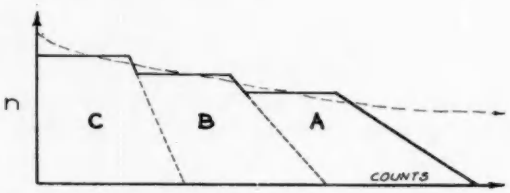

Fig. 14.

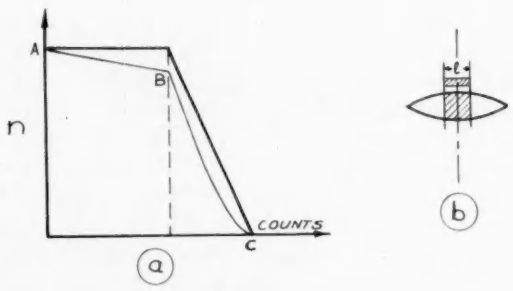

Fig. 15.

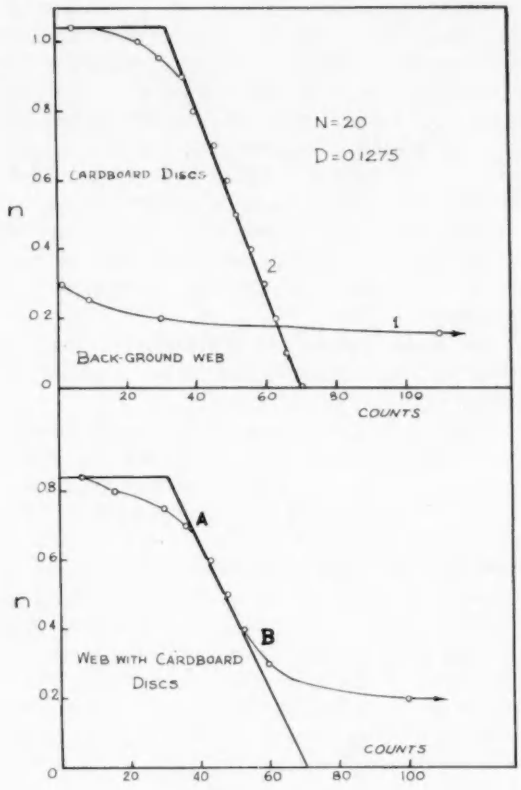

Figs. 16 and 17.

"ideal" sample of black paper disks, such as has already been described. The web itself was scanned separately (curve 1, Figure 16), the disks also separately (curve 2, Figure 16), and then the disks were superimposed on the web and the two were scanned together, the gain of the scanning amplifier remaining constant throughout. The curve then obtained is shown in Figure 17. It is at once obvious that, whereas with the disks alone the clipping level necessary to clip out the maximum pulse was $n = 1.05$, the presence of the background in Figure 17 so reduces the contrast between particle and background, and consequently the height of the maximum pulse, that the latter is clipped out at $n = 0.85$. As a result, the length of the straight part of the curve AB (Figure 17) is so reduced as to be insufficient to allow a reliable value of slope to be obtained from it. (The slope drawn in Figure 17 is that calculated from the known number of particles present.) If this is so in the case of black paper disks on a web background, it will be even more the case for actual neps, since then, as explained above, the straight part AB will hardly exist at all, being replaced by a smooth curve concave upward in the general case; though possibly some uniform webs with very clearly defined neps might give curves somewhat similar to Figure 17.

(*b*) *The evaluation of counts curves from actual webs.* It becomes plain from the foregoing, that although the mathematical theory of particle scanning developed earlier provides an excellent basis for the counting of solid particles on a uniform background, where the contrast is reasonably good, it is not in itself of much assistance in the assessment by scanning methods of particles of varying optical density superimposed on a background which is itself subject to random fluctuations in density. This fact admitted, the conclusion is not thereby rendered inevitable, that scanning methods are of no use in assessing the nep content of carded webs. It certainly means that they are incapable of measuring the precise number and mean diameter of the neps, as can be done for more ideal samples. Nevertheless, the n-value-counts curve does contain, in its shape and disposition, the essential information regarding both the background (small-pulse irregularity) and the nep content (high-pulse irregularity) of the sample. It is necessary to find a means of extracting the required information from the experimental curve obtained by scanning the web. The information, or parameter, so extracted will not be the actual number of neps present, but will represent that part of the irregularity of the sample which is due to the presence in it of discrete neps, as opposed to that part of the irregularity which is due to the presence of a randomly fluctuating background. Such a value should be closely related to, if not actually proportional to, the total number of neps present.

Figure 18 shows an actual n-value-counts curve for a wool web. Now, it is known that the area below the line ABC depends almost entirely on the fluctuations of the background, which is of no interest or importance from the point of view of the number of neps present. The latter influences far more the area BCD; i.e., it is the shape of the curve between B and D which is most affected by the presence or absence of neps in the sample. The full line DB, for example, would correspond to a fairly neppy web, while the dotted line DB would correspond to

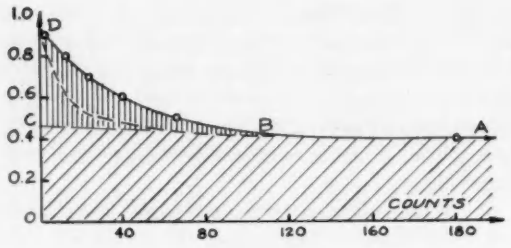

Fig. 18.

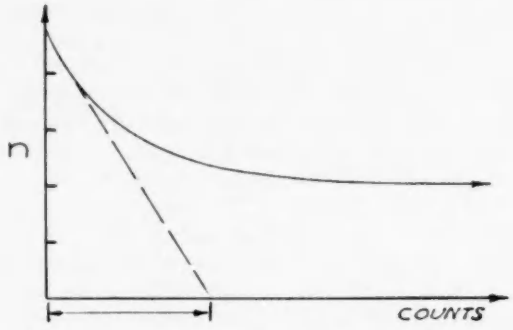

Fig. 19.

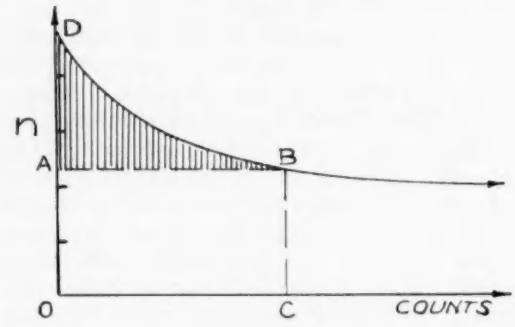

Fig. 20.

a much less neppy sample, that is, to one in which the number of pulses counted at n values sufficiently high to cut out the background (these being the pulses due to neps), is much less than in the former case. The parameter sought, therefore, must be one which varies with the shape of the curve in the region BD.

Two parameters of this sort were investigated, using n-value-counts curves obtained from a series of 34 wool webs of varying nep content. The first (Figure 19) was obtained by drawing a tangent to the experimental curve at the point $C = 0$, producing this tangent to cut the C axis, and measuring the intercept on the latter. Obviously, the steeper the experimental curve at high values of n (i.e., the smaller the nep content of the sample), the less this intercept will be. This may be termed the tangent-intercept parameter. It suffers from one drawback, namely, that it does not take sufficient account of the less dense neps, which give pulses somewhat shorter than the maximum, and is primarily an indication of the number of the denser neps present in the sample.

The second parameter had reference to the area under the upper part of the curve, as shown in Figure 20.

This area must be chosen to be as free as possible from the effects of the background count, yet include as much information about the nep population present as possible. In effect, the level AB (Figure 20) above which the area is evaluated will be a compromise, and one which will need to be experimentally arrived at. The parameter was therefore defined by selecting some arbitrary value of C, and measuring the area lying between the experimental curve and the abscissa of this value of C, i.e., the area ABD in Figure 20. This may be termed the area parameter. Obviously, for any given specimen area ABD can have a wide range of values depending on the choice of C, and is not a unique parameter solely determined by the shape of the experimental curve, as is the tangent-intercept value. Nevertheless, by calculating the area parameters corresponding to a range of C values, for a number of different web samples, and correlating the different values of area parameter so obtained with visual nep counts, the best compromise value of C can be determined.

These two parameters were investigated by scanning a series of wool web specimens, carded from 64's botany wool on a medium card at 28 lb./hr. Each specimen was scanned, as already described, at a number of different n values, and the experimental n-value-counts curve was then drawn. Tangent-intercept and area parameters were obtained from each curve, the latter for a range of C values in each case, and also the number of neps present in the sample scanned was visually estimated in each case, the area of the samples being approximately 140 sq. in. A summary of the results so obtained is given in Table II, together with values of the web weight per unit area.

TABLE II. Tangent-Intercept and Area Parameters for a Range of Webs

Sample No.	Visual nep count	Area parameter for various values of C					Tangent intercept parameter	Web weight (g./sq. m.)
		$C=50$	$C=75$	$C=100$	$C=125$	$C=150$		
1	4	4.0	5.25	5.75	6.40	7.70	10	5.5
2	4	4.99	6.55	7.20	9.25	10.81	11	6.6
3	5	5.05	6.06	6.46	7.66	9.00	13	5.0
4	8	5.30	6.40	7.74	7.50	8.50	30	5.6
5	8	5.08	7.66	10.09	11.30	12.50	37	6.8
6	9	5.47	6.78	8.32	9.30	10.51	16	6.3
7	10	7.33	8.40	9.10	9.98	11.68	32	5.1
8	11	5.99	6.90	7.55	10.08	11.13	33	7.5
9	11	6.33	6.96	7.82	9.68	11.08	18	6.2
10	12	6.65	8.26	10.50	11.20	12.40	31	6.7
11	12	6.36	8.19	9.99	11.15	13.80	48	6.7
12	13	6.10	8.05	10.73	12.98	15.75	40	6.7
13	13	6.14	7.86	11.03	14.85	16.06	61	8.0
14	14	7.37	9.80	11.46	15.50	16.14	62	4.5
15	15	9.74	10.50	11.60	13.22	15.15	37	5.0
16	15	6.86	9.67	10.74	12.07	13.20	46	5.5
17	16	9.03	11.70	15.30	16.14	17.26	57	6.7
18	18	9.75	12.38	14.00	14.90	15.48	56	5.2
19	20	11.10	13.12	14.05	14.90	15.48	56	5.2
20	22	10.75	13.47	15.50	17.22	18.30	78	7.4
21	22	7.44	8.48	10.90	13.58	14.90	27	6.4
22	24	6.85	10.29	13.79	15.99	17.45	46	6.8
23	26	10.68	13.47	15.02	18.05	20.55	58	6.8
24	26	9.46	12.80	15.50	17.17	18.20	53	8.0
25	27	13.80	17.27	20.48	21.50	22.55	79	6.3
26	28	10.92	10.92	14.85	17.46	21.36	99	4.6
27	30	11.93	17.32	18.03	19.20	20.35	82	5.5
28	33	10.15	13.30	20.05	16.57	18.50	117	6.3
29	33	10.93	17.90	14.95	22.40	23.55	55	7.5
30	36	11.75	20.33	22.80	24.44	25.40	103	8.0
31	39	11.29	16.14	19.30	21.00	23.22	88	6.5
32	44	8.85	15.12	20.35	24.44	26.45	61	7.6
33	44	9.40	16.52	20.80	23.20	25.15	141	6.3
34	52	8.80	16.02	22.60	26.30	29.80	119	8.1

Correlation coefficients were obtained by the product moment method [4] for each of the parameters so obtained against visual nep count, with the results shown in Table III.

The correlation coefficients for the area parameter are shown, plotted against the C value for which they are derived in Figure 21. The derivative value of C which gives the area parameter most closely correlated with visual nep count is $C = 100$, but the correlation coefficient is high and fairly constant for all values of C between about 100 and 150. This procedure may therefore be considered as not unsatisfactory, in that it gives a parameter, derived from the experimental scanning data, and correlated with the actual visual nep count by the very good correlation coefficient of 0.962, if the value of C chosen for evaluating the parameter is 100 in all cases.

TABLE III. Correlation Coefficients of Area and Tangent-Intercept Parameters against Visual Nep Count

Parameter	Correlation coefficient
Tangent-intercept	0.809
Area, for $C=$ 50	0.733
75	0.880
100	0.962
125	0.938
150	0.923

The correlation of the tangent-intercept parameter with visual count is not so good as that of the area parameter (0.809). This is in line with the criticism already recorded of this parameter, namely that it largely ignores the less dense neps in the sample.

The webs used in the foregoing tests were of fairly low weight per unit area, and the neps present were well formed and in good contrast with the background. It was felt that further tests should be made on a less uniform and heavier set of web samples, in which greater variation in the size and quality of the neps, as well as in the uniformity of the web itself, might be found. Accordingly, a fresh set of 40 samples was prepared using a heavier rate of production on the card (38 lb./hr. as against 28 lb./hr. in the previous series). The card actually used was only half the standard width in both cases, i.e., 30 in., but the rates of production given are for a standard 60-in. card. These webs were scanned as before, and the area parameter for a value of $C = 100$ was obtained in each case, and correlated as before against visual nep count. The results are given in Table IV.

The correlation coefficient between visual nep count and area parameter is very much lower in this series of tests than in the previous set, and the difference must apparently be attributed to the nature of the web samples themselves. In the second series, the webs being produced at a greater rate than in the first, the background was both more dense and more irregular, resulting in less contrast between

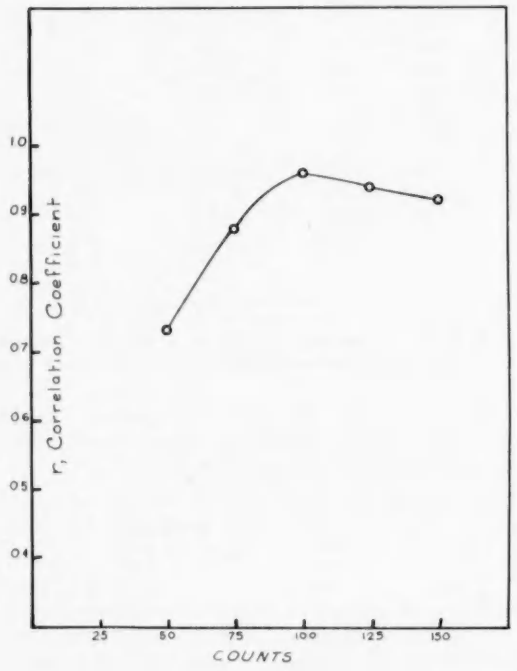

Fig. 21.

TABLE IV. Area Parameter and Visual Nep Count for Variable Series of Webs

Sample No.	Visual nep count	Area parameter for $C = 100$	Web wt. (g./sq. m.)
1	6	10.21	9.0
2	7	9.58	9.5
3	10	10.52	7.5
4	12	15.35	8.7
5	12	11.46	9.3
6	12	8.63	9.0
7	13	13.36	9.8
8	13	14.77	11.3
9	13	12.63	8.0
10	14	12.69	9.5
11	15	12.54	10.4
12	16	11.50	8.7
13	17	11.47	8.9
14	17	10.38	11.5
15	18	13.38	9.0
16	18	11.51	8.3
17	18	10.69	8.7
18	18	12.55	14.0
19	18	13.38	9.5
20	19	13.13	8.4
21	20	13.65	7.7
22	21	12.30	12.4
23	21	11.45	9.8
24	21	9.90	9.3
25	22	13.48	9.2
26	22	14.15	7.8
27	22	13.40	11.7
28	23	13.51	10.3
29	23	11.79	9.3
30	23	13.85	11.5
31	26	13.85	9.0
32	27	13.65	12.7
33	28	15.24	14.0
34	28	14.87	14.0
35	29	13.75	10.3
36	29	14.58	11.0
37	30	13.26	11.0
38	31	16.58	8.7
39	31	15.66	10.7
40	37	12.52	11.5

Coefficient of correlation between visual count and area parameter = 0.56.

neps and background. This, allied to the fact that the size, shape, and average density of the neps were all considerably more variable in the second case, not only made the visual count much more uncertain, but also produced the equivalent electrical effect in the scanner; i.e., it tended to blend the nep pulses with the background pulses, so that the area parameter was invaded, as it were, by the background, and so was less characteristic of the nep population than in the previous set of results. This point may be better appreciated by considering the regression lines of the area parameter on visual nep count in the two cases. Linear regression equations were obtained by the method of least squares in both cases, with the following results.

$$\textit{First Set:} \quad A_{100} = 5.69 + 0.370N$$
$$\textit{Second Set:} \quad A_{100} = 9.97 + 0.139N$$

A_{100} being the area parameter for $C = 100$, and N the visual nep count in both cases. On comparing these equations, it is at once obvious that the contribution of the nep pulses to the area parameter has decreased (smaller coefficient of N) and the effect of the background has increased (larger constant) in the second case as compared with the first.

Final Conclusions

The correlation coefficient of 0.56 is statistically significant at the 95% level, but for practical nep counting it is too low. It is a little difficult to form a critical judgment as to the accuracy and usefulness of this set of results. The correlation coefficient only shows the extent to which the visual nep count and the area parameter obtained from the scanner are related; it does not necessarily indicate the value of the latter as a measure of neppiness, unless it can be assumed that the former is in fact an accurate index of the nep content of the samples tested. Much experience has shown, however, that visual nep counts are, on the whole, unreliable as a means of determining neppiness; reproducibility of count between different observers is not generally very good, and even one observer tends to vary in his standards over a period of time. Thus, it is possible that the low correlation coefficient obtained in the second set of tests reflects, not so much unreliability of the scanning apparatus, as errors in the visual counts against which the scanning data have been compared. This is the more likely, because this set of web samples were, as already stated, of the type in which visual counting is at its most difficult. It has been shown that, using samples in which visual counting can be carried out with fair accuracy, the scanning results correlate closely with the visual count. There seems therefore to be no more *a priori* reason to suppose that the performance of the machine should show a sudden deterioration when the character of the web samples is altered, than that the deterioration should equally have occurred in the accuracy of the visual counts obtained from the samples; and in favor of the scanning data there is this to be said, that they at least remain purely objective, whereas an increasingly large element of subjectivity enters into the visual method as the quality of the webs deteriorates.

A further point bearing on the matter is that in visual counting, no account is taken of nep size; a nep is counted as one individual irrespective of whether it is large or small. In scanning, however, it is plain that a large nep will give more full-amplitude pulses than a small one, and will consequently contribute more to the area parameter obtained from the scanning curve. As a result, the area parameter tends to be a function both of nep size and nep number, i.e., $A = f\ (N,\overline{D})$ whereas the visual count depends on N only. In the same way, visual counting takes no account of nep density, whereas the latter will to some extent influence the area parameter, though not to the same extent as nep diameter. This means that for web samples in which the neps are large and irregular, the area parameter will tend to overemphasize the neppiness, if the latter is to be judged on nep number only.

It is, however, questionable whether or not in practice the "neppiness" of a web ought in fact to be judged on nep number only; in the past it has been so judged, mainly because nep number obtained by visual counting was the only readily obtainable value related to nep content. It is at least arguable, however, that the area parameter obtained in the manner indicated is a better index of total neppiness than a visual count based on the number of neps alone, because it is more closely related to the total proportion of the material in the web that has been agglomerated into neps by the carding process. It would seem that this point can hardly be settled without a considerable volume of data, obtained under practical conditions, in which the two measures of neppiness are compared as regards their ultimate correlation with the known effects of neppi-

ness in later processing, such as end breaks in worsted spinning and yarn irregularity in the final product. In this way the relative values of the two methods of estimating neppiness could, and should, be compared.

It would appear that the present apparatus represents almost the practical limit of usefulness of optical scanning methods as applied to nep counting. If the parameter obtained from it in the present work is rejected as an unsatisfactory measure of the nep content, it is difficult to envisage any change of method or principle which could give a satisfactory one, if optical scanning techniques are retained, since the factors involved are fundamental to the character of the samples investigated rather than to the apparatus employed. It should finally be stated, however, that the second set of web samples utilized in the present work, deliberately produced under conditions unrelated to commercial practice, would in general find no counterpart in the ordinary run of mill experience. Normal carded webs, as commercially produced, would approximate much more closely to the first set tested, and in this case the scanning method showed itself to be in fairly close agreement with visual counting data.

Literature Cited

1. Anon. (North Carolina State College), *Textile World* (May 1952).
2. Cooke-Yarborough, E. H., *British J. Appl. Phys.*, Supplement No. 3, S147 (1954).
3. Courshee, R. J.,*British J. Appl. Phys.*, Supplement No. 3, S161 (1954).
4. Fisher, R. A., *Statistical Methods for Research Workers*, 4th ed. 121, Oliver & Boyd (1932).
5. Hawksley, P. G. W., *Nature* **169**, 985 (1952).
6. Hawksley, P. G. W., *British J. Appl. Phys.*, Supplement No. 3, S125 (1954).
7. Helliwell, E. H., and Ball, H. J., *Textile World* **95**, 5,112 (1945).
8. Hoare, E. R., *Nature* **169**, 519 (1952).
9. Institute of Physics Conference on the Physics of Particle Size Analysis, held at Nottingham, England (April 1954).
10. Lagerkrantz, C., *Acta Physiologica Scandinavica, Supplementum* 93, 52 (1952).
11. Meyer, E. W., British Patent Application 25647/51.
12. Roberts, F., and Young, J. Z., *Nature* **166**, 231 (1951).
13. Roberts, F., and Young, J. Z., *Nature* **169**, 963 (1952).
14. Stenersen, R. S., Diploma Thesis, Leeds University (1935).
15. Wolff, H. S., *Nature* **165**, 967 (1950).

Manuscript received January 24, 1956.

Effect of Alkaline Hydrolysis on the Properties of Cyanoethylated Cotton

Laurence W. Mazzeno, Jr., Robert M. Reinhardt, J. David Reid, and John B. Dickson

Southern Regional Research Laboratory,[1] New Orleans, Louisiana

Abstract

Cyanoethylated cotton has been subjected to treatment with excess 1% aqueous sodium hydroxide at temperatures of 22°, 60°, and 97° C. Rates of cleavage of cyanoethyl groups at these temperatures have been determined. Resistance to rotting is destroyed by removal of part of the cyanoethyl groups. Heat resistance is decreased by the alkaline treatment, but only to the extent that nitrogen is removed. It appears that heat resistance is directly proportional to the nitrogen content regardless of the previous history of the sample. Dyeing characteristics, measured by a differential staining technique, show reversion to the color of untreated cotton even though only half the nitrogen is removed.

Physical properties are not adversely affected by alkaline hydrolysis. Tenacity increases as groups are cleaved but does not return to the original value of the gray yarn. This is the usual case with other cellulose derivatives. The knot strength data do not indicate brittleness. Hydrolysis has little effect on elongation.

Introduction

Research on cyanoethylated cotton has been greatly intensified during the past few years in an effort to produce a commercially successful textile product. To date the process has reached the pilot plant stage with production of fiber, yarn, and fabric. It is estimated that by the middle of 1955 at least 14,000 lb. of cotton yarn and 15,000 yd. of fabric had been cyanoethylated and distributed for commercial evaluation. There remain many problems, however, the solution of which would improve the prospects of general commercial acceptance.

In particular, commercial exploitation of chemically modified cotton could be more effectively directed to promising outlets if the properties important for specific end uses were better known. As an example, the rot resistance and heat resistance might be satisfactory for a projected end product, but a greatly reduced value of some other property, functionally important, could prevent success. Again, after a cyanoethylated cotton textile of satisfactory quality has been produced, it is of almost equal importance to avoid any subsequent treatment which might destroy or lower the usefulness of the product. Unless this precaution is taken, inferior products may be offered on the market, or the customer himself, through ignorance, may reduce the value of the goods by damaging treatment. Among the detrimental conditions to which cyanoethylated cotton may be exposed is alkaline hydrolysis.

Scattered investigations of alkaline hydrolysis of cyanoethylated cotton have been reported [6, 9, 16], but the field has not yet been fully explored. Additional knowledge is desired, especially in view of the fact that cotton yarns and fabrics are treated with alkaline solutions of various concentrations and temperatures in many textile finishing processes, as well as in laundering. The present paper, one of a series from this laboratory [6, 12, 17, 18] on the subject of cyanoethylated cotton, describes experiments designed to determine the effect of dilute sodium hydroxide solution at various temperatures on the chemical and physical properties of cyanoethylated cotton.

The reversibility of the cyanoethylation reaction has been studied for simple alcohols [3], polyvinyl alcohol [21], and with cellulose [6, 12, 14]. With dilute alkali, hydrolysis results largely in cleavage

[1] One of the laboratories of the Southern Utilization Research Branch, Agricultural Research Service, United States Department of Agriculture.

of the cyanoethyl group at the ether link. The effect of cleavage of part of the cyanoethyl groups on the properties of the textile has not been previously investigated. By partial hydrolysis of a high nitrogen sample the product can be compared with another unhydrolyzed sample of approximately equal nitrogen content. The hydrolyzed materials will probably be substituted differently, as compared with materials prepared by direct cyanoethylation. It is not within the scope of this paper to determine this variation in constitution, but rather to indicate its probable effect on textile properties since the object is to provide technologically useful information. However, the desirability of quick control tests has been kept in mind, and from the data herein it is possible to suggest a tentative battery of such tests for the important properties determining the usefulness of a cyanoethylated cotton.

With a view to systematic determination of the effect of dilute sodium hydroxide solution on the properties of cyanoethylated cotton, the effect of cleavage has been studied at three temperatures, 22°, 60°, and 97° C. The data thus obtained not only give a qualitative idea of the degradation which may occur during commercial treatments, such as scouring or vat dyeing, but also by suitable mathematical handling permit calculation of the effect of the alkali at other temperatures. An immediate use made of the data was in the calculation of the proper times and temperatures for hydrolysis to obtain the range of nitrogen contents desired in this study. The tests covered not only the usual physical properties such as breaking strength, elongation, knot strength, and twist, but also, and more particularly, the special properties such as change in dyeing characteristics and in rot- and heat-resistance, the latter two of which are considered to be the chief assets of cyanoethylated cotton.

Experimental

Materials and Methods

In all experiments the base material was a raw cotton 12's/5 yarn of the type used for sewing bags. Cyanoethylation of the yarn was carried out at 60 ± 1° C. with a 60% add-on of 2% sodium hydroxide solution with a subsequent immersion in commercial grade acrylonitrile, as described by Daul et al [6]. Differences in degree of substitution were regulated by varying the time of reaction. Uniformity was assured by continuous shaking of the flasks containing the cotton and the acrylonitrile, using a shaking apparatus which held the flasks in a constant-temperature bath. The reaction was stopped by immersing the samples in 5% acetic acid and washing with water. Throughout the preparation of the cyanoethylated samples, the yarn was free to shrink. The yarn treated as above to various nitrogen contents was hydrolyzed with 1% aqueous sodium hydroxide in a constant temperature water bath with continuous agitation. Again the yarn was free of mechanical constraint. The temperature was held constant to ± 1° C. and the time of hydrolysis varied. After hydrolysis the yarn was removed, soured, thoroughly washed in water, and dried. Nitrogen content, carboxyethyl content, physical properties, oven-aging resistance, and soil-burial resistance were determined on the original and the hydrolyzed yarns. Heat resistance tests were carried out at 160 ± 2° C. and 200 ± 3° C. in a mechanical convection oven. Resistance to microbiological attack was determined by burial in soil beds prepared in accordance with ASTM specifications [1]. Textile testing was carried out under standard conditions, of 70° F. and 65% relative humidity, using methods of the ASTM and Federal Specifications [7]. Tenacity was computed on the basis of the cotton count of the yarns actually broken. The two parts of the broken yarns were cut off at the jaws and accurately weighed. Gauge length before breaking was 10 in., and from length and weight the reciprocal linear density in units of cotton count was computed. Tenacity (defined as breaking load per unit linear density) is expressed as breaking load in pounds multiplied by the cotton count; the usual term for tenacity in units of this kind is "count-strength product" or "yarn break factor." The knot break factor was computed similarly, employing, however, cotton count already determined.

Treatment of Data

The resistance of textile products to deterioration, as in oven aging, is measured by the rate of change of some property, usually strength. Rate constants are a logical quantitative expression of such resistance. Empirical equations for this purpose are applied to the hydrolysis of cyanoethylated cotton. Equations for handling other physical and chemical properties of textiles in a similar manner are found in the literature [4, 11, 13, 15, 19, 20]. The equations applied which define physical rate constants,

will be recognized as mathematically the same as for a first-order chemical reaction. This is only coincidence, however. There is an obvious reason for precluding assumption of a first-order reaction: while the loss of nitrogen for any given sample is an exponential function, the half-life for this reaction is dependent on the original nitrogen content. However, as an approximation which is useful in practical applications the data will be treated as if complying with first-order reaction requirements.

The basis of the mathematics consists in two empirical facts. (1) Fraction of strength remaining (S/S_o) and fraction of nitrogen remaining (N/N_o) plot against time as straight lines on semilog paper, with strength or nitrogen on the log scale and time on the arithmetic scale. The slope of this line provides the rate constant. (2) Logarithms of the rate constants corresponding to different temperatures plot as straight lines against the reciprocal of the absolute temperature. Values of k used throughout the paper are calculated by regression methods rather than read directly from the plots.

The use of rate constants and temperature coefficients affords the maximum information with a minimum expenditure of effort and cost when oven-aging experiments are so planned. The result is to permit estimation of strength remaining at any given time and temperature. The usual procedure has been to conduct one series of oven-aging tests at constant temperature and variable time and another at constant time and variable temperature. A more useful procedure is to select two temperatures, fairly well apart from a rate standpoint, and two ranges of time each of which is sufficiently long at least to halve the strength: the object is, of course, to secure enough spread in temperature and time to ensure reasonably accurate results. The data then permit computation of the values of A and B in the temperature equation

$$\ln k = A + \frac{B}{T}$$

Application of this equation at the two temperatures gives

$$\ln k_2 - \ln k_1 = B\left(\frac{1}{T_2} - \frac{1}{T_1}\right)$$

which may easily be solved for the temperature coefficient B. From this, the value of the constant A is readily determined. The value of k at other temperatures may be read directly on a plot of the two known values of k on a logarithmic scale against the reciprocal of the absolute temperature.

Results and Discussion

A sample of cotton yarn containing 5.7% nitrogen was prepared and the amount of hydrolysis with 1% aqueous sodium hydroxide was determined for times of from 5 to 60 min. at 97° C. Reduction of nitrogen content was due to cleavage and not to conversion to carboxyethyl groups, inasmuch as the increase in carboxyethyl content is only 0.6% (0.02 group per anhydroglucose unit) over the original after the full 60 min. of treatment. The data are given in Table I. In order to obtain samples of varying nitrogen content with a more easily controlled rate of hydrolysis, samples were hydrolyzed at 60° and 22° C. The results are shown in Table II.

TABLE I. Effect of Alkaline* Hydrolysis on Cyanoethylated Cotton Yarn

Time of hydrolysis, Min.	N, %	Carboxyethyl, %	Breaking strength, lb.	Elongation, %	Yarn number	Soil burial: % of original breaking strength retained 1 Wk.	2 Wk.	3 Wk.	Dyeing†: Color expected from N content	Color obtained
0 (original)	5.7	0.5	7.0	17.0	1.75	99	96	97	Purple	Purple
5	2.9	0.5	6.7	12.8	2.18	81	9	0	Bluish purple	Dark green
10	1.4	0.5	7.1	14.1	2.24	14	0	0	Bluish green	Dark green
15	0.8	0.6	7.0	13.2	2.34	0	0	0	Dark green	Green
20	0.5	0.7	6.9	13.7	2.36	0	0	0	Green	Green
30	0.4	0.9	7.1	12.4	2.46	0	0	0	Green	Green
45	0.2	1.0	6.5	12.6	2.35	0	0	0	Green	Green
60	0.2	1.1	7.0	13.4	2.32	0	0	0	Green	Green

* 1% aqueous NaOH used. Temperature 97° C.
† Calco Identification Stain No. 2. Dyeing in 1% solution at boil for 1 min. Untreated blank thread dyed green.

TABLE II. Hydrolysis of Cyanoethylated Yarns with 1% Aqueous NaOH

Temperature 22° C.			Temperature 60° C.		
Time, hr.	% N	% Carboxy-ethyl	Time, hr.	% N	% Carboxy-ethyl
— (original)	4.9	0.4	— (original)	4.9	0.4
8	4.8	0.3	0.5	4.5	0.4
16	4.8	0.4	1	4.4	0.4
32	4.6	0.4	2	3.9	0.4
64	4.3	0.4	4	2.7	0.4
96	4.3	0.4	6	1.8	0.6
120	4.1	0.5	8	1.4	0.8
160	3.6	0.5	16	0.6	1.2
240	3.7	0.6	24	0.4	1.5

A semilog plot, Figure 1, of fraction of nitrogen remaining versus time of hydrolysis gives a straight line for the portion of the curve down to a loss of approximately 80% of the nitrogen. At this point the curve begins to level out; however, the nitrogen content has been reduced so much that the figures are not significant in view of experimental error. It will be noted that N/N_o, the fraction of nitrogen remaining, is used instead of N alone where N is the nitrogen content remaining and N_o is the original nitrogen content. This is done to minimize differences in original nitrogen content of samples, and as will be shown later, the curves on different samples are comparable. The slope of the line is, as usual, the rate constant k.

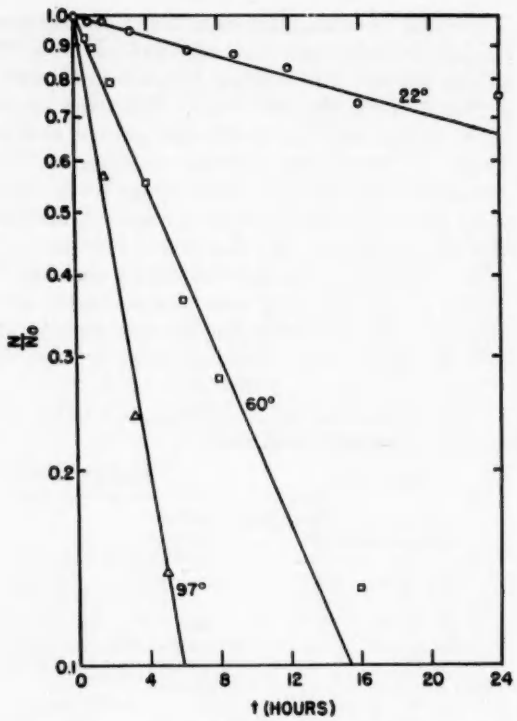

Fig. 1. Fraction of nitrogen remaining after alkaline hydrolysis. Values shown for 22° C. hydrolysis are $t/10$; for 60° C. hydrolysis, t; for 97° C. hydrolysis, $t \times 20$.

As may be seen in Figure 2, there is a linear relationship between ln k and the reciprocal of the absolute temperature. This plot or the equation of the straight line can be used for the calculation of the rate of hydrolysis at other temperatures.

In addition to time and temperature, concentration also can be taken into account quantitatively by using the data in the paper by Fordemwalt and Kourtz [9] to estimate the effect of sodium hydroxide on fraction of nitrogen remaining after hydrolysis. When rate of hydrolysis k is plotted against sodium hydroxide concentration (three concentrations), the points fall roughly on straight lines through the origin. Rate constant is proportional to concentration, and when proportionality factors are plotted on a logarithmic scale against the reciprocal of the absolute temperature (four temperatures), the points fall approximately on a straight line. The proportionality factors at any temperature can be computed from the equation for the straight line, or they can be read off the plot.

The physical properties included in Table I are not adversely affected. Breaking strength remains constant while elongation decreases in the first five minutes and remains constant throughout the remaining reaction time. Loss in weight is, of course, reflected in the yarn number.

Although these physical properties have not been much affected by hydrolytic cleavage, the rot resistance is seriously impaired and the dyeing characteristics are altered drastically. As may be noted from the table, the cyanoethylated cotton no longer follows the expected pattern of dyeing with Calco Identification Stain No. 2 [2] after hydrolysis has taken place. The sample containing 2.9% nitrogen, which would dye purple if cyanoethylated to this content directly, now displays an affinity for the green dye with the same shade as an unhydrolyzed sample of 0.8% nitrogen.

Rot Resistance

Rot resistance is greatly affected by hydrolysis. Even as short a reaction time as 5 min., under the conditions used, which produced a sample with 2.9% nitrogen, is sufficient to destroy the rot resistance of the sample. Complete loss of breaking strength occurs in less than two weeks' burial. Normally a sample of this yarn with a nitrogen content of 2.8% retains 100% of its breaking strength after 6 weeks' soil burial and approximately 70% after 22 weeks [12]. Soil burial of a series of cyanoethylated samples (2 to 7% nitrogen), which had been cleaved to approximately half their nitrogen content and to essentially no nitrogen content also showed complete loss of rot resistance. This same phenomenon of loss of rot resistance has been observed on the partial saponification of acetylated cotton [10]. It is believed that the partial hydrolysis removes the more accessible substituents first, which in turn leaves these more accessible regions unprotected against microbiological attack.

The change in dye shade with change in rot resistance suggests the possibility of use of this technique as a rapid test for soil burial resistance. However, while our results show correlation between differential staining and rot resistance, the data are too meager to permit a definite conclusion. Buras et al [5] found the same kind of relation between rot resistance and dyeing for acetylated cotton with a combination of two dyes. With respect to control testing, this is an important possibility, since soil burial tests are prohibitively long.

[2] The mention of trade names and firms does not imply their endorsement by the Department of Agriculture over similar products or firms not mentioned.

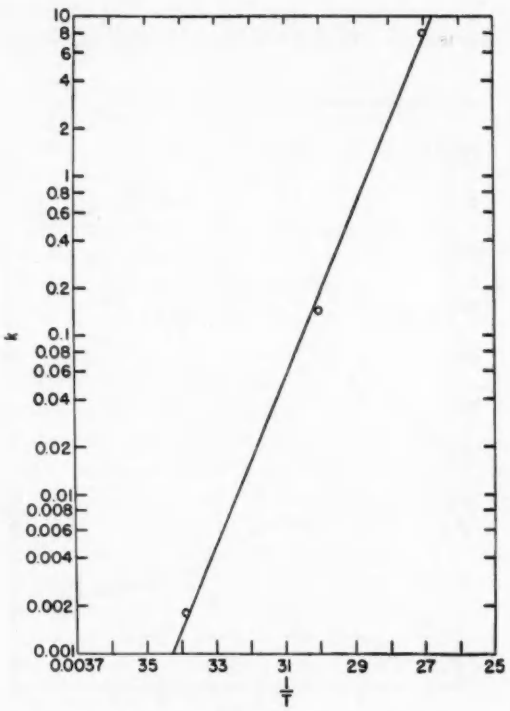

Fig. 2. Effect of temperature on the rate of hydrolysis of cyanoethylated cotton with 1% aqueous NaOH.

Heat Resistance

Since heat resistance is one of the outstandingly improved properties of cyanoethylated cotton, the effect of hydrolysis on this property is important. The series of hydrolyzed samples with various nitrogen contents was selected as before and subjected to oven aging for varying lengths of time at 160° and 200° C. The former is the usual temperature employed for this type of test. It was hoped that the higher temperature would give results comparable with the 160° C. tests, but more rapidly, and thus considerably reduce the time of a laboratory control test.

It is apparent from Figures 3 and 4 that the phenomenon of oven aging is different from that of rot resistance. The evidence is that resistance to heat is uniquely a function of the nitrogen content regardless of the previous history of the sample. As may be seen from the figure, all of the points are

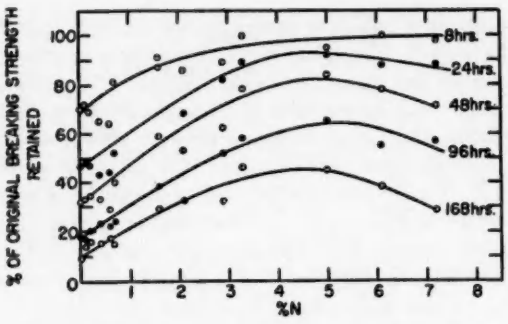

Fig. 3. Oven-aging of cyanoethylated cotton (and hydrolyzed cyanoethylated cotton) at 160° C.

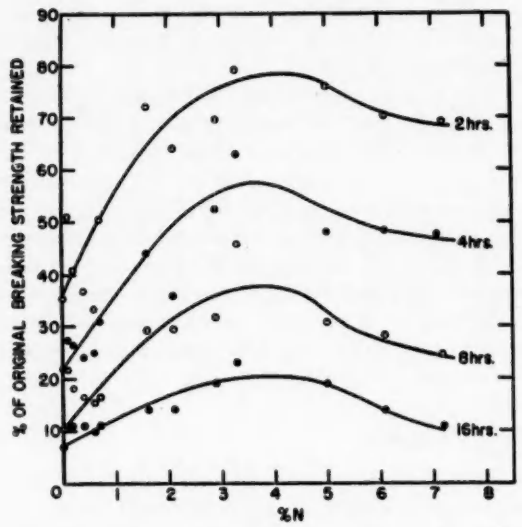

Fig. 4. Oven-aging of cyanoethylated cotton (and hydrolyzed cyanoethylated cotton) at 200° C.

essentially on the same curve whether the nitrogen is directly introduced by cyanoethylation or is the cyanoethyl residue after hydrolysis. It is known, of course, that microbiological decomposition may cause a large decrease in tensile strength with little change in fluidity [2], whereas the same decrease in tensile strength resulting from heat degradation is accompanied by a greatly increased fluidity [15]. From this it has been assumed that the cellulose splitting enzyme, produced by the mold or bacteria, acts on an accessible amorphous area to "cut" the fiber without much effect on the degree of polymerization. On the other hand, when the fiber is exposed to elevated temperatures oxidation takes place throughout the fiber with corresponding decrease in degree of polymerization. These assumptions are compatible with the results obtained in the present case.

Oven-aging data in terms of half-strength life are plotted against nitrogen content in Figure 5. Half-strength life is the time required by oven aging to reduce the strength to half its original value, and its use provides a better understanding of rate than does the rate constant. The half-strength life is calculated from the rate constant equation

$$k = -\frac{\ln (S/S_o)}{t}$$

where k is rate constant, t is time in hours, and S is strength after oven aging and S_o the original strength before aging. Solving for $S/S_o = \frac{1}{2}$, the equation simplifies to

$$t_{\frac{1}{2}} = \frac{0.693}{k}$$

These data are given in Table III which also includes the calculated values for the temperature

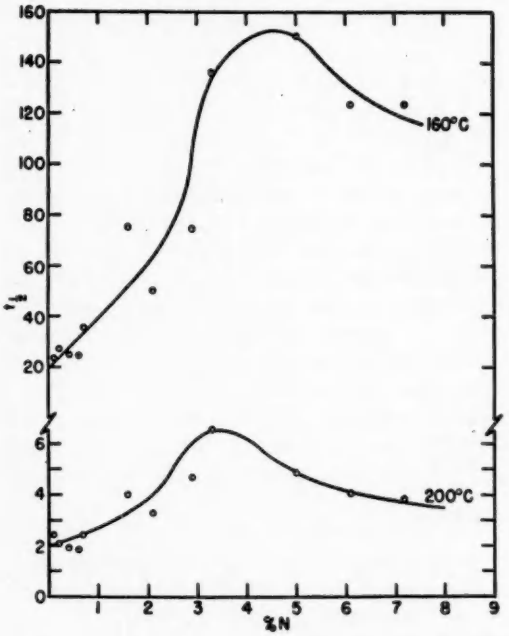

Fig. 5. Half-strength life on oven-aging vs. % nitrogen.

TABLE III. Oven Aging of Cyanoethylated Cotton Yarn before and after Hydrolysis

Nitrogen content		160° C. Oven-aging rate		200° C. Oven-aging rate		
Before hydrolysis, %	After hydrolysis, %	Constant k_{160}	Half-strength life = $\frac{0.693}{k}$, hr.	Constant k_{200}	Half-strength life = $\frac{0.693}{k}$, hr.	$B = \frac{\ln k_{160} - \ln k_{200}}{0.0001951}$
2.1	2.1[a]	0.0138	50.2	0.211	3.28	−14,000
2.1	0.7	0.0197	35.2	0.287	2.42	−13,800
2.1	0.1	0.0291	23.8	0.284	2.44	−11,700
3.3	3.3[a]	0.0051	135.9	0.106	6.54	−15,600
3.3	1.6	0.0092	75.5	0.174	3.98	−15,100
3.3	0.2	0.0256	27.1	0.331	2.09	−13,100
5.0	5.0[a]	0.0046	150.5	0.143	4.85	−17,600
5.0	2.9	0.0093	74.6	0.148	4.68	−14,200
5.0	0.4	0.0278	24.9	0.361	1.92	−13,200
7.2	7.2[a]	0.0056	123.7	0.182	3.80	−17,800
7.2	6.1	0.0056	123.7	0.172	4.03	−17,500
7.2	0.6	0.0284	24.4	0.377	1.84	−13,300
					Av.	−14,700

[a] Not hydrolyzed.

coefficients B, as previously described. As may be noted, the average value is −14,700. This is an empirical constant which may be used in the calculation of the approximate extent of degradation in oven aging of cyanoethylated cotton.

From Figure 5 it is evident that there is an optimum range of nitrogen content which affords best resistance to heat. This range is from about 3 to 5%, resistance falling off rapidly below 3% and more slowly above 5%. A study of the data of Grant et al [12] reveals the same trend in their oven-aging experiments on cyanoethylated 12's/5 yarn: heat resistance increased up to 4.5%, but was lower at 5.5% than at 4.5%.

Physical Properties

Preparation of the series of cyanoethylated and hydrolyzed yarns afforded opportunity to make a fairly extensive determination of their physical properties. Properties so determined are listed in Table IV.

Tenacity increases, but only slowly, as the cyanoethyl groups are cleaved by hydrolysis. The tenacity does not return to its original value upon removal of the cyanoethyl group. The tenacity ratio (fraction of gray yarn tenacity remaining) of hydrolyzed cyanoethylated samples is not identical with that of directly cyanoethylated material, but rather approaches a value lower than the value for cotton. This is nominally the tenacity of cellulose regenerated from cyanoethylated cotton, and the value is reasonable, since the tenacity of regenerated cellulose made by other methods is usually lower than that of the original cellulose, excluding the effect of stretching and so forth. The greater the nitrogen content before hydrolysis, the lower will be the tenacity of the partially or wholly regenerated fiber.

The fraction of knot strength is not plotted for the reason that a cursory inspection of Table IV shows that the results would be similar to the straight yarn strength. Knot strengths were determined because a low value in this property is indicative of brittleness. The data do not indicate brittleness, knot strength declining, if anything, less rapidly with increasing nitrogen content than straight tenacity itself. It was noted, moreover, that in the higher substitutions, the break was not at the knot in most samples tested.

Moisture regain values increase as cyanoethylated groups are cleaved. This is reasonable, since more hydroxyl groups are available to accept the moisture. Further, although a plot is not given here, the values for hydrolyzed samples would fall on a line higher than those for directly cyanoethylated samples. Stated more simply, nitrogen contents being equal, hydrolyzed samples have a higher moisture regain value than the unhydrolyzed.

The effect of these chemical treatments on break-

TABLE IV. Effect of Alkaline Hydrolysis on the Physical Properties of Cyanoethylated Cotton

Original N content, %	Hydrolysis*	N content after hydrolysis, %	N/No	Breaking strength, lb.	Yarn number	Tenacity	Tenacity ratio	Fract. tenacity remaining after hydrolysis	Elongation at break, %	Knot strength, lb.	Knot break factor	Knot ratio	Ply twist multiplier	Moisture regain, %
(Blank)†	—	—	—	9.55	2.40	22.9	1.000	—	9.8	8.67	20.7	1.000	4.51	6.12
—	M	—	—	9.13	2.40	21.9	0.956	—	11.0	7.78	18.8	0.908	4.68	6.59
—	S	—	—	8.99	2.48	22.3	0.972	—	10.9	8.10	20.3	0.981	4.55	6.60
(Control)‡	—	—	—	9.28	2.43	22.6	0.987	—	12.0	7.96	19.3	0.932	4.65	6.95
—	M	—	—	8.38	2.46	20.6	0.900	—	11.5	7.47	18.5	0.894	4.76	6.77
—	S	—	—	8.38	2.51	21.0	0.917	—	11.7	7.62	18.7	0.903	4.86	6.65
2.1	—	—	1.00	9.23	2.43	22.4	0.978	1.00	11.9	7.61	18.3	0.884	4.77	6.04
2.1	M	0.7	0.333	9.14	2.26	20.7	0.904	0.92	12.2	7.85	17.3	0.836	5.14	6.87
2.1	S	0.1	0.048	8.80	2.51	22.1	0.965	0.99	11.9	8.43	20.8	1.005	4.85	6.78
3.3	—	—	1.00	9.18	2.14	19.6	0.856	1.00	11.3	7.13	15.4	0.744	5.04	4.79
3.3	M	1.6	0.485	8.58	2.33	20.0	0.873	1.02	11.3	7.54	17.3	0.836	4.85	6.45
3.3	S	0.2	0.061	9.12	2.46	22.4	0.978	1.14	10.7	7.52	18.3	0.884	4.62	6.81
5.0	—	—	1.00	7.54	2.03	15.3	0.668	1.00	12.4	6.80	13.9	0.672	5.39	3.82
5.0	M	2.9	0.580	7.85	2.08	16.3	0.712	1.07	12.9	7.01	14.8	0.715	5.13	5.88
5.0	S	0.4	0.080	7.87	2.34	18.4	0.804	1.20	13.0	6.99	16.3	0.787	4.94	7.50
7.2	—	—	1.00	6.50	1.52	9.9	0.432	1.00	18.3	6.84	10.3	0.498	6.63	3.15
7.2	M	6.1	0.847	6.40	1.64	10.5	0.459	1.06	19.2	6.19	10.1	0.488	6.58	4.47
7.2	S	0.6	0.083	7.21	2.20	15.9	0.694	1.61	16.9	6.98	15.3	0.739	5.45	7.54

* M represents mild hydrolytic conditions: 1% aqueous NaOH, 5 min., 95° C., S represents severe hydrolytic conditions: 1% aqueous NaOH, 30 min., 95° C.
† Blank is untreated raw 12's/5 yarn. ‡ Control is yarn treated with 2% caustic.

ing elongation is chiefly of importance as an illustration of the necessity of taking change in textile structure into account in interpreting the changes in physical properties. On examination of Table IV, it is to be observed that the figures for elongation increase, and it might be concluded that cyanoethylation considerably increases the break elongation of yarn (from about 10% in the gray state to almost 20% after treatment). Furthermore, it would be concluded that hydrolysis has little or at least only an erratic effect on this property. However, since twist is the most important structural property of a yarn subject to change, the ply twist and the cotton count of the yarn actually tested for twist were determined as part of the original testing program. Figure 6 shows break elongation plotted against computed twist multipliers. It is seen that the points fall essentially in a straight line, as is already known to be the case for untreated gray yarns [8]. It is to be concluded, therefore, that when change in structure is taken into account, any effect on break elongation by cyanoethylation, or cyanoethylation followed by hydrolysis, is absent or slight. This conclusion is supported by the finding of Grant et al [12] to the effect that single-fiber tests show, if anything, a decrease in fiber break elongation as a result of cyanoethylation.

In the interpretation of the results of similar investigations on fabrics it is of equal importance that any change in structure be determined and taken into account. Fabrics present a more complicated problem than one-dimensional yarns, as interlacing yarns add another dimension, and crimp adds a third.

Summary and Conclusions

It is important to note that conclusions from this investigation apply only to cyanoethylated cotton prepared with 2% sodium hydroxide solution by the method described. There is evidence from other work done in this laboratory (as yet unpublished) that the use of higher concentrations of sodium hydroxide results in products which do not have the same properties at a given nitrogen content, especially with respect to resistance to soil burial.

The action of 1% sodium hydroxide on cyanoethylated cotton is to remove cyanoethyl groups, the amount depending upon the time and temperature of the reaction and original nitrogen content of the sample. The reaction is substantially all cleavage of

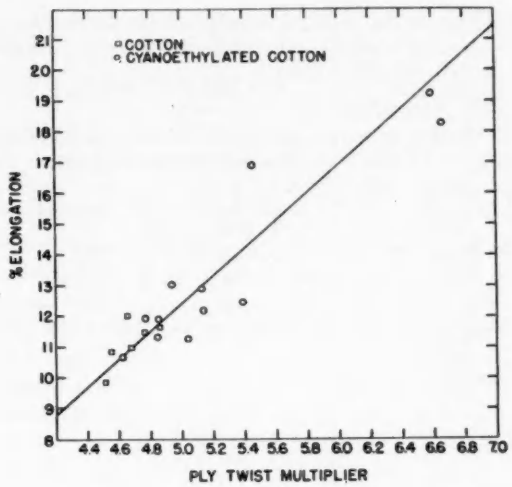

Fig. 6. Effect of twist on the elongation of cotton and cyanoethylated 12's/5 yarn.

the group with regeneration of the cellulose, conversion from cyano- to carboxyl group being negligible.

The rates of cleavage of cyanoethyl groups with 1% sodium hydroxide at 97°, 60°, and 22° C. have been determined. A plot of ln k versus $1/T$ is a linear relationship.

Alkaline aftertreatment at temperatures much above 25° C. should be avoided or the value of cyanoethylated cotton for many purposes will be destroyed.

Rot resistance is destroyed by cleavage. This property is not entirely a function of the nitrogen content, but also of accessibility of amorphous regions of the cellulose.

Cleavage of the cyanoethyl groups does not adversely affect the usual physical properties of the original cyanoethylated yarns. The yarn becomes stronger as hydrolysis proceeds, but at the stage of complete hydrolysis (regenerated cellulose), the original strength has not been restored. This result is the same for regenerated cellulose made by other methods which do not reorient the cellulose molecules.

Heat resistance of cyanoethylated yarns is reduced by hydrolysis but only to an extent roughly proportional to the loss of nitrogen. Such resistance is a direct function of the nitrogen content.

Resistance to oven aging increases as nitrogen content increases, and then declines slowly. The optimum nitrogen content for oven-aging resistance would seem to be from about 3 to 5%.

From oven aging at 160° and 200° C. rate constants (in terms of fraction of strength remaining after heating) half-strength life and temperature coefficients before and after hydrolysis have been computed for nitrogen contents up to 7.2%, the limit in this investigation. Temperature coefficients provide for estimating the effect of change in temperature on rate of oven aging.

Dyeing characteristics are changed by the cleavage reaction. Partially hydrolyzed samples, dyed with a mixture of differential dyes, are much changed in color and shade from samples of comparable nitrogen contents which were not hydrolyzed. This effect is probably due to difference in availability of regions accessible to the dyes.

A battery of quick laboratory tests for important properties is desirable. From data acquired in this investigation, the following are tentatively suggested: (*a*) breaking strength of yarn (strip tensile if fabric is used), (*b*) Kjeldahl nitrogen, (*c*) oven aging at 200° C., testing samples after 2- and 8-hr. exposure, and (*d*) a multidye test for possible prediction of resistance to microbiological attack.

Acknowledgments

The authors wish to acknowledge gratefully the aid of Wilbur F. McSherry for textile testing, Julian F. Jurgens for Kjeldahl nitrogen analyses, Audrey V. Castillon and Lorraine A. Leitz for mathematical calculations.

Literature Cited

1. American Society for Testing Materials, "Standard Methods of Test for Resistance of Textile Materials to Microorganisms," A.S.T.M. D684–54, p. 128–129, Philadelphia (1954).
2. Blum, R., and Stahl, W. H., TEXTILE RESEARCH JOURNAL **22**, 178–192 (1952).
3. Bruson, H. A., *Org. Reactions* **5**, 79–135 (1949).
4. Busse, W. F., Lessig, E. T., Loughborough, D. L., and Larrick, L., *J. Appl. Phys.* **13**, 715–724 (1942); correction, *ibid.* **16**, 120 (1945).
5. Buras, E. M., Jr., Cooper, A. S., Keating, E. J., and Goldthwait, C. F., *Am. Dyestuff Reptr.* **43**, P203–208 (1954).
6. Daul, G. C., Reinhardt, R. M., and Reid, J. D., TEXTILE RESEARCH JOURNAL **25**, 246–253 (1955).
7. Federal Specifications CCC-T-191b, Govt. Print. Off., Washington, D. C. (rev. ed. Jan. 1956).

8. Fiori, L. A., Brown, J. J., and Sands, J. E., TEXTILE RESEARCH JOURNAL **24**, 428–433 (1954).
9. Fordemwalt, F., and Kourtz, R. E., TEXTILE RESEARCH JOURNAL **25**, 84–99 (1955).
10. Goldthwait, C. F., Buras, E. M., Jr., and Cooper, A. S., TEXTILE RESEARCH JOURNAL **21**, 831–840 (1951).
11. Grant, J. N., Couturier, G. M., and Rhodes, M. W., TEXTILE RESEARCH JOURNAL **21**, 867–875 (1951).
12. Grant, J. N., Greathouse, L. H., Reid, J. D., and Weaver, J. W., TEXTILE RESEARCH JOURNAL **25**, 76–83 (1955).
13. Larrick, L., *Textile World* **95**, No. 5, 107–109, 194, 196, 198, 200, 202 (1945).
14. MacGregor, J. H., *J. Soc. Dyers Colourists* **67**, 66–73 (1951).
15. Orr, R. S., Weiss, L. C., Humphreys, G. C., Mares, T., and Grant, J. N., TEXTILE RESEARCH JOURNAL **24**, 399–406 (1954).
16. Redmond, J. R., et al., *Am. Dyestuff Reptr.* **43** P 774–779 (1954).
17. Reinhardt, R. M., Markezich, A. R., Moore, H. B., and Reid, J. D., TEXTILE RESEARCH JOURNAL **26**, 6, 423–429 (1956).
18. Schuyten, H. A., and Weaver, J. W., TEXTILE RESEARCH JOURNAL **24**, 1005 (1954).
19. Sippel, A., *Kolloid, Z.* **112**, 80–84 (1949).
20. Walker, R. C., and Roseveare, W. E., *J. Appl. Phys.* **17**, 482–491 (1946).
21. Wright, J. F., and Minsk, L. M., *J. Am. Chem. Soc.* **75**, 98–101 (1953).

Manuscript received March 13, 1956.

Definition and Measurement of Crimp of Textile Fibers

Ernst Alexander,[1] Menachem Lewin, Helmut V. Muhsam,[1] and Miriam Shiloh

Institute for Fibers and Forest Products Research, Ministry of Agriculture, Israel

Abstract

Two fundamental concepts are defined, the effective crimp diameter and the effective wave number. The corresponding figures for these concepts are calculated from the measurements of the width values of the plane projection of a rotating fiber and from the measurements of the crimp ratio. These figures are obtained for a fiber under a certain load, and take into account the spatial nature and the statistical aspect of crimp. An effective curvature is determined as well. Results are obtained for 90's Merino and 52's Scotch-Blackface wool fibers. It is shown that the higher quality wool fibers are associated with lower effective crimp diameters and higher effective wave numbers.

Introduction

The natural crimp of the wool fiber is one of the main reasons for wool's pre-eminence in high quality fabrics, and artificially crimped fibers are made with the aim of matching the natural crimp of wool.

Although crimp seems to be one of the important properties characterizing the quality of wool and other fibers, no valid definition of crimp seems to have been worked out, and no method for measuring this property seems to have been established.

Several investigations are reported in the literature, in which attempts have been made to define and measure crimp. Methods of measuring crimp in wool fiber and fleece have recently been surveyed [2]. Owing to the complexity of the shape of the crimped fibers, investigators are by no means agreed as to what properties should be used to define the crimp characteristics.

[1] Hebrew University, Jerusalem, Israel.

Duerden in 1929 [3] and Norris [11] were concerned only with measuring the crimp in the stapled wool. They defined crimp as the number of waves per unit length appearing on the staple. Swart and Kotze [14] showed, by using the same method of measurement, that the wave length thus measured on a staple is not constant along the direction of the fibers forming the staple. In these methods for the measurement of crimp, no attempt was made to measure directly the amplitude or depth of the waves in the staple. Their approach was not concerned with the crimp of the individual fibers and dealt mainly with a property of a bulk of fibers in the original staple. However, in this state the fibers are under considerable strains (see Woods [16], Goldsworthy and Lang [6]); therefore the above method cannot present reliable information and may not give the necessary data on the fiber crimp as related to the evaluation of the wool quality. This method of measuring the number of waves per staple length seems to be also of a very limited scope, since it is applicable only to wool with well-defined staple waves, e.g., Merino, Corriedale.

O'Connell and Yeiser [12] were concerned with the effect of crimp on mechanical properties of wet wool, but did not define this property; they only "estimated the amount of crimp in individual fibers" by "rough counts of crimps and ranked fibers in their order of relative crimpiness," differentiating only qualitatively between "low, medium, and high crimp."

The fibers in the staple are subject to deformation owing to their closeness of packing. Therefore when a single fiber is withdrawn from the staple, it departs from its form in the staple [16]. Goldsworthy and Lang [6] have studied the relationship of fiber form and staple crimp in Merino wool by qualitative observations of the behavior of strands formed from individual fibers. Woods [16] and others [2] dealt with the crimp in the individual fibers after they were separated one from another. Woods measured the radius of curvature and the tortuosity at individual points along a single fiber. Since he was concerned only with the relation between crimp and the natural twist of the fiber, he did not attempt to define figures for characterizing the crimp of the fiber as a whole.

Wildman [15] seems to have suggested a method for determination of crimp, based on microscopic measurements of the mean crimp depth, details of which have not been published.

Rainard and Abbot [13] define crimp in terms of what they call "single-fiber bulking capacity." In this method the fiber was stretched inside a slot of a given width, released, and flattened into a plane. A grid of lines parallel to the slot was placed on top of the slot, and the number of intersections of the fiber with the grid lines was counted. This number was used in the definition of bulking capacity. From the description of this method it is evident that during measurements uncontrolled and unknown strains of considerable magnitude must have been present.

Another method of measurement of crimp on a single fiber was suggested by Zart [17] and subsequently simplified by Ecochard [4]. In this method the number of waves per unit length, and the crimp ratio, defined as a percentage shortening of the fiber due to crimp, were measured on a flattened fiber. The crimp ratio was also used by Human and Speakman [8] who, in their short communication dealing with the crimping and heterogeneity of keratin fibers, compared the reduction in crimp after different oxidation treatments.

The main drawbacks of the method of Ecochard [4] have already been pointed out by Millard [10] who stated that the fiber cannot be assumed to be crimped in one distinct plane, and that no uniform shape of crimp exists. He also points out that this method of determination of crimp in textile fibers cannot even be applied to man-made fibers, which are sometimes manufactured with a uniplanar crimp or even a sinusoidal crimp, but which do not remain in this form in later technical processes. Further, it would appear that in view of the marked changes in crimp caused at each stage of handling of the fiber, such handling as suggested by Ecochard cannot assure uniform treatment of each fiber either.

The use of the properties of the force-extension curve of the fibers at low loads and low rates of extension in relation to crimp, as given by Evans and Montgomery [5], is a more promising development. They have defined the following parameters to characterize the crimp.

1. The energy to uncrimp, or the integral of the "crimping force" over the region of uncrimping.
2. The "stiffness of crimp," or the force necessary to "uncrimp" the fiber.

3. The "contraction due to crimp," which is based on a more exact measurement of what has been called the "crimp ratio" by previous authors [4, 8, 17].

These parameters were successfully used by the authors for studying changes in sets of fibers. This method seems to be more accurate than the former ones. But in addition to certain dynamic features it deals with only one aspect of the geometry of the fiber, without paying enough attention to the actual shape of the fiber. Unfortunately no further details of this method have been published.

Zilahi and Dobozy [18] investigated the role of heterogeneous swelling in the formation and origin of certain wool properties, with a view of determining some relation between the internal fiber characteristics governing the shape of the crimp and the swelling potential of the fiber. The authors based a definition of crimp on the following characteristics: the number of waves per axial unit length, the length of an individual wave, and the length of straight line portions and radii of curvature. They conclude that further research is necessary in order to answer many questions connected with crimp.

Recently some papers have been published in which a correlation between the crimp and the chemical and morphological structure of the wool fiber cortex is described [7, 9]. These investigations dealing with single fibers are mainly concerned with the causes of crimp and not with the measurement or the definition of the crimp for a fiber as a whole.

The present paper deals with the geometrical shape of the separate fibers.

Although the definitions and methods of measurements described in the literature differ widely, it is obvious that the concept of crimp was used as a synonym for the general geometrical shape of non-straight fibers. In most fibers this geometrical shape is of a complex statistical nature.

At least two fundamental parameters are necessary for the characterization of crimp, one giving a measure of the amplitude, which is generally called in the literature the "depth" of the crimp; and a second factor which describes the number of crimps per unit length. In the present paper it is proposed to characterize these two factors by defining the effective crimp diameter (E.C.D.) and the effective wave number (E.W.N.). Both figures are defined in such a way as to account for the three-dimensional nature of crimp and for its statistical aspect. The E.C.D. covers the "depth of the crimp" together with what has been called "the bulking capacity" [13]. The E.W.N. measures the number of waves per unit length of the fiber, and may also be related to the number of waves on the staple, as measured by Duerden [3] and Norris [11]. It will be shown (see Appendix II) that an effective radius of curvature can be calculated by using the two parameters given in the present paper; this effective radius of curvature may be related to an average of the radii of curvature as measured by Woods [16] at individual points along single fibers. It will be seen from the methods of calculation that the crimp ratio as used by Zart [17], Ecochard [4], and Human and Speakman [8] is incorporated in the two parameters defined in the present paper.

The measuring methods and instrumentation described in this paper take into account that it is impossible to carry out consistent measurements in the complete absence of strain. All measurements were therefore carried out under well-defined tensions. These tensions were systematically varied, and the changes obtained at different tensions seem to be related to the changes observed by Evans and Montgomery [5].

The Effective Crimp Diameter

In a previous paper [1], measurements of the "effective crimp diameter" have been described. The measurements were performed on vertically suspended wool fibers which were loaded with small weights w, ranging from 50 mg. up to the weight necessary to "uncrimp" the fiber. For each load the horizontal coordinates y_i of a projection of the fiber on a vertical plane were measured at constant vertical intervals with the aid of a vertically moving comparator fitted with an ocular-micrometer. From these the effective crimp diameters were calculated in a way similar to the effective voltage of an alternating electric current. In the equations and tables, values of E.C.D. are represented by D_{eff}.

$$D_{eff} = 2 \cdot \sqrt{\left(\sum_{i=1}^{N} y_i^2 \right) \Big/ N} \qquad (1)$$

where N is the number of measurements.

This method seems to be incomplete for the following reason. For the same load w, different values of D_{eff} are obtained when carrying out the measurements at different planes of projection of the fiber.

It is seen from the few measurements listed in Table I that the values of D_{eff} may increase by up to 60% on passing from one projection plane to another. This is high as compared with the accuracy of the measurements.

TABLE I. Change of Effective-Crimp-Diameter (D_{eff}) with Change of Plane of Projection of the Fibers. (Fibers under Load of 0.2 g.)

Fiber number	D_{eff} (mm.) First plane	Second plane	Third plane	Mean	Standard deviation	Coefficient of variation
1	0.32	0.29	0.20	0.27	0.05	18.5
2	0.41	0.30	0.44	0.36	0.06	16.6
3	0.22	0.25	0.23	0.23	0.01	4.3
4	0.25	0.24	0.26	0.25	0.01	4.0
5	0.27	0.26	0.25	0.26	0.01	3.8
6	0.29	0.26	0.27	0.27	0.01	3.7

Although these differences do not invalidate the method described previously [1] as a simple method of measurement of E.C.D., it was felt that a more accurate approach is desirable. Among the fibers studied by the present authors no fiber exhibiting a well-defined crimp plane was encountered; no such uniplanarity was found on fibers withdrawn from the staple, even in fine Merino wool fibers which exhibit staple crimp of straight waves, suggesting uniplanar crimp of the individual fibers. It was realized, nevertheless, that a method of measurement of the E.C.D. should be independent of the existence or nonexistence of preferred crimp planes.

In order to take into account the three-dimensional distribution of the crimp of the fiber it is proposed to redefine the E.C.P. in the following way:

$$D_{eff} = 2 \cdot \sqrt{\left(\int r^2 \cdot dl \right) \Big/ l_w} \qquad (2)$$

where r is the distance between each point of the fiber and the straight line connecting the endpoints of the section of the fiber under study; l_w is the distance between the endpoints of the fiber section; the integral is to be extended over the whole of l_w.

In practice the measurements are carried out only at a finite number of points N and the formula used is therefore

$$D_{eff} = 2 \cdot \sqrt{\left(\sum_{i=1}^{N} r_i^2 \right) \Big/ N} \qquad (3)$$

It can be readily seen that this definition of E.C.D. is identical with that given previously (Equation 1), provided the crimp of the fiber is uniplanar and the measurements are carried out on a projection plane parallel to this particular plane. In all other cases this new definition gives a higher value of D_{eff} than the previous one, since

$$y_i \leq r_i$$

The measurements of r_i are carried out by rotating the fiber around an axis passing through its end points. The fiber then describes a surface of revolution, and on its projection on a plane parallel to its axis (see Figure 1), the values of $2r_i$ can readily be measured.

The value of D_{eff} obtained in this way for a fiber under a certain load presents an unequivocal measure of a fundamental property of the fiber.

Experimental

The measuring apparatus consisted of a special fastening and rotating device and a projection sys-

Fig. 1. A 52's fiber suspended in a frame and rotated 6 t.p.s. through an axis passing through its endpoints.

tem. The fastening and rotating device is shown in Figure 2. It consists of a frame A fitted with two bearings, B_1 and B_2. Each bearing carries an adjustable jaw, C_1 and C_2. With the help of the axle D and two identical pairs of cogwheels, E_1 and E_2, E_3 and E_4, the two jaws C_1 and C_2 are rotated simultaneously by a suitable motor.

The projection system (see Figure 3) contains a lamp G which illuminates the fiber H in its fastening frame, and a lens I arranged so as to give an enlargement of the rotating fiber by a factor of approximately six. The image of the rotating fiber is formed on a millimetric square scale J of 20 × 20 cm. on an opaque glass plate.

For the measurements an S-shaped hook weighing 10 mg. was tied to one end of the fiber. The other end of the fiber was fixed on the upper jaw (C_1 in Figure 2), while the end carrying the hook hung freely through the opened lower jaw (C_2 in Figure 2). After applying the appropriate load to the hook,

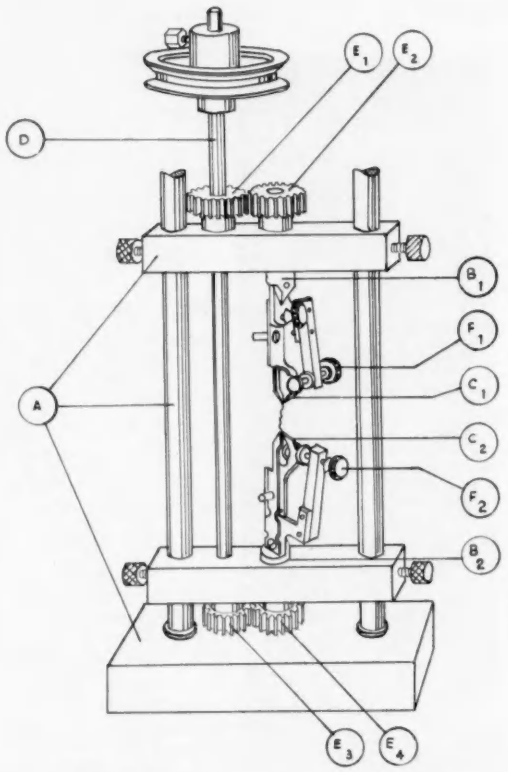

Fig. 2. The fastening and rotating frame.

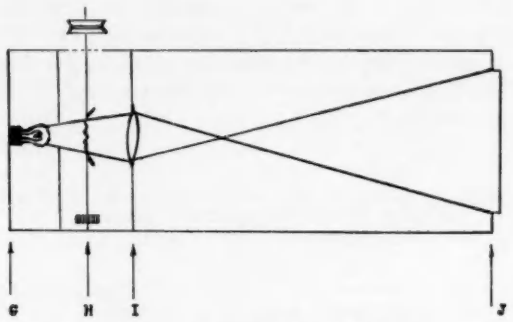

Fig. 3. The projection system.

the lower jaw C_2 could be closed without disturbing the equilibrium of the fiber. Before rotation, the end points of the fiber were brought into coincidence with the axis of rotation by slightly adjusting the jaws with the help of two screws (F_1 and F_2 in Figure 2). This adjustment was necessary as it proved very difficult to clamp the fiber at the exact center of the jaws.

The fiber is then rotated and measurements of $2r_i$ taken along the section of the axis of rotation between two centered points, at constant intervals of about 1 mm.

Several series of measurements of the E.C.D. of the same fiber were performed at various rates of revolution, up to 6 t.p.s., and it was found that no significant deformation of the image occurred (see Figure 1), i.e., the same values were obtained in all cases. The actual measurements were performed at 1 to 2 t.p.s., since it was found that these rates were the most convenient ones.

The values of $2r_i$ were measured between the outside boundaries of the image formed on the opaque glass plate, and therefore, include the image of the fiber itself. This inclusion is of no practical consequence as long as the E.C.D. is large compared with the diameter of the fiber. With increase of load, however, the E.C.D. as measured here decreases to the limiting value of the fiber diameter. If the E.C.D. were defined as a geometrical figure related to the shape of the fiber axis, the diameter of the fiber d_f should have been subtracted from each of the above measured values of $2r_i$. In this case also the values of E.C.D. would be reduced to

$$D'_{eff} = D_{eff} - d_f.$$

The limit of D'_{eff} for a straight fiber will be zero, whereas the limit of D_{eff} will be d_f.

TABLE II. Change in E.C.D. with Load

(The Mean of 50 Fibers)

	52's Scotch-Blackface scoured wool fibers mean diameter: 38μ				90's Merino scoured wool fibers mean diameter: 22μ			
Load, mg.	20	40	60	80	20	40	60	80
Mean D_{eff} mm.	1.4	0.8	0.5	0.4	0.37	0.26	0.21	0.17
Standard error	0.09	0.05	0.03	0.02	0.02	0.011	0.007	0.006
Coefficient of variation	46	44	41	44	35	31	25	26

Results

Since varying the moisture content of wool fibers brings about considerable changes in the fibers [16], all the measurements were performed at 65% R.H. and 20° C. on fibers previously kept at these conditions for 48 hr.

Results obtained for 52's Scotch-Blackface and 90's Merino scoured wool fibers are given in Table II. In both cases measurements were taken on 50 fibers from each quality, loaded with 20, 40, 60, and 80 mg.

The comparison of the E.C.D. of various fibers from the same lot, at any given load, shows that this figure varies within rather large limits. At all loads there are some fibers which show relatively low values of D_{eff}. Among the sample of 50 fibers from 52's Scotch-Blackface fibers, D_{eff} varied around an average of 1.4 mm. from 0.4 to 3.0; and in a sample of the same size from 90's Merino wool fibers, it varied about an average of 0.37 mm. from 0.20 to 0.82. At the higher load of 60 mg., variations from 0.1 to 1.1, around an average of 0.5 mm., were observed for the former; and from 0.14 to 0.40, with an average of 0.21 mm., for the latter. At a load of about 40 to 60 mg., erratically high values of D_{eff} rarely occur, and the distribution of D_{eff} within the sample approaches normality. The coefficient of variation then approaches about 40% for 52's Scotch-Blackface and 20% for 90's Merino.

It has still to be investigated whether the variability of D_{eff} within a sample of wool has any significance for the technical qualities of the wool concerned. However, it might be mentioned that the coefficient of variation of D_{eff} was found to be smaller with respect to 90's Merino than with respect to 52's Scotch-Blackface.

In view of the fairly low variability of D_{eff} (20 to 46% variation) from one sufficiently loaded fiber to another, a small sample of about 15 fibers taken from the same lot will often be sufficient to estimate the average E.C.D. of a lot with a satisfactory degree of reliability. With a sample of this size, it can be determined whether the mean E.C.D. of a lot deviates from a standard value by more than about 20%. Similar samples from each of two lots permits differentiation between them, if the actual difference between the average E.C.D.'s is about 30%.

The present results, incidentally, indicate certain interesting relationships between the E.C.D., the load, and characteristics of the fiber itself, including the fiber diameter, such as an association of high fiber diameters with higher values of E.C.D. Additional relationships which can be deducted from the data will form the subject of subsequent publications.

In Figure 4 the change of the mean E.C.D. values with stress for the 52's Scotch-Blackface and 90's Merino wool fibers is represented.

Measurements of E.C.D. of the same fiber show that repeated loading and unloading cause a reduction in the E.C.D. Partial or full restoration of crimp occurs after a certain time, and this time differs

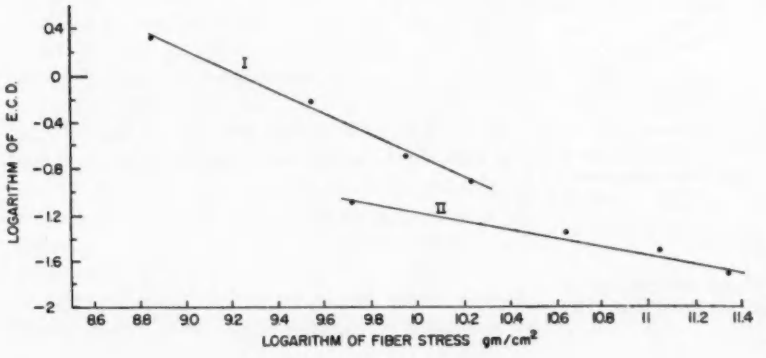

Fig. 4. Change in E.C.D. with stress. I, mean of 50 fibers of 52's quality; II, mean of 50 fibers of 90's quality.

for individual fibers, i.e., the fibers show hysteresis of crimp under the loads applied. Figure 5 shows the relation between the E.C.D. values and the loads applied to a fiber:[2] I, when the fiber was loaded for the first time with increasing weights; II, when the fiber was gradually unloaded in the opposite direction after having remained under the maximum load of I for 14 days; and III, when the fiber was again loaded with the same weights after having been held for another 14 days under the minimum load of II.

It follows that the history of the fiber influences crimp, and should be considered carefully in each set of measurements.

The Effective Wave Number

From the effective crimp diameter an "effective volume" can be estimated, which may be related to the volume actually occupied by a loose fiber assembly, e.g., webs, slivers, felts, etc.

On the other hand the E.C.D. of a fiber represents only one feature of the geometrical shape influencing the physical behavior of the fibers. It is obvious that very differently shaped fibers may yield the same E.C.D., e.g., Figure 6 shows two fibers of the same length and the same E.C.D. with very different curvatures.

Since the E.C.D. can characterize only one aspect of the geometrical shape of a crimped fiber, an additional geometrically independent term is necessary for describing this shape.

[2] These measurements relate to E.C.D. as defined in Equation 1.

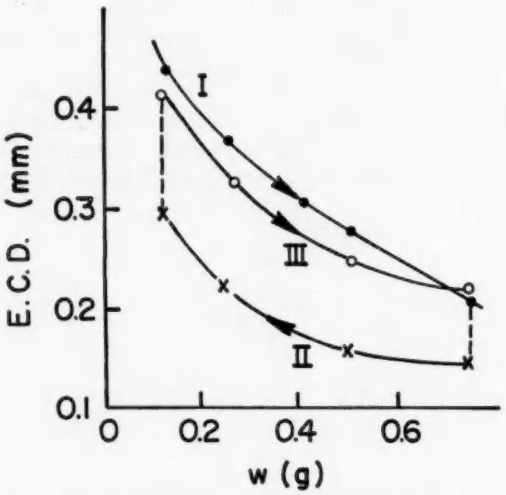

Fig. 5. Hysteresis curve of a single fiber showing change in E.C.D. with load w. I, loading; II, unloading; III, loading.

Fig. 6. Two fibers with the same E.C.D. and different curvature and wave length.

It is generally impossible to define and measure directly the wave length of a crimped fiber. However, an effective wave length or wave number can be calculated. It is proposed to use effective wave number (E.W.N.), defined as the number of waves per unit of fiber length, as the second term. However, it is recognized that E.W.N. alone would not be sufficient to describe crimp.

In the following, a method of deriving E.W.N. is proposed which makes use of the E.C.D. as defined previously, together with the "crimp ratio" (C_r), or "contraction" as used by previous authors [4, 5, 8, 17].

Although it would be possible to use these two measures (E.C.D. and C_r) for characterizing the shape of the fiber, it is desirable and possible to deduce from these two measures an E.W.N. which seems to be a more meaningful measure than the crimp ratio.

In order to arrive at an estimate of the E.W.N., it is sufficient to assume any regular fiber shape, and to calculate the wave number n from the E.C.D. and C_r, with the help of the model of the assumed shape.

The E.W.N. thus estimated gives a characteristic of every fiber, whether regularly or irregularly shaped; in the latter case it can be interpreted as an *average* wave number of the fiber. From this it

will be seen that the thus computed wave number depends only slightly on the particular shape used in the computations.

The regular shapes assumed in the following calculations are: (1) a circular helix and (2) a sine curve. It is assumed that the fiber's D_{eff} was measured, as well as its crimp ratio C_r:

$$C_r = (L - l_w)/L$$

where L is the length of the stretched fiber,[3] and l_w is the distance between the fiber ends under the load w.

In the following calculations, the wave number n is obtained as a function of D_{eff} and C_r.

As the wave-number is given by

$$n = \nu/L = \nu/\nu s = 1/s$$

ν being the total number of waves on the fiber of length L, and s the curve length of one complete wave, it is necessary to find s for any given values of C_r and D_{eff}.

The effective wave number computed from the helix model is called n_1 and that computed from the sine curve model, n_2. The method of calculating these two figures is given in Appendix I.

Results

These two regular shapes were used with the following experimental results, which are presented here as an illustration of the actual estimation of the E.W.N.

Table III shows the values of D_{eff} and C_r as measured on three fibers of different grades. Each fiber was loaded with 10, 20, and 30 mg., respectively.

For these fibers, the distance l_w between the fiber ends and the stretched length L (see footnote 3) were measured, and C_r computed. Then the wave numbers n_1 and n_2 were calculated from the helix and from the sine curve respectively (Equations 4 and 8, Appendix I).

It is seen from Table III that in all cases the wave number n_2 computed from the sine curve are slightly higher than those obtained from the helix n_1; but in view of the considerable difference observed here between various fibers and under different loads, these smaller differences between n_1 and n_2 seem to be of no practical importance. It therefore seems permissible to use either model for the actual calculations, and no preference can be stated.

Under different loads, the wave number of a regularly shaped fiber, homogeneous along its whole length, should remain constant. However, the few empirical data listed in Table III show, in general, a tendency of the average wave number to increase with load. This suggests that the longer waves tend often to disappear before the shorter ones. A lack of homogeneity of the fiber along its length may explain those cases (like the 46's fiber under a weight increase of from 20 to 30 mg.), where this tendency is reversed.

It is seen from Table III that the 90's Merino fiber has approximately a ten-times higher wave number than the 46's and 52's fibers. A high wave number may therefore serve as a good indication of the quality of the wool.

While the E.C.D. and the E.W.N. seem to be highly characteristic for different kinds of wool fibers, it can be seen from Table III that the crimp ratio alone is not significant for such a differentiation.

[3] The stretched length L of the fiber should be defined in a way similar to that given by Evans and Montgomery [5] (see Introduction). However, its actual measurements were taken after loading the fiber to the extent where the E.C.D. approaches the diameter of the fiber.

TABLE III. Estimation of E.W.N.

Fiber grade	w (mg.)	D_{eff} (mm.)	l_w (mm.)	L (mm.)	C_r × 100	n_1 (mm.$^{-1}$)	n_2 (mm.$^{-1}$)
Scotch-Blackface							
46's	10	2.92	40.5	49	17.3	0.061	0.063
	20	1.95	41	49	16.3	0.089	0.092
	30	1.89	42.5	49	13.3	0.084	0.086
52's	10	2.61	50.5	56	9.8	0.053	0.054
	20	1.98	51	56	8.9	0.066	0.068
	30	1.44	51.5	56	8.0	0.087	0.091
Merino							
90's	10	0.21	42	48.5	13.4	0.76	0.78
	20	0.17	42.5	48.5	12.4	0.90	0.93
	30	0.16	43	48.5	11.3	0.92	0.94

APPENDIX I

Computation of the Effective Wave Number

1. *The Circular Helix*

In this case one turn of the helix represents a complete wave. The curve length s of one turn of a helix of radius r and pitch h is

$$s = \sqrt{(2\pi r)^2 + h^2}$$

In the present case,

$$D_{eff} = 2r \quad \text{and} \quad C_r = (s - h)/s$$
$$h = s(1 - C_r)$$

therefore

$$s^2 = (\pi D_{eff})^2 + s^2(1 - C_r)^2$$

and

$$s = \pi D_{eff}/\sqrt{C_r(2 - C_r)}$$

The wave number n_1 of a helix is therefore

$$n_1 = 1/s = \sqrt{C_r(2 - C_r)}/\pi D_{eff} \qquad (4)$$

2. *The Sine Curve*

The curve length s of one wave of a sine curve $y = y_0 \sin(2\pi x/x_0)$, of wave length x_0 and extreme amplitude y_0, is given by

$$s = 4y_0E(k)/k \qquad (5)$$

where $E(k)$ is the complete elliptic integral of the second kind.[4]

$$E(k) = \int_0^{\pi/2} \sqrt{1 - k^2 \sin^2 \varphi} \cdot d\varphi$$
$$(\varphi = 2\pi x/x_0)$$

and

$$k = 2\pi y_0/\sqrt{x_0^2 + (2\pi y_0)^2} \qquad (6)$$

This can be easily seen in the following:

$$s = \int_0^s ds = 4 \cdot \int_0^{x_0/4} \sqrt{1 + (dy/dx)^2} \cdot dx$$
$$= 4 \cdot \int_0^{x_0/4} \sqrt{1 + (2\pi y_0/x_0)^2 \cos^2(2\pi x/x_0)} \cdot dx$$

By introducing

$$\varphi = 2\pi x/x_0$$
$$d\varphi = (2\pi/x_0) \cdot dx$$

we get

$$s = (4x_0/2\pi) \cdot \int_0^{x_0/4} \sqrt{1 + (2\pi y_0/x_0)^2 - (2\pi y_0/x_0)^2 \sin^2 \varphi} \cdot d\varphi$$
$$= (4/2\pi) \cdot \sqrt{x_0^2 + (2\pi y_0)^2} \cdot \int_0^{\pi/2} \sqrt{1 - k^2 \sin^2 \varphi} \cdot d\varphi$$
$$= (4/2\pi) \sqrt{x_0^2 + (2\pi y_0)^2} \cdot E(k)$$

Taking k as given in (6),

$$\sqrt{x_0^2 + (2\pi y_0)^2} = (2\pi y_0)/k$$

it follows that

$$s = 4y_0(E(k)/k)$$

In the case of the sine curve

$$D_{eff} = y_0\sqrt{2}$$

as given in Equation 2 under "The Effective Crimp Diameter,"

$$D_{eff}^2 = \frac{1}{l_w} \int_0^{l_w} y^2 \cdot dx$$
$$= (y_0^2/x_0) \cdot \int_0^{x_0} \sin^2(2\pi x/x_0) \cdot dx = 2y_0^2$$

s, from (5), will be

$$s = 2\sqrt{2}\, D_{eff}(E(k)/k) \qquad (7)$$

and the wave number n_2 will be

$$n_2 = 1/s = \frac{1}{2\sqrt{2}\, D_{eff}} \cdot (k/E(k)) \qquad (8)$$

The crimp ratio C_r is given by

$$C_r = (s - x_0)/s$$

therefore

$$s = x_0/(1 - C_r)$$

From (6) we get

$$x_0 = (2\pi y_0) \cdot \frac{\sqrt{1 - k^2}}{k}$$

so from the last two equations it follows that

$$s = (2\pi y_0) \cdot \left(\frac{\sqrt{1 - k^2}}{k(1 - C_r)} \right) \qquad (9)$$

from (9) and (5),

$$\frac{E(k)}{\sqrt{1 - k^2}} = \left(\frac{\pi}{2} \right) \cdot \frac{1}{1 - C_r}$$

or

$$C_r = 1 - (\pi/2)\sqrt{1 - k^2}/E(k) \qquad (10)$$

[4] Tables for this integral as a function of $\sin^{-1} k$ can be found in the 34th edition of the Handbook of Chemistry and Physics, pp. 234–236 (and in other handbooks).

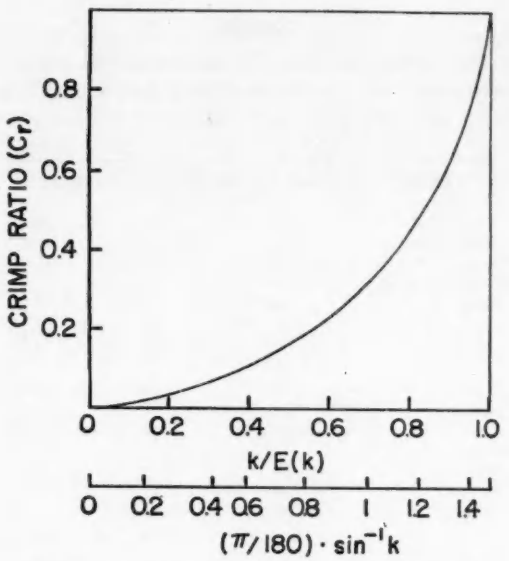

Fig. 7. Graphical representation of the function $C_r(k) = 1 - (\pi/2)\sqrt{1-k^2}/E(k)$.

It is useful to define the function

$$C_r(k) = 1 - (\pi/2)\sqrt{1-k^2}/E(k)$$

This function can be calculated from the tabulated values of $E(k)$, and the values of $C_r(k)$ can be plotted graphically against the similarly calculated values of another function: $k/E(k)$. This is represented graphically in Figure 7.

The wave number n_2 can now be calculated from the measured values of C_r and D_{eff} in the following way. From Figure 7 we get for C_r the corresponding value of $k/E(k)$ directly from the abscissa. By introducing this value into Equation 8, n_2 is obtained.

APPENDIX II

The Effective Curvature of Fibers

In a way similar to the computation of the wave number, it is also possible to obtain from the measured values of D_{eff} and C_r a figure representing the "effective curvature" of the fiber (or its reciprocal, the "effective radius of curvature"), which could also be used as a parameter which serves to illustrate the geometrical shape of a fiber.

The effective curvature (E.K.) can be estimated by computing the curvature of the two regular fiber shapes also used for the E.W.N.: 1. a circular helix, 2. a sine curve.

Computation of the Effective Curvature

1. *The circular helix.* The curvature K_1 of a three-dimensional curve is given by

$$K_1^2 = (d^2x/dS^2)^2 + (d^2y/dS^2)^2 + (dz^2/dS^2)^2$$

where S is the curve length of the helix.

The circular helix is given by

$$x = r\cos\theta \qquad y = r\sin\theta \qquad z = r\theta\tan\alpha$$

where r is the radius and α the slope of the helix.

$$(dS/d\theta)^2 = (dx/d\theta)^2 + (dy/d\theta)^2 + (dz/d\theta)^2 = \frac{r^2}{\cos^2\alpha}$$

therefore

$$S = r\theta/\cos\alpha \tag{11}$$

From (11) it follows that

$$\theta = S\cdot\cos\alpha/r$$

so that

$$(d^2x/dS^2) = (d^2x/d\theta^2)\cdot\cos^2\alpha/r^2 = -\cos^2\alpha\cdot\cos\theta/r$$
$$(d^2y/dS^2) = -\cos^2\alpha\cdot\sin\theta/r \qquad (d^2z/dS^2) = 0$$

$$K_1^2 = \cos^4\alpha\cdot\cos^2\theta/r^2 + \cos^4\alpha\cdot\sin^2\theta/r^2 = \cos^4\alpha/r^2$$

and the curvature

$$K_1 = \cos^2\alpha/r$$

which is constant along the helix.

It is now necessary to calculate α in terms of the known values of D_{eff} and C_r. In the present case,

$$D_{eff} = 2r$$

The crimp ratio is

$$C_r = (S - z)/S$$

By introducing $z = r\theta\tan\alpha$ and S from (11), we obtain

$$C_r = \left(\frac{r\theta}{\cos\alpha} - r\theta\tan\alpha\right)\Big/\left(\frac{r\theta}{\cos\alpha}\right) = 1 - \sin\alpha$$

so that

$$\cos^2\alpha = 1 - (1 - C_r)^2 = C_r(2 - C_r)$$

and from (4) (Appendix I),

$$n_1^2 = C_r(2 - C_r)/\pi^2 D_{eff}^2$$

and

$$\cos^2\alpha = n_1^2\pi^2 D_{eff}^2$$

therefore

$$K_1 = 2n_1^2\pi^2 \cdot D_{eff} \qquad (12)$$

2. *The sine curve.* The curvature K_2 of a plane curve $y(x)$ is given by

$$K_2 = \frac{y''}{(1 + y'^2)^{3/2}}$$

For

$$y = y_0 \sin (2\pi x/x_0)$$
$$y' = (2\pi/x_0)y_0 \cos (2\pi x/x_0)$$
$$y'' = -(2\pi/x_0)^2 y_0 \sin (2\pi x/x_0)$$

and

$$K_2 = \frac{-(2\pi/x_0)^2 y_0 \sin (2\pi x/x_0)}{[1 + (2\pi/x_0)^2 y_0^2 \cos^2 (2\pi x/x_0)]^{3/2}}$$

In order to obtain an average value of $K_2(x)$, we calculate

$$\bar{K}_2 = \frac{1}{s} \cdot \int_0^s K_2 \cdot ds$$

with $s = 1/n_2$ (see Appendix I) (s being the curve length of one complete wave).

$$\bar{K}_2 = n_2 \cdot \int_0^s K_2 \cdot ds$$
$$= 4n_2 \cdot \int_0^{x_0/4} \left[\frac{-(2\pi/x_0)^2 y_0 \sin (2\pi x/x_0)}{1 + (2\pi/x_0)^2 y_0^2 \cos^2 (2\pi x/x_0)} \right] \cdot dx$$

Introducing

$$u = (2\pi y_0/x_0) \cos (2\pi x/x_0)$$

gives

$$\bar{K}_2 = 4n_2 \cdot \int_{(2\pi y_0/x_0)}^{0} \frac{du}{1 + u^2} = -4n_2 \cdot \tan^{-1} (2\pi y_0/x_0)$$

when introducing x_0 from (6) (Appendix I), we obtain

$$\bar{K}_2 = -4n_2 \cdot \tan^{-1} (k/\sqrt{1 - k^2}) = -4n_2 \cdot \sin^{-1} k$$

When disregarding the sign of the curvature, the average of the absolute value of the curvature is consequently given by

$$|\bar{K}_2| = 4n_2 \cdot \sin^{-1} k \qquad (13)$$

In Figure 7 the $C_r(k)$ values were plotted against the $k/E(k)$ values on a linear scale, from which the wave numbers n_2 can be read. An additional nonlinear scale of $\sin^{-1} k$ (in radians, so as to get K_2 in mm.$^{-1}$) is plotted in the same figure, and with the aid of this scale, the average curvatures of the sine curve can be obtained.

Results

The following values of curvature (in mm.$^{-1}$) were obtained (see Table IV) for the same fibers listed in Table III.

TABLE IV. Estimation of the Effective Curvature

Fiber grade	w (mg.)	$K_{1_{eff}}$ (mm.$^{-1}$)	$K_{2_{eff}}$ (mm.$^{-1}$)
Scotch-Blackface			
46's	10	0.21	0.20
	20	0.31	0.28
	30	0.26	0.24
52's	10	0.14	0.13
	20	0.17	0.16
	30	0.22	0.20
Merino			
90's	10	2.40	2.17
	20	2.55	2.49
	30	2.68	2.43

It is seen from Table IV that there are slight differences between the curvatures obtained from the two representations, and the helix model is associated with higher curvatures.

It seems that the general picture of these figures resembles those obtained from the E.W.N.

Summary

A new approach to the problem of defining and measuring crimp, or the geometrical shape of fibers, is reported in the present paper.

In previous methods the stresses under which measurements were performed were not controlled, and the spatial arrangement of crimp, as well as its irregular, statistical aspect was not considered sufficiently. The present paper attempts to account for these factors.

Two fundamental concepts are defined, the effective crimp diameter (E.C.D.) and the effective wave number (E.W.N.).

The E.C.D. gives the average distance between the nonlinear fiber and the straight line connecting its end points. It therefore covers the "depth of the crimp" and the "bulking capacity." It is obtained from measurements of the width of the plane projection of the rotating fiber. For this purpose a special apparatus containing a fastening and rotating device was designed.

The E.W.N. is defined as an average number of waves per unit length of the fiber. A figure for the E.W.N. for a given fiber can be obtained from the

E.C.D. (D_{eff}) and the crimp ratio C_r which is defined as the relative shortening due to crimp of the distance between the fiber ends. This can be done only with the help of a geometrical model. Two models, a circular helix and a sine curve, were used. From the helix model the E.W.N. (n_1) is found to be

$$n_1 = \frac{1}{\pi D_{eff}} \cdot \sqrt{C_r(2 - C_r)} \qquad (4)$$

and from the sine curve model,

$$n_2 = \frac{1}{2\sqrt{2}\, D_{eff}} \cdot [k/E(k)] \qquad (8)$$

where $k/E(k)$ is derived from C_r.

The E.W.N. is related to the length of the waves by which the irregular crimp can be approximately represented.

Each measurement for determining the E.C.D. and E.W.N. is performed under a well-defined stress, by application of weights to the suspended fiber. The spatial nature of crimp is accounted for by the rotation of the fiber. At the same time, the E.C.D. and the E.W.N., being statistical averages, take the variability of the amplitude and the wave length of crimp waves into consideration.

It is shown that an effective radius of curvature or an effective curvature K is determined with the help of the same models. For the helical model,

$$K_1 = 2n_1^2\pi^2 D_{eff} \qquad (12)$$

and for the sine curve model,

$$K_2 = 4n_2 \sin^{-1} k \qquad (13)$$

It is found that both the E.C.D. and E.W.N. assume different values for different types of wool. For a single wool fiber the E.C.D. decreases and the E.W.N. increases slightly with increasing loads. Fibers of the same batch do not differ considerably in E.C.D., the coefficient of variation being fairly low. A small sample is therefore sufficient to determine the average E.C.D. of a lot.

The E.C.D. shows hysteresis. Repeated loading of a fiber causes a reduction in the E.C.D. values, with partial or full restoration after rest.

Merino 90's fibers show smaller E.C.D. values (about 0.1 mm.), than those of Scotch-Blackface 52's and 46's (about 1 mm.), when compared under the same loads; while the E.W.N. values obtained for the 90's fibers are higher than those of the other grades (about 1 mm.$^{-1}$ for the 90's fibers, and 0.1 mm.$^{-1}$ for the 52's and 46's). A similar trend is observed for the values of the curvature.

It is possible, therefore, to differentiate between wools of different qualities by the E.C.D. and E.W.N.

Literature Cited

1. Alexander, E., Lewin, M., and Shiloh, M., *Bull. Research Council Israel* **4**, No. 1, 75 (1954).
2. Anonymous, *Wool Sci. Rev.* **11**, 40–50 (1953).
3. Duerden, J. E., *J. Textile Inst.* **20**, T93–100 (1929).
4. Ecochard, F., *J. Textile Inst.* **45**, P675 (1954).
5. Evans, T. F., and Montgomery, D. J., TEXTILE RESEARCH JOURNAL **23**, 689 (1953).
6. Goldsworthy, Y. E., and Lang, W. R., *J. Textile Inst.* **45**, T755–773 (1954).
7. Horio, M., and Kondo, T., TEXTILE RESEARCH JOURNAL **23**, 23, 373 (1953).
8. Human, J. P. E., and Speakman, J. B., TEXTILE RESEARCH JOURNAL **24**, 58 (1954).
9. Mercer, E. H., TEXTILE RESEARCH JOURNAL **24**, 29 (1954); *J. Textile Inst.* **45**, T365 (1954).
10. Millard, F., *J. Textile Inst.* **46**, P220 (1955).
11. Norris, *et al.*, *J. Textile Inst.* **21**, T481 (1930); **22**, T224 (1931); **22**, T241 (1931).
12. O'Connell, R. A., and Yeiser, A. S., TEXTILE RESEARCH JOURNAL **24**, 629–632 (1954).
13. Rainard, L. W., and Abbott, D., TEXTILE RESEARCH JOURNAL **20**, 301–316 (1950).
14. Swart, J. C., and Kotze, J. J. J., *Empire J. Exp. Agr.*, p. 69 (1937).
15. Wildman, A. B., International Wool Textile Organization Technical Committee Proceedings, 1939. Unpublished. (Surveyed in [2]).
16. Woods, H. J., *J. Textile Inst.* **26**, T93 (1935).
17. Zart, A., *Melliand Textilber.* **10**, 329 (1947).
18. Zilahi, M., and Dobozy, O. K., *Acta Tech. Acad. Sci. Hung.*, Tomus IX, Fasciculi 1–2 (1954).

Manuscript received December 15, 1955.

Letters to the Editor

Short communications in the form of Letters to the Editor are intended to provide prompt publication of significant new research results and to permit an exchange of views on papers previously published in the JOURNAL. These communications are not submitted to formal review as are research papers, and the editors do not assume any share of the author's responsibility for the information given or the opinions expressed. When work previously published in the JOURNAL is the subject of critical comment, the authors of the original paper are given an opportunity to submit a reply, which will be published concurrently when possible.

The Distribution of Ortho- and Para-Cortical Cells in Wool and Mohair

Biochemistry Unit
Wool Textile Research Laboratory
C.S.I.R.O.
Melbourne, Australia

To the Editor
TEXTILE RESEARCH JOURNAL

Dear Sir:

It is now well established that the cortex of fine crimped wool contains two types of cortical cells which differ greatly in their chemical and physical properties [2 through 4], and that the ortho- and para-cells, formerly termed *S* and *H* cells, respectively, in this laboratory, are grouped to form a bilateral structure, as shown in Figure 1*a*.

In a previous communication [2], it was demonstrated that ortho- and para-cells could also be differentiated in Lincoln wool fibers but that the distribution was radially differentiated, with a central core of ortho-cells, as in Figure 1*c*. This was tentatively correlated with the relatively small amount of crimp in Lincoln wool, and subsequent investigations indicate that this feature is associated with poor crimp or the absence of crimp in wools from other breeds and fibers from other animals.

An interesting example was found in a sample from a mutant Merino fleece with no crimp, kindly supplied by Dr. B. F. Short of the C.S.I.R.O. Sheep Biology Laboratory. Most of the cross sections (Figure 1*b*) have a core of two or three deeply stained cells surrounded by lightly stained cells. The differentiation in this case is not as marked as in normal Merino wool, but the two types of cells presumably correspond to the ortho- and para-cells of normal wool.

Further examples of radially differentiated ortho-para distributions were found in samples of both Australian mohair and South African mohair (Figure 1*d*), which have little or no crimp. This was an unexpected result, as Dusenbury and Menkart [1] have suggested, that on the basis of acid sensitization and uniform dyeing, kid mohair can be classified as a "pure *ortho*-fiber." We have examined samples of this material kindly supplied by Dusenbury, and find that ortho- and para-cells may be differentiated, although not so clearly as in adult mohair, and that their distribution is not so orderly.

The discrepancy between the uniform dyeing reported by Dusenbury and Menkart and our own findings is probably related to the choice of dye. In our experience methylene blue gives excellent ortho-para differentiation in cases where other basic dyes give a uniform dyeing of the cortex. The ortho-para nature of mohair cortex is further supported by the separation of two types of cortical cells from mohair digests by Ward and Bartulovich with the aid of an aqueous chloral hydrate density gradient column [5].

We conclude that the radially differentiated ortho-para distribution may be a fairly general feature of wools and wool-like keratin fibers with little or no crimp, the terms ortho and para being understood to indicate relative differences in the reactivity of individual cells toward basic dyes rather than a direct correlation with the ortho- and para-cells of fine crimped wools. Although a general classification of keratin fibers in terms of the ortho- and para-components of fine wool, as suggested by Dusenbury and Menkart [1], is attractive, it may require modification and elaboration to include the spatial distribution of the two types of cell and the

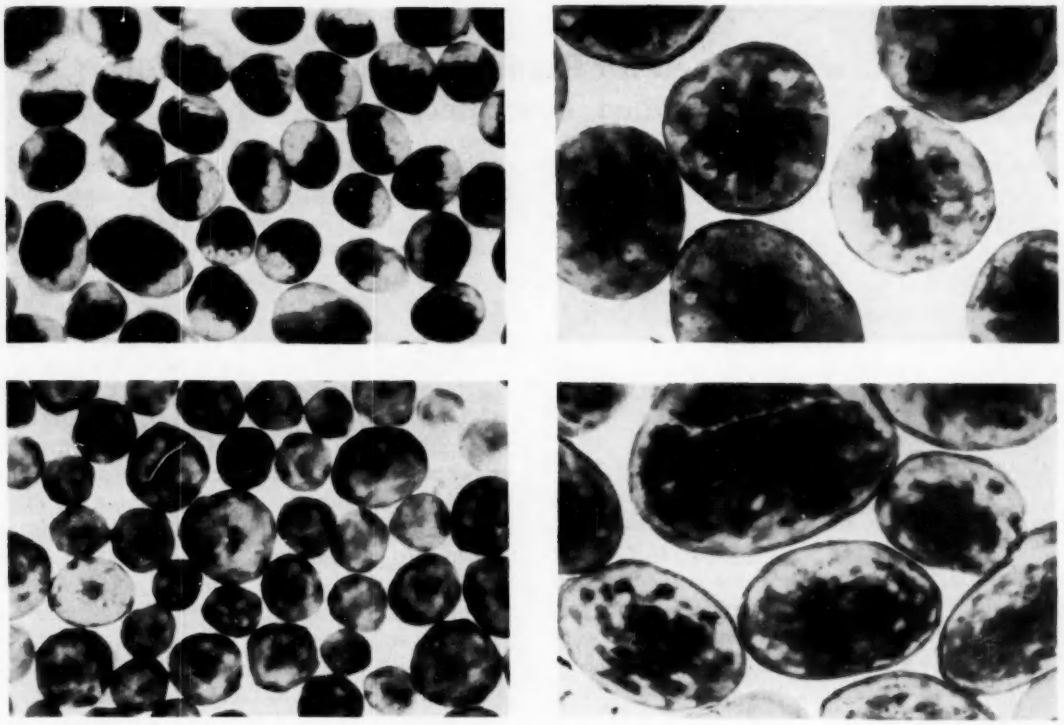

Fig. 1. Cross sections of wool and mohair dyed with methylene blue illustrating the transition from a bilateral asymmetry of basic dye affinity in the cortex of Merino wool (*a*) to one of radial asymmetry in crimpless Merino wool (*b*), Lincoln wool (*c*), and mohair (*d*). (× 500).

less pronounced contrasts in dye affinity found, for example, in kid mohair.

We would like to acknowledge the assistance of R. Moore in cutting some of the sections.

Literature Cited

1. Dusenbury, J. H., and Menkart, J., Proceedings of the International Wool Textile Research Conference, Australia, 1955 (in press).
2. Fraser, R. D. B., and Rogers, G. E., *Aust. J. Biol. Sci.* **8**, 288 (1955).
3. Horio, M., and Kondo, T., TEXTILE RESEARCH JOURNAL **23**, 373 (1953).
4. Mercer, E. H., TEXTILE RESEARCH JOURNAL **23**, 388 (1953).

R. D. B. FRASER
T. P. MACRAE

A Fabric Designed for Rapid Preparation of Uniform Raveled Test Specimens

Engineer Research and Development Laboratories
Corps of Engineers, U. S. Army
Fort Belvoir, Va.

To the Editor

TEXTILE RESEARCH JOURNAL

Dear Sir:

The use of 1-in., raveled fabric test strips, for the determination of the tensile strength lost during soil burial, weathering, and pure culture tests, is one of the accepted methods employed by investigators for determining the microbiological degradation of fabrics that have been impregnated with various types of fungitoxicants. The usual method of preparation is to remove warp yarns from oversize strips until the width is 1 in. across the remaining warp. This is a time-consuming task and requires care to ensure accuracy in raveling. A variation of plus or minus one yarn from the prescribed number required to give a 1-in. warp can affect the mean breaking strength by an amount that is statistically significant.

Another serious objection to this method of preparation is that any raveling performed after exposure to either weathering or fungicidal treatment may not take into consideration dimensional changes caused by shrinkage. A strip raveled to 1 in. after weathering or impregnation with a fungicide may have a different thread count per inch than the unexposed or untreated specimen of the same fabric. This change in the thread count per inch can be a significant factor when the breaking strength of one type of treatment is compared with that of another.

To overcome these disadvantages, a specification was prepared by the Fungus Control Section of the Engineer Research and Development Laboratories, U.S. Army at Fort Belvoir, Virginia, for the weaving of a fabric that could be quickly and accurately raveled into replicate test strips. On the basis of this specification several thousand yards of duck, weighing 10.3 oz./sq. yd. with 54 warp threads per inch was manufactured.

The specification called for the incorporation of colored warp yarns at definite intervals to facilitate the cutting and raveling of the test strips. The colored threads (Figure 1, A) are spaced at two intervals, a wide and a narrow spacing which alternate with each other. The wide spacing including the bounding yarns, is composed of a definite number

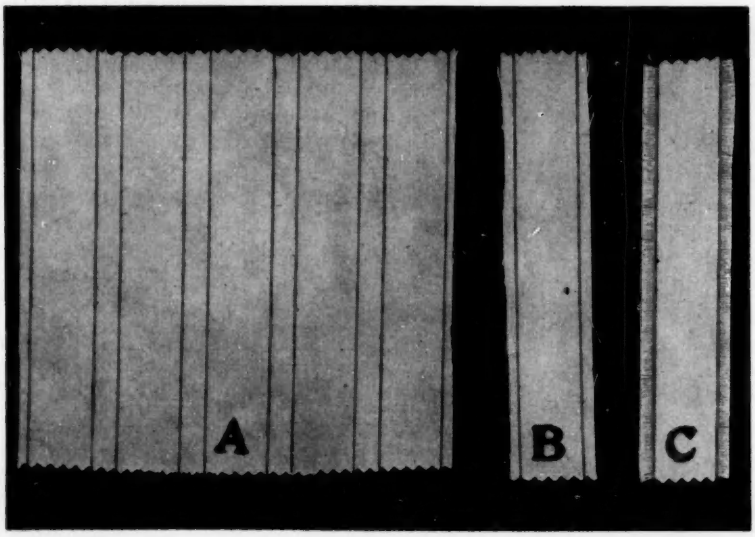

Fig. 1. Standard fabric for preparation of 1-in. raveled fabric test strips.

of yarns as near to one inch as the weaving process will allow. The narrow spacing not including the bounding yarns is approximately a quarter of an inch in width.

Cutting the fabric through the narrow interval will give strips that are approximately 1½ inches in width (Figure 1, B). Removing the warp threads up to, but not including the colored ones, from each side of the strip will leave a uniform number of threads in the warp direction (Figure 1, C). It is never necessary, either during the cutting or ravelling, to measure the warp to assure replicate specimens. Should it be necessary to ravel after exposure to weathering or subsequent to impregnation, any resulting shrinkage or dimensional changes will be self-compensated; the raveling to the colored threads will automatically result in uniform strips having a definite number of yarns in the warp. Accurately raveled strips in any quantity can be prepared by unskilled personnel at a fairly high rate per hour without fatigue or eye strain. The accuracy of the raveling can be checked rapidly by observing whether ravelling can be checked rapidly by observing whether or not the last yarn thread on either side is a colored one. The number of test strips prepared per hour has been increased over 500% by the use of this specially woven fabric.

In order to compare the breaking strength of a 1-in. raveled strip with that of strips having one and two warp threads over or under the required number, five samples, each containing fifty specimens for breaking, were prepared. The samples were conditioned at 70° plus or minus 2° F. and 65% relative humidity. Breaking strengths were made on a Scott tester. An analysis of variance showed a highly significant difference between sample means. The data obtained in these tests and other information may be had by writing to the author.

Plans are now being formulated by a number of Defense Agencies and other interested laboratories for the adoption of a standard test fabric of this type. A portion of the adopted fabric will be treated with a standard fungicide that it is to be agreed upon by the cooperating agencies. These two standard fabrics will be used to correlate the test results of the various laboratories and will serve as a medium for checking the biological activity of the soil-burial beds, the effects of weathering, actinic degradation, and for other tests used in fungicidal evaluations.

Acknowledgments

The author is indebted to Dr. J. M. Ashcroft, Consulting Mycologist, Engineer Research and Development Laboratories, U.S. Army, Fort Belvoir, Virginia, for his assistance with the statistical analysis of the observed data and to J. W. Proctor, Wellington Sears Company, Inc., New York, New York, for his cooperation in the manufacturing of this special fabric.

SAMUEL SHAPIRO

INDUSTRIAL SECTION

Lubrication of the Textile Spindle Bearing

J. P. Vidosic and R. D. Cheverton

Georgia Institute of Technology, Atlanta, Georgia and
Carbide and Carbon Chemical Company, Oak Ridge, Tennessee

Abstract

A great amount of power is consumed in overcoming friction in the high-speed textile spindle. Its proper lubrication is therefore a tremendously important engineering problem. An experimental study of this problem is reported in this paper. We attempt primarily to uncover and to analyze some of the factors involved in order to arrive at the characteristics of the oil-lubricated, cast-iron bolster spindle.

Introduction

It has been established that of the total power consumed in a textile plant, the power required by the spinning room is a substantial item. Soo [5] found that 91% of the power consumed in the spinning room was required to drive the spindles.

Much has thus been done by the textile machinery manufacturers, by the mill operators, and by the petroleum industry in solving this extremely important problem of friction. Steel spindles, rolling bearings, porous-metal inserts, centralized force feeds, better lubricants, have all been considered in modern designs. Research and development have been fully accepted as a necessity. As an example, we need only point out that the work being reported was sponsored through fellowships at the Georgia Institute of Technology by The Texas Company.

Textile spindles in use today are probably mostly oil-lubricated. However, an appreciable number of grease-packed rolling-bearing spindles are finding their way into spinning machinery. In either case, the nature of the bearing and the properties of the lubricant deserve serious investigation. The spindles generally may be grouped into plain-bearing and rolling-bearing types. Even though, as indicated, many of the newer frames are equipped with rolling bearings in whole or in part, thousands upon thousands of the plain-bearing spindles are in use today, and many more are being sold as replacements. Thus the investigation to be reported, dealing with the plain, cast-iron bolster spindle, is fully justified.

This plain bolster spindle contains two bearings (see the sectioned spindle dynamometer in Figure 1). A journal bearing is to be found at the top end of the spindle base and a conical or step thrust bearing at the bottom.

Power Losses

The original investigation [4] in this series, using a power dynamometer developed by Newell and the Research Division of the West Point Manufacturing Company, revealed the general power requirements. Tables I through III depict the large power-consumption variation with spindle speed, package size, and oil viscosity. The conclusions reached from the analysis of these data are that

1. The spindle driving power increases with speed.
2. The spindle driving power increases with package size.
3. The spindle driving power increases with oil viscosity.

It was realized early that air friction must contribute largely to the power consumption of the spindle. Stucki [6] investigated this problem by weighting the spindle down with solder wire. In this way, a reasonable smooth surface with a diam-

eter only slightly larger than the empty bobbin replaced the rough yarn surface, thus reducing air friction at this point to a minimum. Table IV depicts the increase in air friction with package size and speed. Notice also that the percentage of the total power used to overcome air friction decreases with lubricant viscosity. This obviously is so because the air friction at any given speed remains reasonably constant while bearing friction and therefore total power demand increases with the more viscous oil. It can be concluded readily from these data that methods of air shielding the bobbin are most worthy of consideration.

Gunson [2] studied, in addition, the wobble or vibration of the textile spindle. Table V shows the

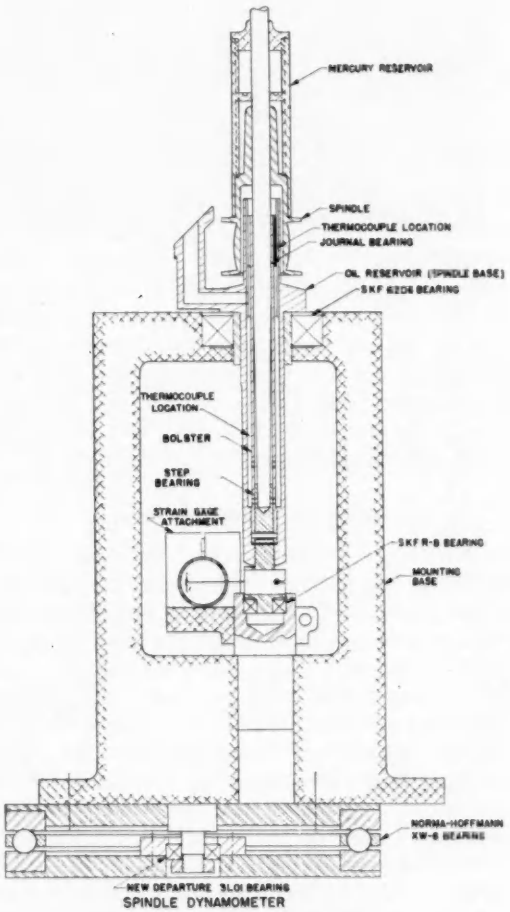

Fig. 1. The spindle dynamometer.

TABLE I. Increase in Single Spindle Power Requirements Caused by Change in Speed from 4,000 to 9,000 r.p.m.

Oil viscosity at 100° F. Saybolt seconds	Package size: Empty	38.5% Full	68% Full	Full
70.8	176%	278%	377%	423%
102.6	173%	248%	330%	379%
183.0	160%	231%	286%	342%
216.0	146%	231%	287%	331%

TABLE II. Increase in Single Spindle Power Requirements Caused by Change in Package Size from Empty to Full

Oil viscosity at 100° F. Saybolt seconds	Spindle speed, r.p.m.: 4,000	9,000
70.8	39.5%	164%
102.6	35.6%	137%
183.0	28.6%	118%
216.0	30.0%	127%

TABLE III. Increase in Single Spindle Power Requirements Caused by Change in Oil Viscosity from 70.8 to 216.0 SSU at 100° F.

Package size (per cent full)	Spindle speed, r.p.m.: 4,000	9,000
Zero	57.9%	39.9%
38.5	54.7%	42.4%
68.0	55.3%	25.8%
100	47.2%	20.8%

TABLE IV. Approximate Percentage of Total Spindle Power Consumed to Overcome Air Friction

Oil viscosity at 100° F. Saybolt seconds	Package size: Empty	Full
	At 5,000 r.p.m.	
70.8	4.2%	45%
102.6	3.2%	41%
189.0	2.8%	34%
216.0	2.5%	32%
	At 10,000 r.p.m.	
70.8	7.0%	67%
102.6	5.7%	62%
189.0	4.3%	60%
216.0	4.4%	57%

TABLE V. Approximate Increase in Spindle Wobble Amplitude Between 4,000 and 10,000 r.p.m.

Oil viscosity at 100° F. Saybolt seconds	Package size: Empty	Full
43.8	550%	1000%
69.5	82%	1525%
97.5	114%	666%

tremendous increase in spindle-tip wobble with speed, at least in these tests. It also shows some effect, though not too conclusively, of the viscosity upon the resulting vibration. This wobble is probably due to many factors. Spindle unbalance, bolster clearance, resonant frequencies, and oil whirl are probably all factors that contribute their share. Possible corrections cannot be made based on these runs, but it definitely indicates that a serious problem exists. Thus further experimentation is warranted.

These preliminary investigations show clearly that the effects of the many variables are quite complex, interrelated and difficult to separate.

It thus becomes evident that a more basic understanding of the mechanism of the spindle bearing and its lubrication is required. Whether or not the bearing operates hydrodynamically becomes a particular question that must be answered. The type and composition of the optimum lubricant can be quite different if boundary lubrication is present. The design might require reconsideration if "perfect" lubrication is not the nature of the present spindle. These problems, and there are many others, could be handled satisfactorily only after the fundamentals became better known. The succeeding investigations were thus directed to this end.

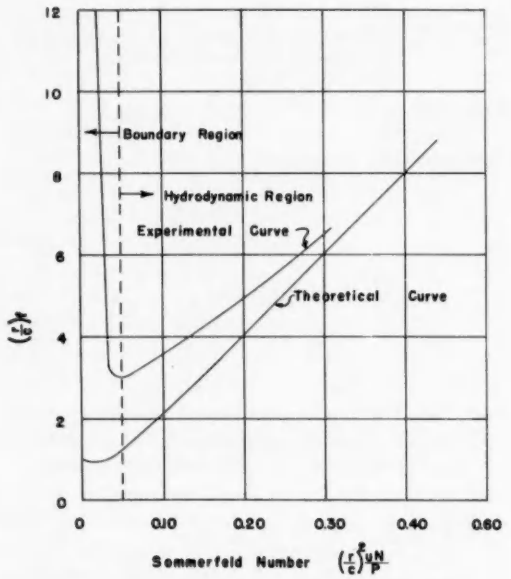

Fig. 2. Friction curves for a full journal bearing.

Sommerfeld Curves

Friction curves for full journal bearings take the form shown in Figure 2. The Sommerfeld number is a dimensionless combination of the variables involved in the lubrication theory

$$S = \frac{\mu N}{P}\left(\frac{r}{c}\right)^2$$

where

μ = lubricant viscosity in reyns
N = speed in r.p.m. (or r.p.s.)
P = load per unit projected area
r = journal radius
c = radial clearance

Plotted against this number is the factor $(r/c)f$ where f, the coefficient of friction, is the ratio of the friction force to the total load W on the bearing. When the bearing is so designed and operated that its Sommerfeld number is to the right of the minimum ordinate, Reynold's hydrodynamic theory of lubrication governs. The bearing will then operate at a safe minimum of friction and under conditions of stable equilibrium. On the other hand, if the Sommerfeld number is below the critical value, uncertain conditions of operation with high friction losses are possible. Consequently, if the Sommerfeld friction curve were to be obtained for the spindle bearing, some of the fundamental characteristics of the spindle would become better known. It is certainly apparent that if this curve is to be established, accurate measurements of friction, load, speed, viscosity, and bearing dimensions must be made.

Laboratory Dynamometer

Cheverton [1] thus proceeded ingeniously to redesign the original dynamometer into a precise laboratory instrument. Pulley, belt, and spindle air-friction losses had to be eliminated from the power readings; a torque device that would measure only the bearing friction was required; the operating temperature of the lubricant had to be established and the spindle speed carefully controlled. The ambient temperature during any test run had to be maintained, etc. All of this was possible with the use of the spindle dynamometer shown in Figure 3.

The torque-measuring device is identified as 1 in Figure 3. A small 75 ST aluminum, cantilever beam with two AB-7 strain gauges of the SR-4 type

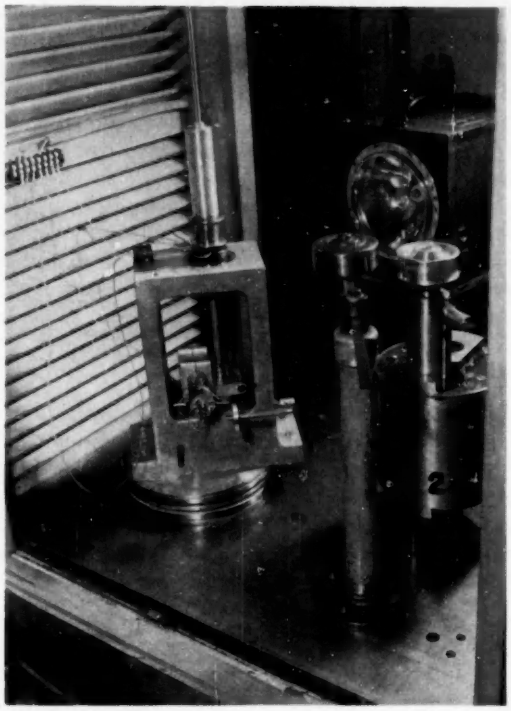

Fig. 3. The spindle dynamometer with its operating equipment. 1. Torque-measuring device. 2. Nine-speed transmission.

cemented on it constitutes the heart of this device. The spindle oil reservoir is mounted, as may best be seen in Figure 1, on two ball bearings. These bearings are in turn supported by the large cast-aluminum base made bulky in the attempt to dampen vibration. This base is mounted on a ball thrust bearing so that its center of rotation is removed from that of the spindle. The force in the spindle-driving belt is thus controlled. A cord attached at one end to the base passes over a pulley and vertically down to a pan upon which can be placed weights for varying the load on the spindle bearing. The line of action of this load is in the same vertical plane as the action line of the belt pull and parallel to it so that the load on the pan is a direct measure of the radial load on the spindle's journal bearing, disregarding the very small friction of the pulley and thrust bearing which was proved negligible. Furthermore, this correspondence in the lines of action could be maintained throughout a run without a change in the load by means of the thrust-bearing adjustment.

Now to get back to the friction torque, a fine thread wrapped at one end about an extension at the base of the oil reservoir and at the other to the free end of the aluminum cantilever beam strained the SR-4 gauges in proportion to the torque moment on the reservoir due to the friction transmitted through the bearings. A Foxboro SR-4 time axis was used to record the strain upon the beam and thus friction.

Control of the spindle speed—an essential—is made possible by means of a synchronous motor and the nine-speed transmission (see Figure 3). With a motor speed of 1800 r.p.m., approximately a 2:1 belt ratio, and the multistage transmission, nine different speeds between 400 and 12,000 r.p.m. are obtainable. The exact speed during any run is measured and checked frequently by use of the stroboscope appearing in Figure 3. An idler pulley and suitable belt tensions are applied in order to prevent excessive slippage as well as provide smooth running and very nearly constant speeds.

The operating lubricant temperatures are established from measurements made on two thermocouples. One of these is immersed in the oil reservoir while the other is silver-soldered in a groove on the outside surface of the journal bearing (see Figure 1).

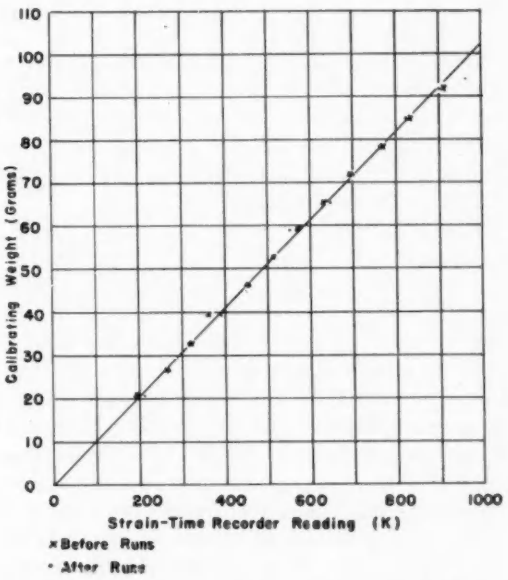

Fig. 4. Calibration record of torque-measuring device.

Williams [7] incorporated mercury slip rings so that temperature measurements could be made continuously without interference with the friction reading. Using the temperatures at these two points, as indicated on a Foxboro portable, assuming a reasonable temperature gradient through the bearing and applying heat-transfer theory, the oil-film temperature can be established closely. The absolute viscosity of the lubricant at the operating temperature is then read off ASTM charts drawn for the oils being used.

All of the operating equipment is installed in an air-conditioning unit with glass sides. Heating elements with a fine rheostat control and a circulating fan are used to maintain the ambient dry-bulb temperature at the desired level. In order to eliminate the transfer of vibrational effects to the spindle, running equipment is mounted on a heavy cast-iron plate characterized by a high natural frequency.

Hydrodynamic Characteristics

The apparatus just described was used by Cheverton and Williams in a series of tests designed to reveal the hydrodynamic characteristics of both spindle bearings—the journal and the pivot. The apparatus satisfied all expectations. It proved quite accurate and precise in the measurement of the many variables involved in bearing lubrication. Calibration curves such as that of the torque-measuring device, Figure 4, attest to this.

Sufficient data were thus obtained to enable the investigators to plot friction curves. These curves could then be analyzed and compared with curves plotted from data computed by applying the hydrodynamic theory to the particular bearing being studied to establish the type of lubrication present.

Some of the data are plotted in Figure 5. Notice that the abscissa is spindle speed. Since the load was constant and viscosity of each oil nearly constant during each run, the spindle speed is directly proportional to the Sommerfeld number. Thus this results only in a change of scale. Similarly, the ordinate in Figure 5 is the strain-time recorder reading. But again since speed is the only variable, K becomes directly proportional to $(r/c)f$. The figure thus shows that the two spindle bearings do operate hydrodynamically. Also that the friction within the bearing rises with viscosity, another hydrodynamic characteristic. This same data plotted in the normal way, Figure 6, indicates quite clearly the hydrodynamic nature of the spindle. It tends to indicate, however, that the bearing may not operate as a full or 360° bearing. It also tells us nothing about either of the two bearings—journal and pivot—separately. It should be noted also that a difference exists between the experimental and theoretical curves over and above the fact that the first is for an infinitely long bearing. The theoretical curve is based on journal friction, while in the test runs bearing friction is measured. Bearing friction is less than that of the journal by approximately a ratio equal to

$$\frac{1 - n^2}{1 + n^2}$$

where n is the attitude at which the journal is running. Thus the two curves would tend to approach each other if either were obtained in terms of the friction involved in the other. There seems to be little doubt, however, that for Sommerfeld numbers (expressed here in the fully dimensionless form), below about 0.07, boundary lubrication exists.

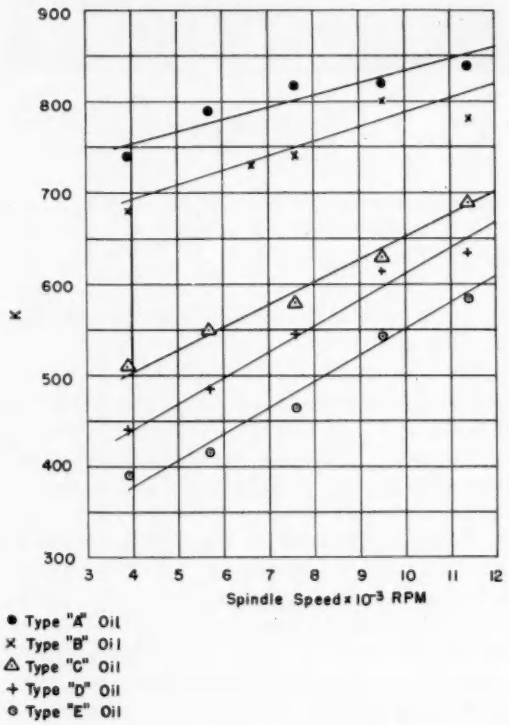

Fig. 5. Modified friction curve.

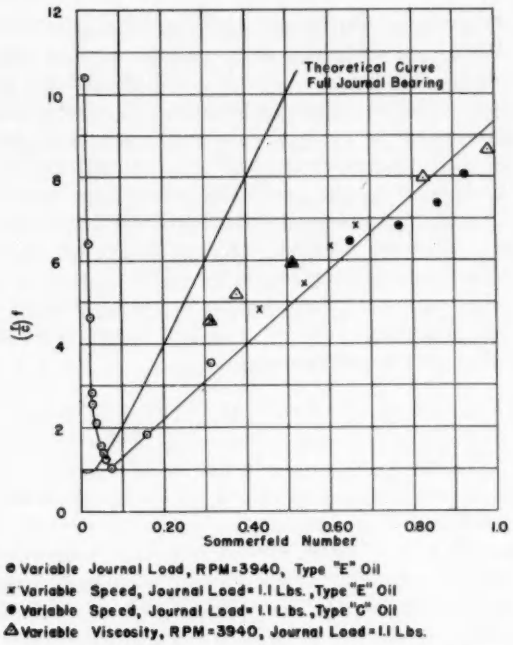
Theoretical Curve
Full Journal Bearing
Sommerfeld Number
● Variable Journal Load, RPM=3940, Type "E" Oil
× Variable Speed, Journal Load= 1.1 Lbs., Type "E" Oil
● Variable Speed, Journal Load= 1.1 Lbs., Type "G" Oil
△ Variable Viscosity, RPM=3940, Journal Load=1.1 Lbs.

Fig. 6. Spindle friction curve.

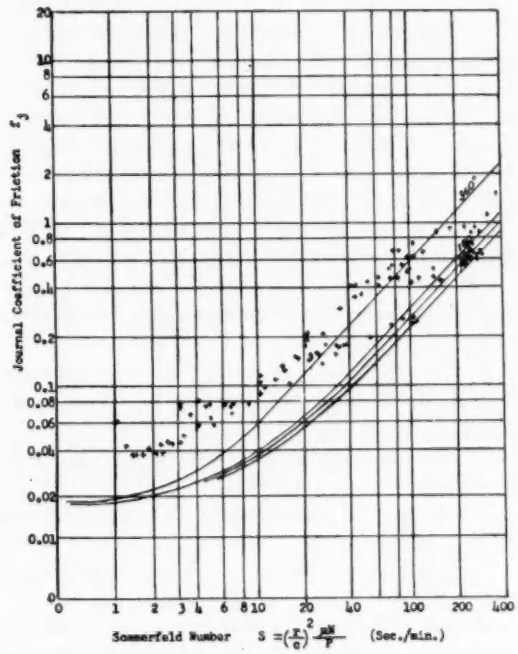

Fig. 7. Spindle friction curves with vertical load constant.

Additional data were obtained and studied in an attempt to investigate the possibility of the bearing running under a partial rather than a complete film. Figure 7 is a plot of these data. Notice that for convenience, primarily, this chart varies somewhat from the previous one. The coordinate axes are reciprocal hyperbolic sine scales, the Sommerfeld number is computed as seconds per minute, the ordinate is journal friction, and the solid curves are the hydrodynamic theory corrected for end flow. Thus the comparison here is more direct. We see then that the friction in the spindle is larger than it should be, at least at the lower Sommerfeld numbers. This is probably accounted for by the high friction on the pivot bearing. In the medium range of Sommerfeld numbers the spindle appears to operate as a full journal bearing. On the other hand, the lightly loaded spindle operates as a partial bearing, at a bearing arc of somewhere between 140 and 180°, above Sommerfeld numbers of about 100.

Pivot Bearing

It must be recalled that the spindle contains two bearings—a journal to support radial forces and a pivot or conical bearing that handles axial loads. The friction that has been analyzed is the total of both bearings. It would be advantageous to deduct the pivot friction from this total. However, Reynold's pressure equation has not been applied to this type of bearing. An exact solution is apparently not known. As attempt was nevertheless made by Williams to evaluate the pivot friction.

The data obtained at increasing vertical loads are plotted in Figure 8 along with the theoretical 360° curve. The curve extends only to a Sommerfeld number of 100 because of the change of bearing arc that occurs, as already noted, above this value. The top enveloping line is assigned the magnitude of the greatest vertical load of 1303.45 g., the bottom line, that of the smallest load of 300.55 g. From the geometry of the figure, the coefficient of friction is then extrapolated to zero vertical load, leaving only the journal-bearing friction.

We notice that because of similar triangles

$$AB:BC = EB:BD$$

Thus

$$(f_{jA} - f_{jB}):(f_{jB} - f_{jC}) = (1305.45 - 300.55):(300.55 - 0) = 3.34$$

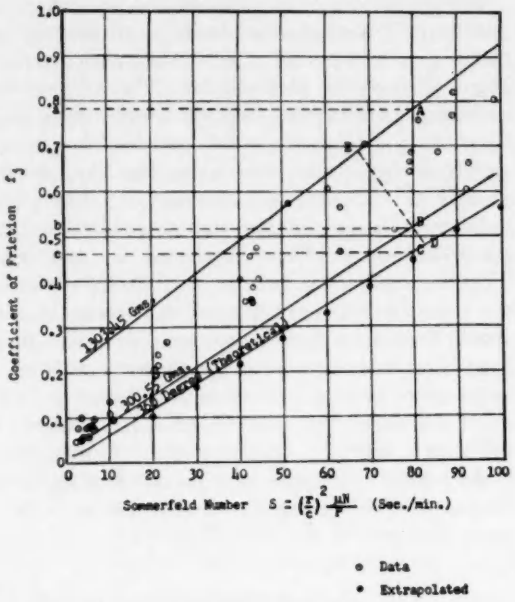

Fig. 8. Spindle friction curves at various vertical loads.

and so

$$f_{jC} = f_{jB} - \frac{f_{jA} - f_{jB}}{3.34}$$

The values thus extrapolated to zero vertical load are shown as solid dots. The close agreement with the 360° line adds some confidence to this attempt at pivot friction separation. An analysis of the lines in Figure 8 reveals that at a Sommerfeld number of 10 the pivot accounts for approximately 79% of the spindle friction. This percentage drops gradually, but it is still about 38% at 100 Sommerfeld number. It is thus evident that the pivot bearing contributes excessively to the total friction present. This must be a result of boundary lubrication. Indeed, a visual inspection of the bearing, even after several hundred hours of running-in, revealed a highly polished spot which results because of the metal-to-metal contact.

Spindle Vibration

Another problem of considerable importance but which was not particularly studied in these investigations is that of spindle vibration. Such vibrations, along with oil whip, which according to Hagg [3] becomes critical when the angular velocity or whirl of the journal center about the bearing center approaches the natural frequency of the spindle, can be quite troublesome because a break in the oil film can result. It appears that operating conditions were such as to result in a critical damping region. Certainly such conditions can be both power-consuming and detrimental to the production of uniform thread. Examination of several such charts reveals two general vibration patterns. One, probably due to oil whip, is characterized by fairly steady high and low traces with some irregularity in between. The other is a continuous oscillation of high frequency, probably a damped resonant vibration.

Summary and Conclusions

Absolute generalization is not justified on the basis of results obtained in this series of investigations. Additional tests are needed to verify the conclusions here indicated. Also the work should be extended to include the effect of the thread tension load, of the moving point application of the thread load, of spindle unbalance, of oil whip, and of pivot-bearing characteristics. However, based on the presently available data, the following conclusions are quite reasonable.

1. Much power is wasted in the spindle bearings.
2. This power increases with speed, package size, and lubricant viscosity as might be expected.
3. The journal bearing within the spindle operates as a hydrodynamic bearing of 360°, up to about a Sommerfeld number of 100 sec./min., and as a partial bearing from here on, dropping to a bearing arc of 140° at a Sommerfeld number of about 400 sec./min.
4. The pivot bearing at the end of the spindle operates in the boundary range of lubrication, thus wasting as much as four times the power lost in the journal bearing. Some modification in design seems desirable at this point.
5. The spindle as presently designed when considered in toto may be operating too close to the critical Sommerfeld number.
6. Vibration and oil whip become critical under some conditions of operation.
7. Shielding of the spindle to reduce air friction could be advantageous.

Thus, indications are that the lubricant to be used in the cast-iron bolster spindle should have the capacity to handle both hydrodynamic and boundary conditions. It should be selected to give a minimum Sommerfeld number of around 10 sec./min. for the

speed and radial load at which it is to operate. Secondly, it should contain polar-type materials, if the boundary conditions in the pivot bearing are to be handled at a minimum of power loss. Mechanically the pivot end should be redesigned in the attempt to eliminate boundary and gain hydrodynamic operation. Possibly, hydrostatic lubrication might be utilized for more efficient operation, friction- as well as vibration-wise. In any case, the spindle should be well balanced in order that high frictional losses resulting from excessive vibration might be minimized.

Acknowledgments

It is indeed a pleasure to acknowledge the excellent work performed by the five graduate students who conducted the research and provided the data that form the basis of this paper. Their names have been given in the body of the paper while their theses are listed under literature cited. As indicated, this research was conducted under fellowship arrangements. For this our sincere appreciation is extended to The Texas Company and to Harry R. Robinson, the Assistant Director of the Lubricating Oil Research Department.

Literature Cited

1. Cheverton, R. D., "A Basic Investigation of the Full Floating Textile Spindle Bearing," Master's thesis, Georgia Institute of Technology, Atlanta, Ga. (June 1953).
2. Gunson, W. E., "The Effects of Various Oils upon the Power Consumption and Wobble in the Cotton Spindle," Master's thesis, Georgia Institute of Technology, Atlanta, Ga. (September 1951).
3. Hagg, A. C., "The Influence of Oil-Film Journal Bearings on the Stability of Rotating Machines," *Trans. ASME* **68**, p. A-211 (1946).
4. Newell, R. L., "Power Characteristics of the Textile Spindle," Master's thesis, Georgia Institute of Technology, Atlanta, Ga. (June 1949).
5. Soo, Shao-Lee, "A Study of the Effect of Lubrication on the Dynamics of Spinning Spindles," unpublished Master's thesis, Georgia Institute of Technology, Atlanta, Ga. (1948).
6. Stucki, A. C., "Air Friction, Its Role in Textile Spindle Power Consumption," Master's thesis, Georgia Institute of Technology, Atlanta, Ga. (June 1950).
7. Williams, J. F., Jr., "An Analysis of the Full Floating Textile Spindle Bearing," Master's thesis, Georgia Institute of Technology, Atlanta, Ga. (December 1953).

Manuscript received December 15, 1955.

A Copper Process for Prolonged Microbiological Protection of Cellulosic Fabrics by Chemical Modification

Edward Abrams[1] and Robert R. Bottoms[2]

Abstract

A new process for prolonged mildew resistance of cellulosic materials has been developed. The process consists of treating cellulose with a dilute solution of copper formate followed by a heat treatment. Heat treatment is an important part of the process. Cotton fabric treated by this process is resistant to pure cultures of cellulolytic organisms both before and after exposure in the Weather-Ometer, and it survives for relatively long periods in biologically active soil. It is believed that in fabric treated by this process, the copper is bound to the cellulose and gives the effect of cross-linking. The copper is insoluble in most copper solvents such as ammonia.

Introduction

Copper in a variety of forms has been used as a fungicide for many years. All of the copper fungicides apparently act as poisons. As such, it is necessary that they have some degree of solubility to affect cellulolytic microorganisms. This solubility, whatever its degree, ultimately results in the complete loss of the fungicide from the cellulose that it is protecting. The process that is the subject of this paper is also based on a copper salt, namely copper formate, but apparently the reaction product of this copper compound and cellulose does not act as a poison for cellulolytic microorganisms. Rather the copper appears to be involved in a cross-linking between adjacent molecules in the amorphous regions of cellulose.

NCG[3] Fabric Preservative Process

The process was invented by Dr. Bottoms and has been developed and evaluated at the Southern Research Institute over a period of more than 6 years. It has been applied to cotton, rayon, and other cellulosic textiles, and to wood and paper.

For purposes of this paper, we will designate the treatment as the NCG Fabric Preservative Process. Basically, the process involves the treatment of any cellulosic material with a solution of certain organic copper compounds. For prolonged resistance to microbiological degradation, copper formate is the only compound that should be used. A maximum of 0.8% copper, based on the weight of the finished fabric, is all that is required for prolonged mildew-resistance. Lesser amounts of copper will also give good protection, and the threshold value is about 0.2% copper.

The process is a simple one. Preferably, the fabric is impregnated with an aqueous solution of copper formate in a padder at room temperature. The fabric is then dried and is autoclaved at a pressure of 15 p.s.i., which corresponds to 120° C. Autoclaving for 20 to 30 min. is sufficient to convert the brilliant green copper formate to the characteristic tan color of the NCG-treated fabric. Cotton fabric thus treated resists soil burial for 14 weeks without significant loss in strength. Wood treated to retain as little as 0.3% copper has resisted the ravages of marine borers and the like in the bay at Miami for over two years.

Copper formate applied to cellulosic material by impregnation alone leaches out readily. Moreover, the copper formate in the cellulose does not inhibit cellulolytic organisms such as *Chaetomium globosum*, nor does it protect cellulose when exposed to bio-

[1] Head Textile Section, Southern Research Institute, Birmingham, Alabama. Present address: National Cylinder Gas Company, Chicago, Illinois.

[2] Research Engineer in Charge, Crestwood Research Laboratories, National Cylinder Gas Company, Crestwood, Kentucky.

[3] NCG is the registered trademark of National Cylinder Gas Co., 840 N. Michigan Ave., Chicago 11, Illinois.

logically active soil. But, after autoclaving at 120° C. and 15 p.s.i. pressure for 20 to 30 min., the copper formate is converted to another copper compound. This copper compound does not leach out in water, in dilute ammonia, or in various chelating agents. And the cellulosic material is now mildew-resistant and will withstand prolonged exposure in soil beds.

Testing and Evaluation

Copper naphthenate was selected as the control in the testing and evaluation of the NCG preservative process as a fabric fungicide.

Ideally, the evaluation of a fabric fungicide should be carried out under actual conditions of use. But it is obvious that such a procedure is not practical. For, if a fungicide is designed to protect fabrics for years in all climates, use tests would require vast amounts of treated fabric with exposures in widely varied climates. A practical solution to this problem has been the development of accelerated tests which simulate the action of Nature. These tests include contact of the treated fabric with pure cultures of known cellulose-destroying organisms under ideal conditions of incubation. Organisms like *Chaetomium globosum* will completely destroy untreated cotton in from 10 to 14 days.

Another test concerns the reaction of the fungicide with the fabric in the presence of sunlight. There is evidence to show that some compounds stimulate the photochemical deterioration of cellulose. By exposing treated fabric to the rays of a powerful carbon arc lamp for a relatively short period of time, as for example, 200 hr., the effect of ultraviolet rays can be determined. An added feature of this test is a cycled water spray that simulates rain. Many compounds, that otherwise would be excellent fabric fungicides, are rejected because they are not stable to sunlight.

Unfortunately, the Weather-Ometer does not correlate too well with outdoor exposure so that the ultimate test of resistance to sunlight is outdoor exposure. However, the Weather-Ometer can be used effectively to screen treated fabrics for resistance to weathering conditions. If a treated fabric loses strength or loses its mildew-resistance as a result of exposure in the Weather-Ometer, there is no need for further tests. On the other hand, treated fabrics that pass this test are worthy of prolonged outdoor exposure tests.

When a fabric fungicide has survived the pure culture and Weather-Ometer exposure tests, it is subjected to the most severe microbiological laboratory test in use at the present time. This is the soil-burial test in which treated strips of fabric are buried in fertile soil. The beds are maintained at ideal conditions of temperature and humidity for the growth of cellulose-destroying molds. In these beds, untreated cotton fabric will become completely disintegrated within 7 to 14 days, whereas treated fabrics will survive in accordance with their ability to resist the attack of molds and bacteria. It is recognized that this test may be more severe than any conditions which will be encountered in the field. Nevertheless, there are treatments that will pass this test. Moreover, the knowledge that a treatment will resist such severe conditions serves as a safety factor in the protection of military and civilian fabrics designed for less severe exposures.

In all of these tests, the action of the microorganisms is measured by changes in breaking strength. The data shown in the tables have been collected over a period of 6 years and each result is the average of hundreds of determinations.

Table I shows that three samples of cotton fabric treated with the NCG preservative, having copper contents of 0.11, 0.45, and 0.82%, lost from 4 to 9% of their strength as a result of processing. Most chemical modifications of cellulose result in loss in strength. But such losses are not considered sig-

TABLE I. Evaluation of NCG Preservative Process as a Fungicide for Cotton Fabric by Various Standard Tests

Sample No.	Copper content, %	Residual B.S. after NCG treatment	Residual B.S. after C.g., %	Weather-Ometer exposure: Residual B.S., %	Weather-Ometer exposure: Residual B.S. after C.g., %	Soil-burial test Residual strength, %, after: 3 wk.	6 wk.	9 wk.	14 wk.
Untreated	—	—	0	98	0	0	0	0	0
1	0.11	96	100	107	54	56	0	0	0
2	0.45	93	102	111	102	101	99	95	91
3	0.82	91	104	106	101	104	102	105	92
Copper naphthenate	0.80	100	101	103	101	100	104	95	85

nificant when they amount to less than 10% of the original breaking strength. Since the copper naphthenate treatment is merely a physical absorption, there was no reduction in strength because of the application of the copper naphthenate.

Chaetomium globosum had no effect on the NCG-preservative-treated fabric, or on the copper naphthenate–treated specimens, whereas the untreated specimens lost all of their strength in 14 days.

Weather-Ometer exposure for 200 hr. had no effect on the breaking strength of all treated samples. The slight increase in strength was due to the shrinking of the fabric.

After Weather-Ometer exposure, subsequent testing with *C. globosum* showed that the sample containing the lowest level of NCG treatment, 0.11% copper, did not resist the growth of *C. globosum*. But, at the level of 0.45% copper and above, each sample resisted *C. globosum* after weathering.

The soil-burial test showed that at the level of 0.11% copper, the sample barely survived the 3-week burial period. The higher concentrations of copper protected the samples beyond 14 weeks of burial. In this respect, they appeared to be the equal of copper naphthenate samples containing 0.8% copper.

It was mentioned previously that Weather-Ometer exposure cannot be considered the equivalent of outdoor exposure. To test the effectiveness of the NCG preservative process during outdoor exposure, large strips of fabric treated by the NCG preservative process and others treated with copper naphthenate were exposed on open-back wooden racks on the roof of one of the buildings at Southern Research Institute. The racks faced south and were inclined at an angle of 45°. Untreated fabric was also included in this experiment. Sufficient fabric for monthly tests for a period of 12 months was exposed. After each month of exposure, sufficient fabric for copper analysis and for 10 breaking strength determinations of each type of fabric was removed from the rack.

TABLE II. Effect of Outdoor Exposure* on NCG-Treated Fabric

Treatment of fabric	Residual breaking strength, % Months of exposure						
	0	1	2	3	4	5	6
Untreated	100	79	72	62	59	58	60
Copper naphthenate	100	87	80	71	68	65	65
NCG-treated fabric	100	91	87	84	84	77	79

*Exposed on roof at SRI, facing south at 45° inclination.

The results for the first six months of exposure appear in Table II. Since the reported portion of the exposure period was during the winter months, it is quite likely that the degradation observed after six months is not as great as may be found during the summer months. At any rate, the untreated fabric lost 40% of its strength and the copper naphthenate-treated fabric lost 35% of its strength, whereas the NCG-treated fabric lost only 21% of its strength. Certainly, it is too early to draw conclusions, but the trend is unmistakable. This experiment is being continued and will be prolonged, if possible, until the NCG-treated fabric is completely deteriorated.

The Role of Heat in the NCG Preservative Process

1. *General Considerations*

An essential part of the NCG-treating process is the application of heat to the copper formate–impregnated fabric. The heating step may be carried out in an autoclave with steam under pressure, or it may be accomplished in air at atmospheric, reduced, or increased pressure. Also, heating may be accomplished in gases other than air, as for example, nitrogen or hydrogen at atmospheric, reduced, or increased pressure. The upper limit of temperature in the heating step depends somewhat on the nature of the cellulosic material. It is desirable to avoid excessive heat, but in most cases, 200° C. is probably the upper limit. The preferred temperature range for the heat step is 100° to 125° C.

The duration of the heat treatment to effect the desired chemical reactions resulting in chemical union of copper with cellulose is not critical and depends largely on the size, form, and species of the cellulosic material undergoing treatment. Ordinarily, from 10 min. to 1 hr. appears to be sufficient for the heating step. But, in any case, the duration of heating is dependent upon the complete conversion of copper formate to a copper-cellulose complex. This becomes evident by a change in color from brilliant green to tan or light olive in the case of autoclaving or brown when dry heat is used. On exposure to air the brown color becomes olive green. Both the brown and olive green colors are believed to be the results of side reactions and do not contribute to the mildew resistance imparted by the NCG-treating process. The colors may be removed by a rinse in dilute ammonia. This is equally true for the pale tan color that is characteristic of autoclaved fabric.

Table III lists various heating procedures. Table IV gives the results of tests on the fabrics described in Table III.

2. *Autoclaving*

Although copper formate may be converted to bound copper by various heating procedures, the preferred method is by autoclaving. For this reason the autoclaving of copper formate–impregnated cellulosic materials has been thoroughly studied. Table V gives the results of tests on cotton fabric samples impregnated with copper formate solution to give three different retentions of copper, of about 0.4, 0.8, and 1.9%. For each level of copper there were four autoclaving periods: ½, 1, 2, and 3 hr.

These experiments suggested that an autoclaving period, not to exceed 30 min., might be preferable, since prolonged autoclaving resulted in little more fixation of copper but was accompanied by a progressive loss in breaking strength.

TABLE III. Effect of Heating in NCG Preservative Process

Conditions	Color of fabric
1. Flowing steam at atmospheric pressure	Olive green
2. Steam in autoclave at 15 p.s.i., 120° C.	Tan
3. Dry air at 120° C. at atmospheric pressure	Olive green (after 2 hr.)
4. Nitrogen at 120° C. at atmospheric pressure	Olive green (after 2 hr.)
5. Nitrogen at 20° C. at 15 p.s.i.	No change
6. Nitrogen at 120° C. at 15 p.s.i.	Olive green (after 2 days)
7. Hydrogen at 120° C. at 15 p.s.i.	Olive green (after 2 days)
8. Air at 120° C. at 15 p.s.i.	Olive green (after 2 days)

TABLE IV. Results of Tests on Cotton Fabric Treated With Copper Formate and Heated in Various Ways

Heating conditions described in Table III	Temperature of treatment, ° C.	Copper content, %		Growth of *Chaetomium Globosum*	
		Original	After 4% ammonia	Original	After 4% ammonia
1	95–100	0.76	0.21	None	None
2	120	0.75	0.33	None	None
3	120	0.72	0.31	None	None
4	120	0.73	0.34	None	None
5	20	0.75	0.07	Heavy	Heavy
6	120	0.73	0.30	None	None
7	120	0.74	0.30	None	None
8	120	0.73	0.32	None	None

Table VI shows that somewhat higher proportions of copper were bound when the autoclaving pressure was increased from 5 to 15 p.s.i. There was a slight tendency for breaking strength to be reduced as autoclaving pressure was increased, but in most cases this was less than 10%.

TABLE V. Effect of Autoclaving Time on Cotton Fabric Treated by the NCG Preservative Process

Sample No.	Autoclave time, hr.	Copper content, %, after		Fixed copper, %	Residual breaking strength, %
		Autoclaving*	Ammonia leach		
1	½	0	0	—	96
2	1	0	0	—	94
3	2	0	0	—	92
4	3	0	0	—	91
5	½	0.37	0.23	62.0	95
6	1	0.30	0.25	83.5	89
7	2	0.41	0.27	66.0	78
8	3	0.32	0.23	72.0	75
9	½	0.79	0.42	53.0	93
10	1	0.75	0.35	46.5	88
11	2	0.85	0.50	59.0	83
12	3	0.91	0.52	57.0	75
13	½	2.03	0.76	37.5	92
14	1	1.84	0.72	39.0	89
15	2	2.04	0.91	44.5	84
16	3	1.83	0.89	48.5	74

* In each case the heating was carried out in an autoclave with steam at 15 p.s.i.

TABLE VI. Effect of Autoclaving Pressure on Cotton Fabric Treated by NCG Preservative Process

Concentration of copper in copper formate solution, %	Autoclave pressure, p.s.i.	Copper content of fabric, %		Fixed copper, %	Residual strength, %
		As treated	After ammonia leach		
0.5	5	0.46	0.16	35.0	97
	10	0.43	0.20	46.5	94
	15	0.47	0.32	68.0	93
1.0	5	0.49	0.20	41.0	93
	10	0.59	0.29	49.0	92
	15	0.52	0.39	75.0	91
2.0	5	1.47	0.49	33.0	96
	10	1.35	0.50	37.0	91
	15	1.48	0.63	42.5	89

Autoclaving time—30 min.

It is suggested that effective copper fixation in the NCG preservative process may be induced by autoclaving at 15 p.s.i. of steam for the shortest time that will give a color change from green to tan. This appears to be 20 to 30 min.

At this point, it is well to emphasize the fact that the ammonia leach that has been mentioned frequently is not part of the NCG preservative process. It is merely a test for the fixation of copper in the treated fabric. Ammonia is a well-known copper solvent. Even metallic copper will dissolve in ammonia in the presence of oxygen to give a characteristic blue copper-ammonia complex. In the ammonia leach test, fabric samples are placed in a large volume of 4% ammonia for 2 hr. The fabric is stirred frequently. After 2 hr., the fabric is removed, is washed in running tap water, and is placed in fresh ammonia for a second 2-hr. period. This is repeated until the ammonia solution remains colorless.

Comparison of Copper Formate with Other Compounds in NCG Preservative Process

In the effort to determine the mechanism of the NCG preservative process, the question of the specificity of copper formate was studied. Similar cotton fabric samples were treated with solutions of copper acetate and with copper propionate in which the copper content was 1.0%. Comparing the results in Table VII with those in Table VI, it appears that the fabric samples pick up more copper (about 0.5%) from the copper formate solution than from the copper acetate or copper propionate solutions (about 0.3%). Moreover, the samples treated with copper acetate and copper propionate tended to retain or fix less copper, about 40% for copper acetate, and 50% for copper propionate, than samples treated with copper formate containing an equivalent amount of copper. The copper formate–treated samples fixed about 75% of the absorbed copper. Since the copper content of the various treating solutions was the same, the difference in copper retention appears to be a function of the anion. The phenomenon may be analogous to the reaction reported by Heuser in "The Chemistry of Cellulose," [1] that the swelling of cellulose in acids appears to be a function of their anions because the effect of the hydrogen-ion concentration upon swelling is negligible. Moreover, it is conceivable that the extent of the swelling is dependent upon the nature of the anion. Thus, the formate ion may make the cellulose more receptive to copper ions than treatment with the acetate or propionate ions. At any rate, it has been established that copper formate is specific for the NCG preservative process in the sense that it was the only compound of those tested that gave prolonged mildew-resistance. Table VIII lists other compounds that have been used, with a lesser degree of success, in the NCG preservative process. In no case did the end results appear to equal those of copper formate. This is indicated in Table IX.

All the compounds were applied to cotton fabric from water solutions. After drying, the fabrics were autoclaved for 30 min. at 15 p.s.i. The color of the fabrics, treated with the copper compounds, changed from blue or blue-green to some shade of tan. The zinc acetate and mercuric acetate solutions did not change the color of cotton, and no change in color was found after autoclaving.

TABLE VII. Effect of NCG Preservative Process on Cotton Fabric Using Copper Acetate and Copper Propionate

(Treating solutions contain 1.0% copper.)

Sample No.*	Autoclave time, hr.†	Copper content, %, after Autoclaving	Copper content, %, after Ammonia leach	Fixed copper, %	Residual breaking strength, %
CA-1	½	0.32	0.13	40.5	85
CA-2	1	0.28	0.11	39.0	82
CA-3	3	0.35	0.16	46.0	81
CP-1	½	0.33	0.16	48.5	82
CP-2	1	0.28	0.14	50.0	76
CP-3	3	0.28	0.14	50.0	74

* CA—copper acetate. CP—copper propionate.
† 15 p.s.i.

TABLE VIII. Compounds Tested in NCG Preservative Process

Aliphatic compounds
Copper formate
Copper acetate
Copper propionate
Copper nonanoate
Mercuric acetate
Zinc acetate

Hydroxy acid compounds
Copper lactate
Copper glycolate

Keto acid compounds
Copper levulinate

Tricarboxylic acid compounds
Copper aconitate

Unsaturated aliphatic compounds
Copper acrylate

Aromatic acid compounds
Copper benzoate

Heterocyclic ring compounds
Copper furoate

Amino acid compounds
Copper glycinate

TABLE IX. Relative Effectiveness of Various Compounds Applied to Cotton Fabric by NCG Preservative Process

Compound	Metal content, %, after autoclaving*	Residual strength, %, after *Chaetomium Globosum*	1-Month soil burial	2-Month soil burial
Copper formate	0.52	100	100	100
Copper acetate	0.54	100	69.0	23.2
Copper propionate	0.45	100	71.3	26.4
Copper lactate	0.53	60	0	—
Copper levulinate	0.45	71	0	—
Zinc acetate	1.03	69	0	—
Copper nonanoate	0.79	79	11.6	0
Copper glycinate	0.40	87	19.8	0
Copper glycolate	0.70	100	45.3	10.6
Copper furoate	0.54	100	94.1	22.2
Copper aconitate	0.92	100	33.7	17.4
Copper acrylate	0.88	100	100	40.1
Copper benzoate	0.36	100	27.6	6.4
Mercuric acetate	0.60	100	31.8	0

* 15 p.s.i. for 30 min.

The metal concentrations listed in Table IX were determined after autoclaving. Most treated fabrics resisted the growth of *C. globosum,* which is a screening test. Only copper lactate, copper levulinate, zinc acetate, copper nonanoate, and copper glycinate failed to pass this mild test for mildew resistance.

In the soil-burial test only copper formate–treated cotton and copper acrylate–treated cotton survived one month of burial, and after the second month, only copper formate–treated cotton still retained all of its strength. Samples of copper formate–treated (NCG-treated cotton) have retained up to 95% of their strength after one year of soil burial.

Mechanism of NCG Preservative Process

Thus far, it has been shown, within the limits of the data available, that copper formate, when applied to cotton fabric or any other cellulosic material by the NCG preservative process, effectively prevents the deterioration of the cellulose by microorganisms for long periods of time.

The obvious question now is: what is the nature of the reaction between copper formate and cellulose during heating? But first, we must prove that heating by autoclaving or otherwise is a necessary part of the process. In Table X, it is seen that when cotton fabric samples are impregnated with copper formate without heating and then are tested with *C. globosum,* the organisms grow to some extent. After 14 days of incubation, the residual strength is only 31.8%. When fabric samples treated in the same way are leached in running tap water for 24 hr., they lose nearly all the absorbed copper formate. The final concentration of copper is only 0.08%. These samples had no resistance to *C. globosum,* and after 14 days were completely deteriorated.

TABLE X. Effect of Autoclaving* on Effectiveness of Copper Formate as a Cotton Mildew Preventive

Treatment	Copper content, %	Residual strength after *Chaetomium Globosum*, %
Copper formate, not autoclaved	0.56	31.8
Copper formate, not autoclaved, leached in water	0.08	0
NCG-treated fabric	0.56	100
NCG-treated fabric leached in water	0.51	100
Untreated	0	0

* 15 p.s.i. for 30 min.

On the other hand, NCG-treated fabric samples with the same pickup of copper formate as the samples just described, were completely resistant to *C. globosum.* Furthermore, water leaching for 24 hr. removed only 0.05% of copper, and the leached samples were also completely resistant to *C. globosum.*

Thus, it is indicated that heating is an essential part of the NCG preservative process. From these results and from the change in color of the fabric after heating, it appears that the copper that is in NCG-treated fabric is not copper formate.

Early in this work, it had been noticed that autoclaved, copper formate–impregnated cotton gave the unmistakable odor of formic acid. This odor was noticeable only on removal from the autoclave. The pH of the fabric sample was found to be about 3.5. After several minutes exposure to the air, no formate odor could be detected, and the pH had risen to 6.5.

To determine whether or not all of the formate was liberated during autoclaving, a radioactive tracer technique was used. Cotton fabric samples were impregnated with copper formate, as described previously. To the copper formate solution was added 10 ml. of a solution of sodium formate (C^{14}). The ratio of formate from sodium formate (C^{14}) to formate from copper formate was about 1 to 3000.

Pieces of cotton fabric were impregnated with this solution and were padded to give a wet pickup of 70%. Two specimens were removed at this point.

One was immediately assayed for total radiocarbon. In Table XI, it is seen that the value for this specimen was 5.42 μc./mole. The other wet sample was used for copper analysis. The copper content was 1.3%.

The remaining wet specimens were dried in a stream of dry air which was then passed through a solution of sodium hydroxide. It was expected that the sodium hydroxide would collect carbon dioxide or formic acid if either were liberated during the process of drying. The sodium hydroxide was then assayed for radiocarbon. The specific activity of the sodium hydroxide solution was 0.43 μc./mole. This figure may have no significance because it is in the range of background radiation. However, radioassay of the dried specimen showed a value of 4.64 μc./mole which was a drop from the wet value of 5.42 μc./mole.

Nevertheless, after the remaining air-dried specimen was autoclaved at 15 p.s.i. for 30 min., the specific activity dropped to 0.57 μc./mole. This value was too low to be considered significant. Thus, it appeared that during autoclaving, practically all of the formate had left the specimen. It does not seem likely that formyl derivatives of cellulose had been formed.

At this point in our investigation, we resorted to X-ray diffraction analysis. X-ray diffraction analysis of cellulose is based on the fact that a crystal behaves like a three-dimensional diffraction grating to X-radiation. It has been found that there is a regularity of interatomic distances in cellulose which may be interpreted as ordered internal structure. This ordered structure is referred to as crystalline cellulose or as crystallites. The cellulose fiber is made up of a multitude of crystallites. For the most part, these are oriented in a direction parallel to the fiber axis. The diffraction found in the X-ray pattern is due only to those crystallites that are in the Bragg position. However, there are regions that are less ordered and are referred to as amorphous regions. These are the regions that are accessible to water, reagents, dyes, and cellulolytic enzymes. Cellulose has a characteristic X-ray diffraction pattern and shows the highest degree of order for ramie, the most crystalline of celluloses. Cotton has a slightly less ordered pattern that is quite similar to that of ramie. And viscose rayon, which is probably the least crystalline of celluloses, with the possible exception of cotton, while still in the unopened boll, shows the lowest degree of order in its X-ray diffraction pattern.

It is sometimes possible to detect chemical modifications of cellulose by X-ray diffraction if the new compound is crystalline or if the old compound either disappears or is diluted. But modifications occurring in the amorphous regions will not necessarily be evident in the X-ray pattern. For example, it is possible to detect an alteration of the position of the cellulose chains with relation to each other in mercerized cotton. This is true only because the lattice arrangement of the crystallites is different from that of native cellulose.

Table XII shows the results of a qualitative experiment in which X-ray analysis has been used. To prepare samples for this study, NCG-treated cotton was Wiley-milled and ball-milled. Untreated cotton was also Wiley-milled and ball-milled. Untreated cotton was combined with cuprous oxide to the extent of 1% copper based on the weight of the cotton, and the mixture was ball-milled. Copper

TABLE XI. Fate of Formate Ion in NCG Preservative Process as Determined by Radioactive Tracer Method

	Specific activity, μc./mole
Copper formate solution	1030
Copper formate–treated cotton fabric, wet*	5.42
Copper formate–treated cotton fabric, dry	4.64
Air used to dry sample	0.43
Copper formate–treated cotton fabric, autoclaved (NCG preservative process)	0.57

* Copper, %—1.3.

TABLE XII. Analysis of X-Ray Diffraction Patterns of NCG-Treated Cotton and Related Materials

Material	X-ray diffraction patterns
NCG-treated cotton, Wiley-milled (60 mesh)	Cellulose pattern plus broad and diffuse lines for Cu_2O
NCG-treated cotton, ball-milled dry for 48 hr.	Broad and diffuse lines for Cu_2O, diffuse cellulose pattern
Untreated cotton, ball-milled with Cu_2O (1% Cu based on weight of cotton)	Strong lines for Cu_2O, diffuse cellulose pattern
Wiley-milled cotton (60 mesh)	Native cellulose pattern
Ball-milled cotton, 48 hr.	Diffuse cellulose pattern
Orange-red powder from autoclaved copper formate crystals	Strong lines for Cu_2O
Orange-red powder from autoclaved copper formate solution	Strong lines for Cu_2O

formate crystals and a copper formate solution (1% copper) were autoclaved at 15 p.s.i. for 30 min. without the presence of cotton. The orange-red powders that appeared on the surface of both the copper formate crystals and the copper formate solution were also examined by X-ray diffraction analysis.

On a qualitative basis, the results suggest that the NCG preservative process did not alter the X-ray pattern of the cellulose. The patterns of the treated and untreated cotton appeared to be identical. This tends to indicate that the crystalline regions, which are responsible for the X-ray diffraction pattern, were not affected by the process. Apparently, the modification that makes the cotton mildew-resistant takes place entirely in the amorphous regions. NCG-treated cotton, both Wiley-milled and ball-milled, gave the characteristic cellulose pattern, although the pattern of the ball-milled cotton was more diffuse. Additional ball-milling would completely obliterate the cellulose pattern. In the patterns for both specimens, there were also broad and diffuse lines for cuprous oxide (Cu_2O). The control, untreated cotton, ball-milled with cuprous oxide, gave an X-ray diffraction pattern similar to the one for NCG-treated cotton, except that the lines for cuprous oxide were stronger. This might have been the result of a larger crystal size.

Finally, the orange-red powder that resulted from the autoclaving of copper formate was cuprous oxide (Cu_2O).

Now, is it possible that the NCG preservative process has resulted in a deposit of crystalline cuprous oxide in the fine structure of the cotton fibers? If cuprous oxide is a good fungicide, the packing of the fine structure of the cellulose with cuprous oxide might be a simple explanation for the effectiveness of the process. However, there are at least two reasons why this cannot be true. First, the copper in NCG-treated cotton is not completely removed by repeated washing with dilute ammonia. It is most likely that free cuprous oxide would be completely removed by ammonia from treated cotton. And, second, cuprous oxide is not an effective fungicide. Table XIII shows the results of an experiment designed to test the effectiveness of cuprous oxide as a fungicide.

For this experiment, a quantity of dewaxed and depectinized cotton fabric and similar fabric treated by the NCG preservative process (0.85% copper) were chopped separately in a Wiley Mill to a uniform size of 60 mesh. Both samples were milled dry in separate ball mills for 48 hr. At the end of this time, both cotton samples were reduced to a fine powder that did not show birefringence under crossed Nicol prisms. An additional control was prepared by adding to dewaxed and depectinized Wiley-milled cotton a quantity of cuprous oxide equivalent to a pickup of 1% copper based on the weight of the cotton. This mixture was also milled for 48 hr.

To test the resistance to mildew of these preparations, 500-ml. Erlenmeyer flasks were prepared with 100 ml. of standard nutrient medium without agar. To each flask was added 1 g. of cotton or cotton powder. Flasks were sterilized and were inoculated with *C. globosum* and were placed on a shake apparatus.

The results listed in Table XIII were recorded after 21 days of incubation. The untreated cotton, whether Wiley-milled or ball-milled, apparently was completely utilized as a food material by *C. globosum*. In the case of the NCG-treated cotton, the Wiley-milled specimen showed only a very slight growth of mycelium which was the result of the germination of the spores. This would also happen if no cellulose were present in the culture flask. The spores, under the influence of moisture and mineral salts, would begin to germinate. However, since native cellulose was not available, they ceased to grow at this stage. On the other hand, ball-milled NCG-treated cotton showed the same heavy growth as untreated cotton. Table XIII shows that cuprous oxide either by itself or in the presence of cellulose was not a good fungicide. It permitted the germination of *C. globosum*. And, when untreated cotton, either Wiley-milled or ball-milled, was present in addition to the cuprous oxide, the cotton was completely digested by the organisms.

TABLE XIII. Resistance of Ball-Milled NCG-Treated Cotton to *Chaetomium Globosum*

Material	Growth of *Chaetomium Globosum*
Untreated cotton	
Wiley-milled	Very heavy, fibers badly deteriorated
Ball-milled	Very heavy, packed solid with mycelia and spores
NCG-treated cotton	
Wiley-milled	Very slight growth of mycelium, no penetration of fibers
Ball-milled	Very heavy, packed solid with mycelia and spores
Untreated cotton and Cu_2O	
Wiley-milled	Very heavy, same as untreated
Ball-milled	Very heavy, same as untreated
Cuprous oxide, Cu_2O	Slight growth of mycelia

The Anomaly of Cuprous Oxide

It has been shown that cuprous oxide is not a fungicide and will not protect cellulosic materials. If we are to accept the evidence of X-ray analysis, it is difficult to understand how cuprous oxide can exist within a cotton fiber so that it is not removed by a copper solvent such as ammonia. Moreover, the cotton is highly mildew-resistant.

Now, if ball-milling destroys the mildew-resistance of NCG-treated cotton, the copper compound which is responsible for mildew resistance must have changed in some way. But, X-ray analysis shows that the compound is cuprous oxide both before and after ball-milling. Since it is known that ball-milling breaks cross-links such as hydrogen bonds, it may be possible that the copper compound in NCG-treated cotton that gives an X-ray diffraction pattern of cuprous oxide, exists as a cross-link in the amorphous regions. In this way, it may act as a barrier to the enzymes of cellulolytic microorganisms. But this hypothesis is difficult to maintain because cuprous oxide, as such, cannot exist as a cross-linking member between adjacent cellulose molecules. However, there is the possibility that the cuprous oxide is physically present on or in the cotton fibers as a by-product of the process in addition to an unknown form of copper that is responsible for the high degree of mildew-resistance of the NCG preservative process. It will be remembered that NCG-treated fabric gives up some of its copper when leached with ammonia. But a point is soon reached beyond which no additional copper is removed. The color of the fabric changes from tan to almost white. Very likely a trace of cuprous oxide remains in the fibers to give a diffuse pattern when analyzed with X-rays.

Evidence for Cross-Linking

Cross-linking in cellulose may be detected in several ways. Reeves and co-workers [3] have recently published a paper entitled: "Insolubility in Cuprammonium Hydroxide as a Means of Detecting Cross-linking in Chemically Modified Cotton." Early in our work, we had attempted to determine the cuprammonium fluidity of NCG-treated cotton as compared with that of untreated cotton. Cuprammonium fluidity of cellulose is a measure of the quality of the cellulose. That is to say, cellulose is permitted to dissolve in a standardized solution of cuprammonium under standardized conditions. After a given period of time, the fluidity, or its reciprocal, the viscosity of the cellulose-cuprammonium solution, is measured. High grade cellulose, having a high degree of polymerization (DP), is very viscous. As the degree of polymerization becomes less, the viscosity in cuprammonium is reduced until the fluidity of the original cuprammonium is hardly changed.

Most celluloses can be dissolved in cuprammonium. But, as Reeves and co-workers have shown, cellulose that has cross-linking has a low degree of solubility in cuprammonium. Attempts to dissolve NCG-treated cotton in cuprammonium were fruitless. Cupriethylene diamine, another cellulose solvent, gave similar results. Moreover, attempts to xanthate NCG-treated cotton were also fruitless. The results of these experiments are summarized in Table XIV.

It is seen that NCG-treated fabric was only very slightly soluble in cupriethylene diamine and cuprammonium. The exceedingly small amount of material that did dissolve in these solvents was probably surface cellulose. Furthermore, cotton treated with the NCG preservative process could not be xanthated to make viscose rayon. The net result of the xanthation was that the treated cotton became slightly stiffer as a result of treatment with sodium hydroxide.

Samples of NCG-treated cotton were immersed in 10% hydrochloric acid. Although untreated cotton was almost completely disintegrated by the acid in a short time, NCG-treated cotton, even after 24 hr., merely broke up into 3 or 4 smaller pieces, each of which maintained its original appearance. The smaller pieces had lost most of their strength.

If cross-linking with copper does take place as a result of the NCG preservative process, then it must occur in the amorphous regions of the cellulose. If this is true, cellulose with higher proportions of amorphous regions should bind more copper than

TABLE XIV. Effect of Various Reagents on NCG-Treated Cotton

Reagent	Untreated cotton	Cotton and copper formate	NCG-treated cotton
Cuprammonium	Very viscous solution	Very viscous solution	Practically insoluble
Cupriethylene diamine	Very viscous solution	Very viscous solution	Practically insoluble
Hydrochloric acid	Completely disintegrated	Completely disintegrated	Breaks into several large pieces
$NaOH-CS_2$	Viscose	Viscose	No change

celluloses of higher crystallinity. Table XV shows the results of an experiment designed to evaluate this theory. The cotton bound 54.2% of the copper from the absorbed copper formate. Viscose rayon which has more amorphous cellulose than cotton bound 90.5% copper under identical circumstances. On the other hand, ramie, which is highly crystalline, did not bind any copper at all. The pure culture tests, after autoclaving, indicated that the copper formate in the ramie, which was still the original green color, had no resistance to *C. globosum*.

Thus, in the NCG preservative process, the binding of copper in these experiments appeared to correlate inversely with the degree of crystallinity of the cellulose.

Moisture Regain of NCG Preservative-Treated Cotton

If, as is suggested by these investigations, the NCG preservative process creates a new type of cross-linking in the cellulose molecule, the ability of cotton fibers to absorb water may be changed. In Table XVI, it is seen that treatment of cotton with 2% formic acid (equivalent to the formate in the NCG preservative process) resulted in an increase in moisture regain from 6.5% to 6.8%. And after autoclaving, this value increased to 6.9%. This is reasonable in view of the known effect of formic acid on cellulose according to Nickerson [2]. When similar cotton was treated with copper formate, the moisture regain rose to 7.1%. Yet after autoclaving —the essential part of the NCG preservative process —the moisture regain dropped to 5.9%.

TABLE XV. Fixation of Copper in Various Cellulose Materials by NCG Preservative Process

Cellulose material	Copper content, %, after: Autoclaving	Copper content, %, after: Ammonia leach	Fixed copper, %	Growth of *Chaetomium Globosum*
Viscose rayon	0.62	0.56	90.5	None
Cotton	0.59	0.32	54.2	None
Ramie	0.63*	0	0	Moderate

* Green color did not change to tan.

TABLE XVI. Moisture Regain of NCG-Treated Cotton in Comparison with Other Treated Cottons
(70° F.—65% R.H.)

Material	Moisture regain, %
Untreated cotton	6.5
Copper formate–impregnated cotton	7.1
NCG-treated cotton	5.9
Formic acid–impregnated cotton	6.8
Formic acid–impregnated cotton, autoclaved	6.9

Summary

1. Copper formate applied to a cellulosic material by impregnation leaches out readily. Moreover, the cellulose thus treated is not mildew-resistant. However, during autoclaving, the copper formate liberates formic acid and is, at least in part, converted to cuprous oxide, as suggested by X-ray analysis. The anomalous copper compound that may be present in addition to cuprous oxide is not readily soluble in water nor can it be removed from cellulose with dilute ammonia. Moreover, NCG-treated cotton becomes mildew-resistant and will withstand prolonged exposure in soil beds.

2. Cuprous oxide alone, or mixed with cellulose, does not appear to inhibit the growth of cellulolytic organisms.

3. Ball-milled NCG-treated cotton is not mildew-resistant. It is most likely that the cuprous oxide is not attached to individual molecules by primary valences. It must then be concluded, in view of the mildew-resistance of NCG-treated cotton, that a copper compound other than cuprous oxide may be bound to adjacent cellulose molecules in the amorphous regions by means of secondary valences or Van der Waal forces.

4. The assumption that the NCG preservative process is limited to the amorphous regions is derived from the following experimental results:

a. Viscose rayon samples, treated with an equivalent amount of copper formate, retained or bound almost twice as much copper as did the cotton fabric samples and were, of course, mildew-resistant.

b. Ramie was difficult to treat with copper formate. After 2 hr. of autoclaving, no reaction appeared to have taken place as evidenced by a color change. The ramie remained green and was not resistant to *C. globosum*. Moreover, the copper was quickly removed with dilute ammonia.

5. Evidence leading to the assumption that copper in some form in NCG-treated cotton is chemically bound rather than physically deposited is:

a. NCG-treated cotton was only very slightly soluble in cuprammonium and cupriethylene diamine. The very small amount that did dissolve was probably readily available surface cellulose. Reeves and co-workers [3] show that insolubility in cellulose solvents is evidence of cross-linking in cellulose.

b. NCG-treated cotton could not be converted to viscose rayon when treated with the xanthation process. The NCG-treated cotton became slightly stiffer after treatment with sodium hydroxide.

c. Treatment of NCG-treated cotton with dilute ammonia resulted in an initial loss of copper after which no additional copper was removed.

In conclusion, it appears that the NCG preservative process deposits copper formate in the amorphous regions of cellulose which, perhaps by ion exchange, attaches copper to OH^- groups. During autoclaving, formic acid is liberated and the attached copper compound bridges across adjacent cellulose molecules. Perhaps the liberated formic acid plays a part in breaking some of the pre-existing hydrogen bonds. Cuprous oxide is also present but does not contribute to mildew-resistance.

With regard to the physical characteristics of NCG-treated cotton fabric, the hand is hardly changed from that of the untreated fabric and the color is light tan. Treated fabrics may be dyed in the same manner as untreated cotton. However, the colors are somewhat modified. The direct dyes are least affected, and in the case of the vat dyes, only one, a yellow, was found that gave a different shade of color. Dyeing does not affect the mildew-resistance of NCG-treated cotton.

Preliminary tests on five human subjects indicate that NCG-treated fabric is neither a primary skin irritant nor a secondary sensitizer. Thus, it will be possible to make mildew-resistant cotton garments from NCG-treated fabrics.

Acknowledgments

It is a pleasure to acknowledge the assistance of Jeanette Esslinger, who was closely associated with the process throughout the more than six years of its development. Thanks are also due Dr. William J. Barrett and his associates for the many analyses required in the course of this work.

Literature Cited

1. Heuser, Emil, *The Chemistry of Cellulose,* John Wiley and Sons, Inc., New York, page 134 (1944).
2. Nickerson, R. F., TEXTILE RESEARCH JOURNAL **21**, 195–202 (1951).
3. Reeves, W. A. *et al.,* TEXTILE RESEARCH JOURNAL **25**, 41–46 (1955).

Manuscript received March 20, 1956.

Physical Properties of Chemically Modified Cottons

Part I: Properties of the Untreated Cottons

Allan W. McDonald,[1] Geraldine Couturier Humphreys,[1] Ora Morlier Kromhout,[1] and James N. Grant

Southern Regional Research Laboratory,[2] New Orleans, Louisiana

Abstract

Six varieties of cottons were given certain chemical treatments, and the resulting changes in their fundamental physical properties were measured. This first report of a series describes the purpose of the work, the methods used to measure the properties, and the types of chemical treatments used. It also furnishes photomicrographs of cross sections of the cotton fibers and the values of the physical properties of the untreated cottons, which are the controls for samples receiving the chemical treatments. Data are given for yarns and fibers of these cottons, and comparisons are made between values of corresponding properties.

In recent years, modification of cotton fibers by chemical means has gained increased importance. By chemical treatment, certain inherent properties of cotton may be improved for a particular use, or new properties may be introduced. These desired changes are usually accompanied by alterations in the micro- and macrostructure of the fibers, yarns, or fabrics. Regardless of their nature, these changes in structure obviously have some effect on other characteristics of the cotton, in addition to changes for which the modification was intended. Furthermore, the extent and effectiveness of these treatments in altering the physical properties depend upon the physical properties of the untreated sample.

In order for industry to make a practical evaluation of a modification for the particular cotton it intends to use, a knowledge is needed, not only of the changes of those properties for which the treatment was designed, but also of the nature and extent of the attendant changes which may or may not be desirable.

The effects on the physical properties of cottons of certain chemical modifications and the dependence of the effects on the variety or growth of the cotton are being investigated at the Southern Regional Research Laboratory. Of necessity, this investigation has been limited to some of the current, more promising chemical treatments, to samples of certain varieties which collectively cover a broad range of inherent properties, and to measurements of those physical properties which are considered to be important in the manufacturing of textiles.

In the over-all study, five chemical treatments being performed at this Laboratory have been selected: acetylation, mercerization, aminization, carboxymethylation, and decrystallization. All possible ramifications of the treatments obviously could not, with practicability, be investigated; therefore, the first four treatments listed were performed only under what was believed to be the optimum condition for producing the most desirable end results. The fifth treatment, decrystallization, has not been applied sufficiently extensively to ascertain an optimum condition of treatment for the most desirable end results; therefore, it was applied in two ways: (*a*) with the yarns free to contract and (*b*) with yarns held at constant length.

The several results of this study will be reported in a series of seven papers. This first, introductory report presents a description of the experimental procedure used, tabulations of properties of the cotton fibers and yarns made from them prior to treatment, and a discussion of the interrelationship of the physical properties of fibers and those of the yarns. The subsequent five articles will present data and discussions of the effects of the individual chemical treatments on the physical properties of the fibers and

[1] Resigned.

[2] One of the laboratories of the Southern Utilization Research Branch, Agricultural Research Service, U.S. Department of Agriculture.

yarns. The final article will treat the interrelationships of the chemical treatments and the varieties or the types of cotton.

Samples

The samples of cotton were chosen from the following six varieties: S×P, Deltapine 14, Stoneville 2B, Coker 100 Wilt, Acala 1517, and Rowden 41B. They were chosen by varieties for the purpose of securing a wide variation in inherent characteristics but not of studying varietal characteristics. Photomicrographs of typical fiber cross sections of samples of the six varieties are shown in Figure 1.

Except S×P, the doubled yarns processed from these cottons had number, direction of twist, and turns per inch, as indicated by 16:Z12/2:S8.1 [1]. The S×P had values of 16:Z10/2:S6.7. Low twists were selected in order to allow rapid penetration of chemicals during treatment and to facilitate the defibering of the yarns. All yarns of each sample were twisted on a single spindle to eliminate the effects of spindle variations on the properties of the yarns.

Experimental Procedure

In order to facilitate chemical treatment, the yarns were wound into 60-yd. skeins. After treatment, the yarns and a set of untreated controls were exposed to standard atmospheric conditions (70° F., 65% R.H.) for several weeks. From each skein, several yards of yarn were separated into the component fibers by the process of defibering [8]. Every effort was made during this process to minimize both straining and breaking of fibers. This resulted in 42 different lots each of yarns and of fibers.

The bundle tenacity of fibers was measured directly by the Pressley method according to standard procedure [2].

At least three length arrays were made on each sample of fibers, according to A.S.T.M. procedure [3]. From these arrays, the length data were calculated, and the modal and two adjacent length groups of the distribution were removed for use in the single fiber measurements [9].

The linear density of a center section, 1.18 cm. long, was determined on a bundle of about 500 fibers from each of the three length groups. A weighted mean, based on the length distribution of the three length groups, was calculated for each lot.

Yarn linear density (weight fineness) was determined from the weight of 2-yd. sections of yarn cut while under a 2-oz. tension. The average linear density for each lot was calculated from several determinations.

Single-fiber breaking load and elongation at break were determined on 100 fibers selected at random from each of the three length groups. They were mounted individually with a polystyrene adhesive on aluminum mounts of ¼-in. gap. The specimen lengths were determined with a traveling microscope for 10 fibers selected at random in every 300 of each lot. Each fiber with an initial load of 0.15 g. was broken individually at a rate of loading of 0.64 g./sec. The complete procedure and description of the instrument used have been presented previously [9, 10]. Means of breaking load and elongation of the modal group, weighted in accordance with their respective per cent by weight in the length distribution, were computed.

The breaking loads and elongations at break of yarns were measured by the single-strand test method [4] on a Scott IP2 tester [2] modified to increase the capacity to 2500 g. Forty specimens were broken for each lot of yarns.

Tenacity and secant modulus, or average stiffness [14], were calculated from the data on fibers and yarns. Other determinations, i.e., maturity [5], crystallite orientation [13], crystallinity [12], wax content [7], and moisture regain have been made on the cottons.

Results and Discussion

In Table I are given the physical properties of the fibers for samples used. All samples, except S×P, which is an American-Egyptian, are American upland cottons. The samples ranged in staple length from 31/32 to 1½ in. [8]. Length measurements on the fibers were in good agreement with their commercial classification. Although the Rowden and S×P were average samples of the varieties, they represented extremes for the series in both length and fineness. Fiber lengths of the other samples were essentially equal and representative of the American upland type cottons [15].

Bundle tenacities at jaw spacings of zero and 2.5 mm. have been given. These measurements indicate that all samples were normal in this property for the types of cotton.

[2] The mention of trade names does not imply their endorsement by the Department of Agriculture over similar products not mentioned.

Fiber maturity count of the processed defibered samples, except Rowden and S×P, were lower than normal for cottons in general; however, the percentages of mature fibers in the unprocessed samples, except Acala 1517, were within the range for normal cotton. Differences between values of measurements of maturity on the unprocessed and processed cottons were discussed in an earlier publication [8].

The fiber properties of the different samples confirm the successful accomplishment of the objective, namely to secure a wide range in physical properties of fibers. Thus, while an individual sample showed extreme values for one or more the fiber properties, in most cases other properties were normal for American cottons. While the sample of Stoneville had an angle of crystallite orientation below the average for American cottons [6], its angle was about average for that variety. The sample of S×P had the lowest per cent crystalline cellulose [12] of any native cotton thus far studied at the Southern Regional Research Laboratory. The densities of these six cottons as measured by the density

TABLE I. Physical Properties of Untreated Cotton Fibers and Yarns

Properties	Samples					
	Acala 1517	Coker 100 Wilt	Deltapine 14	Rowden 41B	Stoneville 2B	S×
Bundle						
Length						
Upper quartile, in.	1.27	1.19	1.18	1.13	1.19	1.56
Mean, in.	1.05	0.95	0.94	0.96	0.97	1.33
C.V., %	29	34	34	25	32	26
Tenacity						
Zero spacing,* g./grex	3.9	3.8	4.0	4.2	4.4	4.6
2.5-mm. spacing,** g./grex	1.8	1.8	1.9	1.8	1.7	2.6
Mature fibers						
Unprocessed, %	70	78	79	90	80	86
Processed, %	66	72	74	87	74	86
Crystallite orientation, deg.†	31.2	32.3	30.1	28.8	25.9	31.3
Wax content, %	0.77	0.64	0.59	0.46	0.63	0.66
Crystallinity,‡ %	81	83	80	80	78	72
Moisture regain, %	6.9	6.8	6.8	6.7	6.7	6.8
Density, g./cc.	1.550	1.550	1.550	1.550	1.550	1.549
Single fibers						
Breaking load						
Mean, g.	5.3	5.1	5.5	7.2	4.8	6.2
C.V., %	39	49	45	45	47	35
Linear density,§ grex	1.69	1.77	1.88	2.55	1.90	1.42
Tenacity, g./grex	3.2	2.9	2.9	2.8	2.6	4.4
Elongation at break						
Mean, %	8.3	8.6	8.1	8.0	5.8	10.2
C.V., %	41	42	38	36	40	32
Secant modulus,‖ g./grex	38	34	36	35	44	43
Yarn						
Breaking load						
Mean, g.	1262	995	1124	950	1029	1724
C.V., %	3	6	4	5	6	3
Linear density, grex	733	719	746	749	725	749
Tenacity, g./grex	1.7	1.4	1.5	1.3	1.4	2.3
Elongation at break						
Mean, %	8.2	7.8	8.1	6.5	6.7	8.9
C.V., %	4	6	4	6	5	4
Secant modulus, g./grex	21	18	19	20	21	26

* Pressley index = zero spacing tenacity × 1.85.

† Angle between positions of maximum and half maximum intensity of the 002 X-ray diffraction arc.

‡ By acid hydrolysis method.

§ Linear density of center section.

‖ Secant modulus (average stiffness) is the ratio of change in stress to change in strain between two points on a stress-strain diagram, particularly the points of zero stress and breaking stress [14].

** Stelometer.

gradient columns [11] were equal for all samples except the S×P which was slightly lower than that of other cottons.

A visual comparison of cottons for linear density, shape, and percentage of mature fibers can be made from photomicrographs of the cross sections in Figure 1. S×P had the highest single fiber tenacity and elongation at break of all samples studied. The low percentage of crystalline cellulose in this sample had apparently less effect on fiber strength than the greater uniformity of fibrillar structure observed in cottons of this species. The Stoneville sample, with low crystallite orientation, had the lowest elongation at break and highest secant modulus of American upland cottons. Since the secant modulus, or ratio of stress to strain taken from the curve, compensates for fiber differences, the elastic properties of cotton are more accurately reflected in this value than any other of the fiber measurements.

In Table I are also given the measurements for

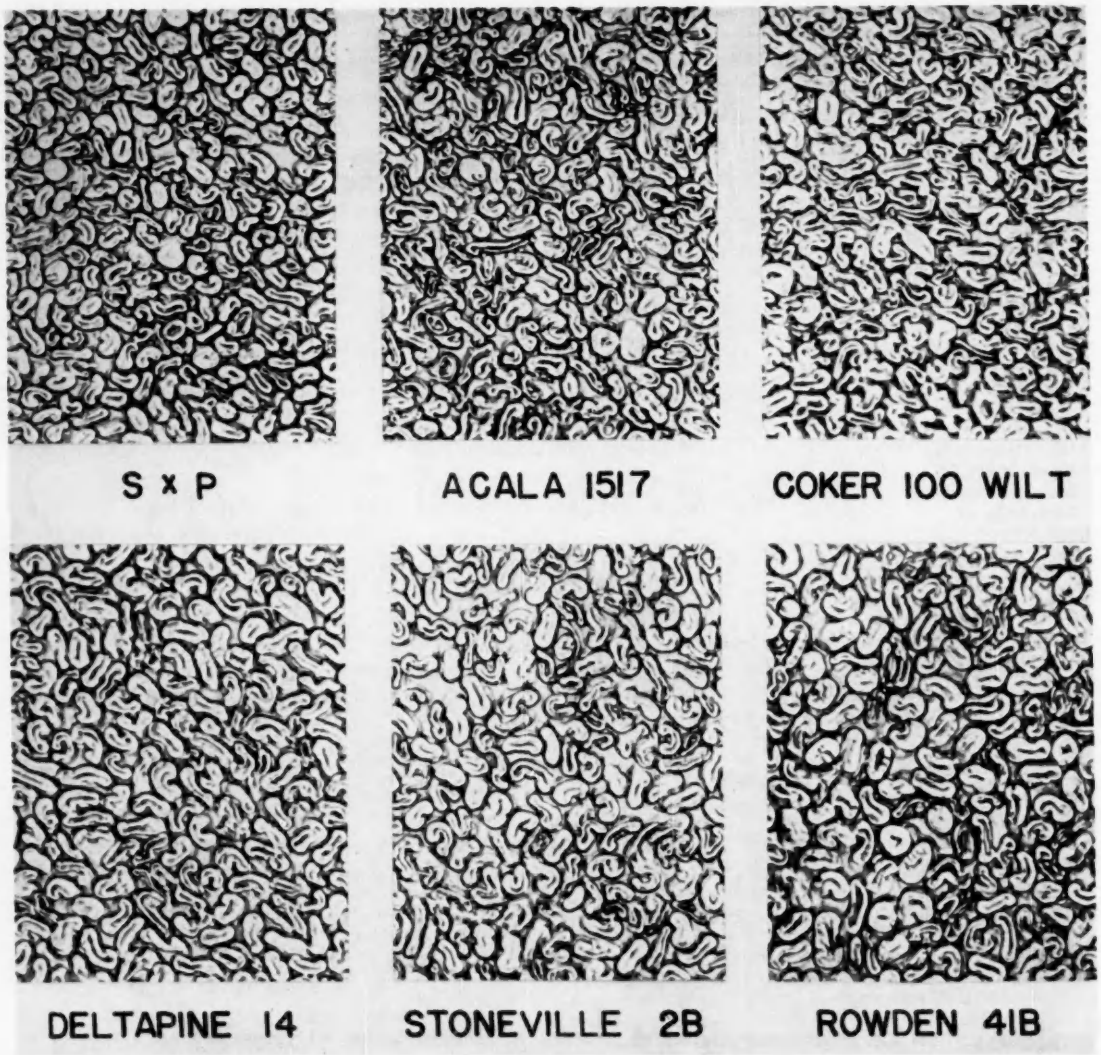

Fig. 1. Photomicrographs of cross sections of untreated cotton fibers of the six varieties. 1000 ×.

properties of the yarns spun from the six cottons. Yarn tenacities are more closely related to single-fiber tenacities and to bundle tenacities at 2.5-mm. jaw spacing than to bundle tenacities at zero jaw spacing, as shown by scatter about lines calculated for the relationships in Figure 2. Also, tenacities of yarns were about one-half those of the single fibers. The low coefficients of variation of breaking load, which are much below those usually observed, are attributed to the spinning with a single spindle and thus to the elimination of variations between spindles. As with tenacities, the elongations of yarns are closely related to the elongations of the fibers (Figure 3), as seen by the curve drawn by inspection through observations for five samples. An exception was the sample of Rowden cotton, which was excluded, the yarns of which had much lower elongation than that expected from elongation of the fibers. Such inconsistency might be expected for cottons with the wide range in fiber size. The close relationships of tenacities and of elongations in fibers and yarns, respectively, resulted in a good relationship of their secant moduli, even though values for fibers are about twice those found for yarns. The fact that the secant modulus of the yarns is lower than that of the fibers can be attributed to the introduction of twist during spinning and to fiber slippage. Although the elongations at break of both fibers and yarns are found to be essentially the same, the tenacity of the yarns at break is about half of that of the fibers. Slippage and unequal tensions at the surface as compared with the axis of the yarn undoubtedly account for this lowering of yarn tenacity.

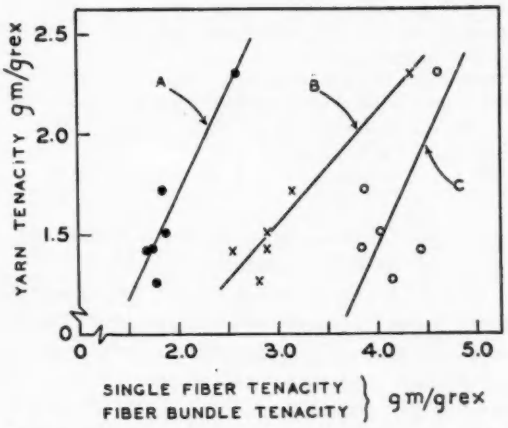

Fig. 2. The relation of tenacities of yarns to tenacities of single fibers at 7-mm. gauge length (curve B) and fiber bundles at zero (curve C) and 2.5 mm. gauge length (curve A).

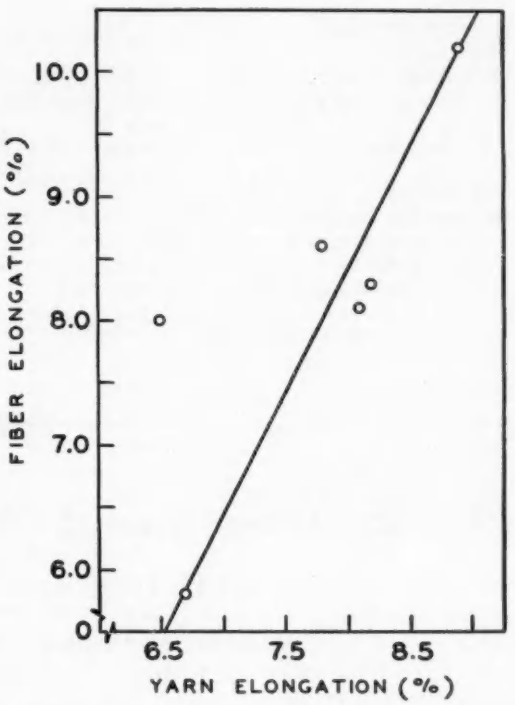

Fig. 3. The relation of single-fiber elongation at break to yarn elongation at break.

Acknowledgments

The authors wish to express their appreciation to the members of the New Products Unit for mechanically processing the yarns; to the members of the Analytical Unit for chemical tests and to those of the Textile Testing Unit for fiber analyses; to members of the Microscopical Properties Unit for photomicrographs; and to those of Colloidal Properties Unit for crystallite orientation and crystallinity values. Appreciation is expressed to Rollin S. Orr, John M. Scott, and Emilie H. Nott, of the Physical Properties Unit, who assisted with individual fiber measurements and in the preparation of the manuscript.

Literature Cited

1. D1244–53T, American Society for Testing Materials, Philadelphia, Pa.
2. D1445–53T, *Ibid.*

3. D414–54T, *Ibid.*
4. D180–54T, *Ibid.*
5. D1442–54, *Ibid.*
6. Berkley, E. E., Woodyard, O. C., Barker, H. D., Kerr, T., and King, C. J., "Structure, Determined by X-ray, and Strength of Cotton Fiber," *U.S. Dept. Agr., Tech. Bull.* No. 949, 64 pp. (1948).
7. Conrad, C. M., *Ind. Eng. Chem., Anal. Ed.* **16**, 745–748 (1944).
8. Grant, J. N., Morlier, O. W., and Scott, J. M., TEXTILE RESEARCH JOURNAL **22**, 682–687 (1952).
9. Morlier, O. W., Orr, R. S., and Grant, J. N., TEXTILE RESEARCH JOURNAL **21**, 6–13 (1951).
10. Orr, R. S., and Grant, J. N., TEXTILE RESEARCH JOURNAL **23**, 505–509 (1953).
11. Orr, R. S., Weiss, L. C., Moore, H. B., and Grant, J. N., TEXTILE RESEARCH JOURNAL **25**, 592–600 (1955).
12. Philipp, H. J., Nelson, M. L., and Ziifle, H. M., TEXTILE RESEARCH JOURNAL **17**, 585–596 (1947).
13. Segal, L., Creely, J. J., and Conrad, C. M., *Rev. Sci. Instr.* **21**, 431–435 (1950). *Instruments* **21**, 431–435 (1950).
14. Smith, H. DeW., *Am. Soc. Testing Materials Proc.* **44**, 543–592 (1944).
15. U.S. Agr. Marketing Service, Cotton Division, "Summary of Fiber and Spinning Test Results from Some Varieties of Cotton Grown by Selected Cotton Improvement Groups, Crop of 1953," Washington, D. C., 38 pp., processed (February 1954).

Physical Properties of Chemically Modified Cottons

Part II: Effects of Partial Acetylation

Allan W. McDonald,[1] Geraldine C. Humphreys,[1] Rollin S. Orr, and James N. Grant

Southern Regional Research Laboratory,[2] New Orleans, Louisiana

Abstract

Yarns manufactured from samples of the same six cotton varieties discussed in the previous paper were partially acetylated to an acetyl content of approximately 24% while held under tension. Certain physical properties of the component fibers, fiber bundles, and yarns were then measured. The changes in most properties were found to be associated with differences in the cottons and the acetyl contents. The averages for breaking loads and tenacities of the fibers were decreased while their linear densities and secant moduli were increased. Breaking loads, linear densities, and secant moduli of the yarns were increased. Elongation of the yarns at break was decreased, while tenacity remained essentially unchanged. The changes were greater for some cottons than for others; whether the changes were advantageous or disadvantageous would depend somewhat upon the use to which acetylated cotton is to be put.

SEVERAL properties induced or augmented by partial acetylation of cotton, such as resistance to heat degradation and reduction of the rate of bacterial decay, are reported in the literature [4, 5, 7]. These and other characteristics of partially acetylated cotton have, among other things, stimulated the study of some of the physical properties of the altered material [2]. Thus far, however, the published results of research have been meager.

This report, the second of a series [9] on modified fibers, gives the results of measurements of certain important physical properties of partially acetylated cotton fibers and yarns, the per cent changes from those of the untreated samples and the dependence of the physical changes on the characteristics of the sample.

In this investigation only one degree of acetylation

[1] Resigned.

[2] One of the laboratories of the Southern Utilization Research Branch, Agricultural Research Service, U.S. Department of Agriculture.

and type of acetylated cotton was studied, namely, one containing about 24% acetyl applied to the gray yarns while they were held under tension. While other percentages of acetyl may prove more useful for certain purposes, this percentage appeared to be more advantageous for many textile products. Therefore, the results are applicable only to this acetyl range, and conclusions must not be construed as pertaining to the other degrees and types of acetylation. The properties of fibers of other degrees of acetylation are now under investigation.

Experimental Procedure

Samples

Both the general characteristics of the cottons and the physical properties of the samples used for acetylation were described in Part I [9].

Treatment

Skeins of yarns of each of the six samples were soaked overnight in a glacial acetic acid bath. Each skein was taken from the bath and placed on two rollers, the lower one surrounded by a glass cylinder [6]. Two pounds' tension, corresponding to approximately 1 to 3% of the breaking load, was then placed on the skeins and remained on them for the duration of the treatment. A solution consisting of 450 ml. acetic anhydride, 1050 ml. acetic acid, and 3 ml. $HClO_4$ was introduced into the cylinder. The skein was rotated continuously in this bath for a length of time ranging from 8 to 12 min. determined previously from trial experiments. The skein was rinsed several times, finally soaked in water, and then air dried. This process was repeated with a new solution for each skein. A more complete description of the process and apparatus is given in the literature [3, 5, 6].

Test Methods

The measurements of physical properties were performed according to the procedures outlined in Part I of this series [9].

Results and Discussion

The influence of partial acetylation with acetyl contents on dry weight basis, degree of substitution, moisture regain at standard conditions, fiber length, and linear densities of the fibers are given in Table I. Data for the untreated fibers from which the per cent changes were calculated are given in the earlier paper [9]. The densities of the fibers from the acetylated samples of these six cottons were also measured and are reported in another publication [10].

While the average acetyl content was 24%, the acetyl contents for the samples ranged from 20.8 to 27.2% (degree of substitution 0.98 to 1.40). Moisture regain, when measured on samples from standard conditions, was found to be decreased about 2.8%, the amounts depending largely upon the acetyl contents of the samples. A reduction in moisture regain of equivalent amount has been observed by other workers [7].

Fiber Length

Both the fiber lengths at the 25% point of the length distribution and the mean length showed a

TABLE I. The Acetyl Contents and Moisture Regains of Six Partially Acetylated Cottons together with Fiber Lengths, Linear Densities of Fibers and Yarns, and Changes in These Properties from Those of the Untreated Cottons

Sample identification	Acetyl content*		Moisture regain at standard conditions	Fiber length				Linear density			
								Fibers†		Yarns	
	%	D.S.‡	(%)	25% point (in.)	Per cent decrease	Mean (in.)	Per cent decrease	Mean (grex)	Per cent increase	Mean (grex)	Per cent increase
Acala 1517	20.8	0.98	4.4	1.26	− 1	1.03	− 2	1.86	10	872	19
Coker 100 Wilt	24.2	1.19	4.0	1.11	− 7	0.84	−11	2.18	23	921	28
Deltapine 14	25.3	1.27	3.9	1.13	− 4	0.88	− 6	2.25	20	943	26
Rowden 41B	23.1	1.12	4.1	1.07	− 6	0.88	− 8	2.97	16	875	17
Stoneville 2B	27.2	1.40	3.6	0.95	−20	0.70	−28	2.29	21	946	31
S×P	22.2	1.07	4.1	1.53	− 2	1.27	− 4	1.64	15	919	23
Average	23.8	1.17	4.0	1.18	− 7	0.93	−10	2.20	18	913	24

* Dry weight basis.
† Linear density for center section of fiber.
‡ Degree of substitution.

reduction in all cases as a result of acetylation. The reduction at the 25% point ranged from 1 to 20% and the mean from 2 to 28%, depending upon the cotton. Only the Stoneville sample showed a decrease of more than 11%. After treatment five of the samples retained their characteristic modal shape of curve for cottons in the frequency length distribution and, except for the Rowden sample, showed no shift of the mode toward lower lengths. The shift in mode for the Rowden corresponded to decreases of 5% in fiber length at the 25% point and 8% in the mean length. All samples, however, showed a decrease in the proportion of longer fibers and an increase in the proportion of shorter fibers but no appreciable shift in the range of fiber lengths in a sample. The redistribution of the fibers varied with the sample and was most pronounced with the sample of Stoneville with the highest acetyl content, which, after treatment, had almost a flat distribution. It is evident, therefore, that the change in the mean length is caused mostly by fiber breakage, probably occurring in the process of defibering the yarns. There may have been some fiber shrinkage since the process does involve a slight swelling, but values for shrinkage and breakage are not easily separated in length distribution measurements.

Linear Density of Fibers

The increases expected in linear density of the center section of fibers, if calculated from the acetyl contents (Table I) to a dry cellulose basis, would range from 26 to 37%, and for the six cottons would average 31%. Since the reduction in moisture was about 2.8%, the range should be from 23 to 34% with an average for the six samples of 28%.

Actually observed increases in linear density of fibers for the six cottons ranged from 10 to 23% (Table I), and the average increase was 18%. The per cent increase in linear density on dry cellulose basis was less than the gain in mass due to acetylation by amounts ranging from 5 to 13%, with that for five samples falling between 10 and 13%. If small decreases in fiber length caused by swelling are assumed, the difference will be slightly greater.

The dye and microscope test of fibers [3] showed that for some samples the distribution of acetyl in the center section was not uniform. The appearance of the samples of Rowden and Acala was spotted, indicating incomplete treatment. The appearance of Coker 100 Wilt and S×P was less spotted, indicating moderately uniform treatment, while that of Stoneville and Deltapine indicated complete treatment. These observations suggested that some fibers in a sample had a higher acetyl content than others. There is also evidence that the finer sections of fibers have a higher acetyl content than do the coarser sections of fibers. This was verified by density measurements for sections of the same fibers which showed that the center sections had about 2% lower acetyl content than their end sections [10]. Also, the density measurement showed that the three length groups used for linear density and other fiber measurements had about 2% lower acetyl content than the composite sample. Since fibers of higher acetyl content were in general more brittle and more easily broken in the defibering process, the center sections were biased about 4% toward the lower acetyl contents. If a comparison is made between the increase in linear density, as calculated from the lower acetyl content, and the measured linear density, there is still a difference unaccounted for of about 3%.

Linear Density of Yarns

The change of observed linear density of the yarns (Table I) ranged from 17 to 31%. If no length change occurred in yarns while held under tension during treatment, the weight gains calculated on a cellulose basis from linear densities of the individual acetylated yarns also were less than the values calculated from the acetyl content, with a range from 0 to 10%.

If a correction is made for moisture regain but not for change in length, the average gain in weight calculated from per cent acetyl was 4% greater than the average gain approximated from linear density. This might be accounted for to some extent by experimental error in the measurement of linear densities of yarns—especially since the sections along the spool were not the same for the acetylated and the control yarns. However, the fact that both fibers and yarns showed trends in the same direction leads to the belief that the discrepancies in loss of weight might be due to other causes.

The data reported by Honold *et al.* [7], for samples of two higher acetyl contents, corrected for moisture regain and shrinkage, show a 3 and 5% difference of the same nature. However, taking other factors into account, they report a difference of less than 3% which is within their experimental error. One possible explanation for the difference is the partial loss of noncellulosic materials during acetylation.

According to the research of McCall and Jurgens [8], it is possible to remove 5% or more of non-cellulosic materials from fibers in certain treatments. If this occurs with acetylation, it would then essentially eliminate the discrepancy between observed per cent gain and that calculated from the acetyl content.

Breaking Load

The observed breaking loads of fibers (Table II) decreased for all the samples except Stoneville, which showed a 3% increase. The range of the changes was +3 to −14% with the greatest decrease found for samples of Acala and S×P. As previously mentioned, an inadvertent selective action occurs in the defibering process, causing some of the weaker and more brittle fibers to be absent from the modal length groups. This means that the measured values of breaking load will be biased toward the high average and decreases in breaking load will be greater than those shown by the per cent change.

It must be remembered, too, that these samples have a relatively high per cent acetyl content attained in a relatively short period of time and that decreases in fiber breaking load found here do not necessarily apply to samples with lower acetyl content or to samples treated under different conditions with the same acetyl content. For example, Bletzinger [1] found in his study that breaking loads of fibers for an upland cotton increased with acetylation. However, the acetyl contents of the fibers (9.43 and 18.3%) were lower than those of the present study, and the times required to attain these acetyl contents were 47 hr. and 37 days, respectively.

The breaking load of yarns (Table II) increased for all samples with the smallest increase found for the S×P. Since increases were not observed in breaking loads of fibers, except for Stoneville 2B, the factors responsible for the increased breaking loads of yarns and the increased yarn to fiber strength ratio are considered to be increased fiber friction, increased cohesion, probably of an electrostatic nature, in conjunction with a decreased moisture regain, and a better fiber adjustment because of slight swelling under a small tension. Increases of 20% in breaking strengths for 16/1 yarns of 19.5 acetyl content were reported by Goldthwait [5].

If the ratio of breaking load of yarn to that of fiber for the untreated [9] and acetylated is calculated, the increase due to acetylation ranges from 22 to 39%, with four of the samples falling into a smaller range of from 27 to 35%. The S×P and Coker 100 Wilt samples represent the low and high extremes respectively. As previously mentioned, the fiber data for these calculations were taken from the observed breaking loads of fibers in the three length groups of acetylated cotton. The ratio might even be increased if calculated from the observed breaking loads of all acetylated fibers in a sample.

Tenacity

The tenacity of the fibers (Table II) was decreased in all cases, due mainly to a dilution effect occasioned by the added acetyl mass. The per cent change in bundle tenacity for three samples is within 3% of the changes observed for single fibers. The other three differed by greater amounts. These differences are to be expected in the light of the differences in the distribution of fibers for the different samples and in the method of bundle preparation (i.e., removal of the short as well as the weaker fibers during the

TABLE II. Breaking Loads and Tenacities of Partially Acetylated Cotton Fibers and Yarns, and Changes in These Properties from Those of the Untreated Cottons

	Breaking load				Tenacity					
	Fibers		Yarns		Fibers		Bundles		Yarns	
Sample identification	Mean (g.)	Per cent change	Mean (g.)	Per cent increase	Mean (g./grex)	Per cent decrease	Zero spacing* (g./grex)	Per cent decrease	Mean (g./grex)	Per cent change
Acala 1517	4.8	− 9	1480	17	2.6	−19	3.5	−10	1.7	0
Coker 100 Wilt	5.0	− 2	1360	37	2.3	−21	3.1	−18	1.5	7
Deltapine 14	5.3	− 4	1475	31	2.4	−17	3.3	−18	1.6	7
Rowden 41B	6.9	− 4	1164	23	2.3	−18	3.2	−24	1.3	0
Stoneville 2B	5.0	3	1402	36	2.2	−15	3.2	−27	1.5	7
S×P	5.3	−14	1813	5	3.2	−27	3.5	−24	2.0	−13
Average	5.4	− 5	1449	25	2.5	−20	3.3	−20	1.6	1

* Pressley index = zero spacing tenacity × 1.85.

preparation of bundles). The tenacity of three of the samples of yarns was increased by 7%. The increases in breaking loads for two samples were sufficient to compensate for the increase in linear density, and no changes were shown in tenacity; one sample, S×P, showed a 13% decrease in tenacity.

A graph of the tenacities of partially acetylated fiber, fiber bundle, and yarn samples, plotted against those of the corresponding untreated controls (Figure 1), shows a fairly linear relationship with yarns grouped at the lower end of the curve and fiber bundles at the upper. The relationship of tenacities of the acetylated to untreated fibers and yarns of these cottons can be expressed by the single equation

$$a = 0.62 + 0.60u$$

where a is the tenacity of the acetylated product and u is the tenacity of the untreated yarn or fiber expressed in g./grex. While the curve for fibers and yarns passes through points for the bundles, the scatter of these points is too great to establish an accurate relationship for the bundles.

The scatter of the bundle test observations at zero spacing shown in the graph, and the dependence of bundle tenacity on gauge length, the amount of which is both unknown and variable, depending upon friction, crimp, and the jaw surfaces, renders this bundle test method a relatively inappropriate one for this type of comparison.

Elongation

Acetylation decreased the elongation at break of single fibers (Table III) from 13 to 33%. The fibers had a relatively large increase in mass, an increase in volume as observed microscopically, and a decrease in moisture. Since the reaction takes place within the amorphous cellulose which is more accessible for chemical reaction [4] and moisture is lost, the internal adjustments in cellulose structure when strained would be more difficult to make in the partially acetylated cottons. The greater rigidity of structure would decrease the "give" and consequently result in a decreased elongation at break and a loss in breaking strength because of the local strains. While the actual elongation would be decreased, the increased percentage recovery from strains at low loads would be expected from such a structure. The greater percentage recovery was found for fibers of

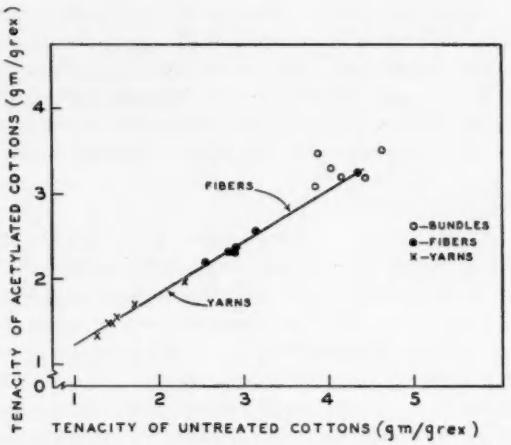

Fig. 1. Relationships of tenacity of acetylated cotton fibers, bundles, and yarns to corresponding tenacity of untreated samples.

TABLE III. The Elongations at Break and Secant Moduli of Partially Acetylated Cotton Fibers and Yarns, and Changes in These Properties from Those of the Untreated Controls

	Elongation at break				Secant modulus*			
	Fibers		Yarns		Fibers		Yarns	
Sample identification	Mean (%)	Per cent decrease	Mean (%)	Per cent decrease	Mean (g./grex)	Per cent change	Mean (g./grex)	Per cent increase
Acala 1517	7.2	−13	6.7	−18	36	−5	25	19
Coker 100 Wilt	5.8	−33	6.2	−21	40	18	24	33
Deltapine 14	5.4	−33	6.4	−21	44	22	24	26
Rowden 41B	6.3	−21	4.7	−28	37	6	28	40
Stoneville 2B	3.9	−33	4.8	−28	56	27	31	48
S×P	7.3	−28	6.9	−22	44	2	29	12
Average	6.0	−27	6.0	−23	43	12	27	30

* Secant modulus (average stiffness) is the ratio of change in stress to change in strain between two points on a stress-strain diagram, particularly the points of zero stress and breaking stress [11].

the Deltapine sample which after cyclic loading to 2.75 g. (approximately 50% of the breaking load) showed 10% more recovery for partially acetylated than for the untreated fibers.

The decrease in yarn elongation (Table III) showed a fairly narrow range of from 18 to 28% with four of the samples having a range of 18 to 22%. The decrease, which in most cases was less than that of the fibers, was to be expected, since the breaking loads of yarns increased while those of fibers decreased.

Secant Modulus

The secant modulus or stress-strain ratio at break of the samples (Table III) increased in most cases for fibers and in all cases for yarns. The average for fibers of the six acetylated samples is 16 g./grex greater than that for the yarns, and the average increases over the untreated for fibers and yarns are 5 and 6 g./grex, respectively. The average increase for yarns is 18% greater than for fibers. If the secant moduli for acetylated samples were plotted against those of the untreated, the points would show considerable scatter from a curve calculated for the data; samples of higher than the average per cent acetyl would usually lie above the curve while those of the lower per cent acetyl would be below the curve. The points representing the yarns would appear at the lower end of the curve and those for the fibers at the upper end. The data implies that the secant modulus of yarns or fibers will be increased about equal amounts for a given acetyl content regardless of the samples.

Conclusions

For partially acetylated cotton with acetyl contents of the order of 24% and prepared by treating yarns while held at constant length, the fibers, when compared with the untreated, were found to have slightly shorter lengths, which are believed to be caused essentially by the breakage of fibers in defibering the yarns. The linear densities were increased by the addition of acetyl mass, but the increases on center sections of modal length groups were less than the amount calculated from the acetyl content of the samples. The slight decreases in breaking loads of individual fibers and the addition of mass caused tenacities of the acetylated fibers to be decreased. The decreases in elongations at break, which were greater than the decrease of tenacities, resulted in most cases in higher secant moduli. The fibers with the higher modulus were, as expected, more rigid and brittle than the untreated fibers and have less ability to absorb energy.

For the yarns, the linear densities and breaking loads were increased on the average about equal percentages, the linear densities by the addition of acetyl mass, and the breaking loads by the intrafiber effects, since the individual fibers in general showed small decreases in breaking loads. Elongations at break were decreased but not to the extent found for individual fibers. The secant moduli for yarns were increased by acetylation; the per cent increases of yarns were more than those for the fibers.

The changes in moisture, length, tenacity, and modulus were functions of the samples used and their acetyl contents. Several interrelations were apparent, but the developments of these interrelationships are beyond the scope of the present paper. However, the extreme undesirable changes found more often in properties of fibers and yarns of S×P, Stoneville, and Acala indicate that acetylation by the method described could be more unsatisfactory in these samples than in the others which were investigated.

Acknowledgment

The authors wish to express their appreciation to A. S. Cooper and his co-workers in the Chemical Modification Unit, who prepared the partially acetylated yarns and measured their acetyl contents, and to Mrs. Ora Morlier Kromhout, J. M. Scott, and Emilie H. Nott, who assisted in initiating the investigation, measured many properties of the fibers and yarns, and assisted in preparation of the manuscript.

Literature Cited

1. Bletzinger, J. C., *Ind. Eng. Chem.* **35**, 474–480 (1943).
2. Buras, E. M., Jr., Cooper, A. S., Keating, E. J., and Goldthwait, C. F., *Am. Dyestuff Reptr.* **43**, P203–208 (1954).
3. Cooper, A. S., Voorhies, S. T., Jr., Buras, E. M., Jr., and Goldthwait, C. F., *Textile Inds.* **116**, No. 1, 97–102, 194–195 (1952).
4. Goldthwait, C. F., Buras, E. M., Jr., and Cooper, A. S., Textile Research Journal **21**, 831–840 (1951).
5. Goldthwait, C. F., McLaren, J., and Voorhies, S. T., Jr., *Textile World* **96**, No. 2, 115–117, 212, 216 (1946).

6. Goldthwait, C. F., Murphy, A. L., Lohmann, I. W., and Smith, H. O., TEXTILE RESEARCH JOURNAL **22**, 540–548 (1952).
7. Honold, E., Poynot, J. M., and Cucullu, A. F., TEXTILE RESEARCH JOURNAL **22**, 25–29 (1952).
8. McCall, E. R., and Jurgens, J. F., TEXTILE RESEARCH JOURNAL **21**, 19–25 (1951).
9. McDonald, A. W., Humphreys, G. C., and Grant, J. N., "Physical Properties of Chemically Modified Cottons," Part I, TEXTILE RESEARCH JOURNAL **26**, 641 (1956).
10. Orr, R. S., Weiss, L. C., Moore, H. B., and Grant, J. N., TEXTILE RESEARCH JOURNAL **25**, 592–600 (1955).
11. Smith, H. DeW., *Am. Soc. Testing Materials Proc.* **44**, 543–592, esp. 589 (1944).

Manuscript received January 23, 1956.

Book Reviews

Plastics for Corrosion Resistant Applications. Raymond D. Seymour and Robert H. Steiner, New York, Reinhold Publishing Corp., 1955. 449 pages. Price $7.50.

Reviewed by Hillary Robinette, Jr., President, Robinette Research Laboratories, Inc., Ardmore, Pa.

Based on a background of wide experience and knowledge, the authors have, in the opinion of the reviewer, produced in this volume a most useful source of information for engineers and others responsible for the choice of materials of construction to combat corrosion through the use of plastics.

Information on the chemical and physical nature of the various plastic materials, along with a brief description of their methods of manufacture, is included in the section dealing with the history of plastic materials. This is followed by a chapter on plastic fundamentals and a chapter relating chemical resistance to molecular structure. Methods of testing are described and methods of application are included.

Separate chapters cover plastic impregnants, casting resins, and chemically resistant mortar cements. A section of the volume is devoted to plastic pipe, valves, and fittings.

Many tables and illustrations are included. The tables make it easy to select the most suitable plastic, and the illustrations are helpful in enabling one to visualize the use of the plastics. This vast amount of comparative data should prove to be most valuable to chemists and engineers as a guide in choosing materials to combat corrosion.

A group of suggested references are included at the end of each chapter, and in addition to an adequate subject index, the volume contains an author index.

Hydrogen Peroxide. W. C. Schumb, C. N. Satterfield, and R. L. Wentworth, New York, Reinhold Publishing Corp., 1955. 669 pages. Price $16.80.

Reviewed by Hillary Robinette, Jr., President, Robinette Research Laboratories, Inc., Ardmore, Pa.

This volume, #128 in the ACS monograph series, is a complete and unbiased presentation of the chemistry and technology of hydrogen peroxide. The authors are to be commended.

The volume meticulously covers the history, discovery, and theories of molecular structure, the mechanisms of formation and decomposition, and the reactions of hydrogen peroxide. There are 669 pages of text, with more than 2500 literature references, providing a complete and exhaustive survey of the existing knowledge about hydrogen peroxide. Illustrations, graphs, and tables have been used freely to clarify the technical aspects of the mechanisms involved in the discussion of the physical and thermodynamic properties of hydrogen peroxide.

The uses of hydrogen peroxide are detailed as a material of synthesis; as a bleaching and oxidizing agent; as a component of fuels for submarines, torpedoes, and rockets; and as an effective bactericide. References are made by the authors to other accepted compounds, and comparisons are drawn between these and hydrogen peroxide.

This volume will prove to be most useful to the chemist and engineer as a working manual and a reference work.